



^T MEASUREMENT OF WATER
POTENTIAL USING
THERMOCOUPLE HYGROMETERS /

by

^A
MICHAEL JOHN SAVAGE ^o—

B.Sc. and B.Sc. (Hons) (Natal)

Submitted in partial fulfilment
of the requirements for
the degree of

DOCTOR OF PHILOSOPHY

in

Department of Soil Science and Agrometeorology

^P University of Natal,

^{PP} PIETERMARITZBURG :

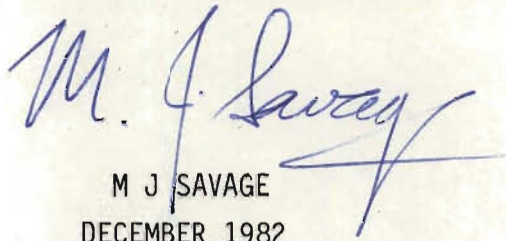
NATAL

^D
(DECEMBER,) 1982.

*Thesis (Ph. D.; Soil science and Agrometeorology) — University of Natal,
Pietermaritzburg, 1982*

DECLARATION

I declare that the results contained
in this thesis are from my own original
work except where acknowledged.

A handwritten signature in blue ink, appearing to read "M. J. Savage". The signature is fluid and cursive, with a long horizontal stroke at the end.

M J SAVAGE
DECEMBER 1982

ACKNOWLEDGMENTS

I wish to express my grateful appreciation to my supervisor, Dr Alfred Cass, for the advice, criticism and patience toward the completion of this work. Sincere appreciation is also extended to: Professor James M de Jager for initiating the project and advice during the course of this work; Professor Herman H Wiebe (Biology Department, Utah State University, Logan, Utah), on sabbatical leave in this Department during 1981/82, for his encouragement and comments on Chapter 5; the anonymous referees for their comments on the research papers emanating from this work; Mr Robert F Grant for cooperation with the research work of Chapter 4.

Special thanks are also due to: Ms Sandra Naidoo for technical assistance (Chapter 5); Mr Peter N Dovey for assistance with electronic details; Mrs Leslie A le Roux for assistance with Figs 2.3 and 2.4; Mrs Susan Davis for the line sketches (Figs 4.1 and 5.2 to 5.5); Mr Anthony G Bruton for assistance with the electron microscope work (Plate 5.1); Mr Bruno Martin for assistance with the photographic work (Figs 2.1, 2.3, 2.4 and 2.7); Grain Crops Research Institute (Cedara sub-centre) for loan of equipment; Department of Agricultural Engineering for use of their computer plotter; Department of Animal Science and Poultry Science for use of their pen chart recorders; Department of Horticultural Science for the citrus trees; Mrs Aileen E Bosman for expertly typing the chapters and Mrs Lucille Shaw the Abstract, Introduction and References.

This project was funded by the Department of Agriculture, the University of Natal Research Fund and the Council for Scientific and Industrial Research and this support is gratefully acknowledged.

Michael J Savage

TABLE OF CONTENTS

iii

	Page
DECLARATION	i
ACKNOWLEDGMENTS	ii
NOTATION	vii
LIST OF TABLES	xiii
LIST OF FIGURES	xvii
ABSTRACT	xxi
INTRODUCTION	1
CHAPTER	
1 THEORY OF THERMOCOUPLE HYGROMETERS	3
1.1 WATER POTENTIAL	3
1.1.1 Introduction	3
1.1.2 Thermodynamic theory of water potential	4
1.1.3 Components of water potential	5
1.2 THERMOCOUPLE HYGROMETERS	6
1.2.1 Introduction	6
1.2.2 Thermocouple psychrometers	6
1.2.2.1 <i>Mechanics of the psychrometric technique</i>	6
1.2.2.2 <i>Energy balance of a thermocouple psychrometer</i>	8
1.2.2.3 <i>Temperature dependence of k_T(theory)</i>	12
1.2.3 Dewpoint hygrometers	13
1.2.3.1 <i>Mechanics of dewpoint hygrometers</i>	13
1.2.3.2 <i>Energy balance of dewpoint hygrometers</i>	14
1.2.3.3 <i>Temperature dependence of dewpoint hygrometers</i>	16
1.3 SUMMARY	16
2 CALIBRATION OF THERMOCOUPLE HYGROMETERS USING THE PSYCHROMETRIC TECHNIQUE	18
2.1 INTRODUCTION	18
2.2 DEFINITION OF THE THERMOJUNCTION STEADY STATE	18
2.2.1 Introduction	18
2.2.2 Theory	18
2.2.3 Materials and methods	21
2.2.4 Results and discussion	23
2.3 TEMPERATURE DEPENDENCE OF PSYCHROMETER CALIBRATION	28

TABLE OF CONTENTS (cont.)

CHAPTER	Page
2.3.1 Introduction	28
2.3.2 Theory	28
2.3.3 Results and discussion	31
2.4 COMPARISON BETWEEN THEORETICAL AND OBSERVED CALIBRATION CURVES	36
2.4.1 Intercept	36
2.4.2 Slope	38
2.5 STATISTICAL ASSESSMENT OF ERRORS IN THERMOCOUPLE PSYCHROMETRIC WATER POTENTIAL MEASUREMENT	43
2.5.1 Introduction	43
2.5.2 Theory	44
2.5.3 Materials and methods	45
2.5.4 Results and discussion	46
2.6 SUMMARY	52
3 CALIBRATION OF THERMOCOUPLE HYGROMETERS USING THE DEWPOINT TECHNIQUE	54
3.1 INTRODUCTION	54
3.2 DEWPOINT COOLING COEFFICIENT DETERMINATION	54
3.2.1 Introduction	54
3.2.2 Materials and methods	54
3.2.3 Results and discussion	55
3.2.2.1 <i>Setting of Π_0</i>	55
3.2.2.2 <i>Π_0 as a function of temperature</i>	57
3.3 CALIBRATION DATA AND SLOPE PREDICTION MODEL	58
3.3.1 Introduction	58
3.3.2 Results and discussion	58
3.4 STATISTICAL ASSESSMENT OF ERRORS IN DEWPOINT HYGROMETER WATER POTENTIAL MEASUREMENT	60
3.4.1 Introduction	60
3.4.2 Theory	62
3.4.3 Results and discussion	63
3.5 SUMMARY	69

CHAPTER	TABLE OF CONTENTS (cont.)	Page
4	LABORATORY MEASUREMENT OF LEAF WATER POTENTIAL USING THERMOCOUPLE PSYCHROMETERS, A SCHOLANDER PRESSURE CHAMBER AND A J-14 HYDRAULIC PRESS	70
4.1	INTRODUCTION	70
4.2	LITERATURE REVIEW	70
4.3	MATERIALS AND METHODS	73
4.4	RESULTS AND DISCUSSION	75
4.4.1	Leaf water potential comparisons	75
4.4.2	Pressure-volume curve	78
4.5	SUMMARY	81
5	<i>IN SITU</i> FIELD MEASUREMENT OF LEAF WATER POTENTIAL USING THERMOCOUPLE PSYCHROMETERS	83
5.1	INTRODUCTION	83
5.2	EFFECT OF CUTICLE ABRASION ON FIELD MEASURED WATER POTENTIAL USING <i>IN SITU</i> THERMOCOUPLE PSYCHROMETERS	85
5.2.1	Introduction	85
5.2.2	Materials and methods	86
5.2.3	Results and discussion	88
5.3	NON-DESTRUCTIVE FIELD MEASUREMENT OF LEAF WATER POTENTIAL USING THERMOCOUPLE PSYCHROMETERS	94
5.3.1	Introduction	94
5.3.2	Materials and methods	96
5.3.3	Results and discussion	102
5.4	TIME RESPONSE OF THERMOCOUPLE PSYCHROMETERS TO LEAF WATER POTENTIAL CHANGES FOLLOWING LEAF EXCISION	108
5.4.1	Introduction	108
5.4.2	Materials and methods	109
5.4.2.1	<i>Laboratory investigation</i>	110
5.4.2.2	<i>Field investigation</i>	110
5.4.3	Results and discussion	112
5.4.3.1	<i>Laboratory investigation</i>	112
5.4.3.2	<i>Field investigation</i>	115

TABLE OF CONTENTS (cont.)

Page vi

5.5 EFFECT OF EXCISION ON LEAF WATER POTENTIAL	119
5.5.1 Introduction	119
5.5.2 Materials and methods	120
5.5.3 Results and discussion	121
5.6 SUMMARY	125
GENERAL DISCUSSION	127
REFERENCES	129

NOTATION

Chapter 1

Symbols not defined fully are defined in the text. The page and equation number indicates where the definition is to be found.

a	defined by Eq. 1.24, p 12, unitless
b	defined by Eq. 1.24, p 12, $^{\circ}\text{C}^{-1}$
B	defined by Eq. 1.16, p 10, $\text{W m}^{-1}\text{K}^{-1}$
C	thermojunction heat capacity, Eq. 1.12, p 8, J/K
D	voltmeter dewpoint gain, p 15, μV^{-1}
D_v	diffusion coefficient for water vapour in air, Eq. 1.19, p 10, m^2/s
e	water vapour pressure, Eq. 1.7, p 5, kPa
e_0	saturated water vapour pressure at temperature T, Eq. 1.7, p 5, kPa
E(rad), E(sen), E(con), etc	terms describing the sensing thermojunction energy balance, Eq. 1.12, p 8, J/s
g	acceleration of gravity, Eq. 1.1, p 3, m/s^2
G	defined by Eq. 1.18, p 10
I	cooling current through sensing thermojunction, Eq. 1.18, p 10, A
k_a	thermal conductivity of air, Eq. 1.14, p 9, $\text{W m}^{-1}\text{K}^{-1}$
k_T	psychrometer calibration constant at temperature T, p 13, $\text{kPa}/\mu\text{V}$
$k_T(\text{theory})$	theoretical calibration constant at temperature T, Eq. 1.23, p 12, $\text{kPa}/\mu\text{V}$
k_w	thermal conductivity of the wire surrounding the sensing thermojunction, Eq. 1.17, p 10, $\text{W m}^{-1}\text{K}^{-1}$
L_v	specific latent heat of vapourization, Eq. 1.19, p 10, $\text{J kg}^{-1}\text{K}^{-1}$
m	mass of water evaporated, p 10, kg
\bar{M}_w	molar mass of water vapour, Eq. 1.4, p 4, kg/mol
n_i	amount of substance of the i th component, Eq. 1.2, p 4, mol
P	system pressure, Eq. 1.2, p 4, Pa; Peltier cooling coefficient, Eq. 1.20, p 10, V
r_c	thermocouple chamber radius, Eq. 1.16, p 10, μm
r_j	thermojunction radius, Eq. 1.13, p 8, μm

NOTATION (continued)

r_w	radius of wire adjoining sensing thermojunction, Eq. 1.16, p 10, μm
R	universal gas constant = $8,3143 \text{ J mol}^{-1} \text{ K}^{-1}$, Eq. 1.7, p 5; electrical resistance of thermojunction and neighbouring wires, p 14, Ω
S	chromel-constantan thermocouple voltage sensitivity to temperature, Eq. 1.11, p 7, $\mu\text{V/K}$
$S_d(\text{theory})$	theoretical dewpoint calibration constant, Eq. 1.25, p 14, $\mu\text{V/kPa}$
\bar{S}_w	entropy change per amount of substance, Eq. 1.2, p 4, $\text{J K}^{-1} \text{ mol}^{-1}$
t	time, p 10, s
T	temperature; gas temperature, Eq. 1.2, p 4, K; block temperature, Eq. 1.11, p 7, $^{\circ}\text{C}$ or K
T_j	thermojunction temperature, Eq. 1.11, p 7, $^{\circ}\text{C}$ or K
T_w	wet bulb temperature, Eq. 1.22, p 11, $^{\circ}\text{C}$ or K
T_{dp}	dewpoint temperature, p 13, $^{\circ}\text{C}$ or K
V	output voltage, Eq. 1.11, p 7, μV
\bar{V}_w	partial molar volume of water vapour, Eq. 1.1, p 3, m^3/mol
$V(T_w)$	output voltage corresponding to the wet bulb temperature T_w , Eq. 1.22, p 11, μV
$V(T_{dp})$	output voltage corresponding to the dewpoint temperature T_{dp} , Eq. 1.25, p 14, μV
V_{25}	output voltage at 25°C , Eq. 1.24, p 12, μV
X_j	j th component of an extensive parameter, Eq. 1.2, p 4
\bar{Y}_j	j th component of an intensive parameter that accounts for work involved per unit amount of substance, Eq. 1.2, p 4
β	slope of the saturation water vapour pressure-temperature curve at temperature T , Eq. 1.19, p 10, Pa/K
γ	defined by Eq. 1.17, p 10
λ	length of wire from sensing thermojunction to chamber wall, p 10, μm

NOTATION (continued)

μ_w	chemical potential of water in a biological system containing liquid water, water vapour and solutes, p 4, J/mol
$\mu_w(0)$	μ_w value of pure free water at a pressure of 101,3 kPa and at the temperature of water in a biological system ($d\mu_w = \mu_w(0) - \mu_w$), p 4, J/mol
π	pi
Π	dewpoint cooling coefficient, p 14, μV
ρ_w	density of water at temperature T, Eq. 1.1, p 3, kg/m^3
σ	Stefan-Boltzmann constant = $5,6697 \times 10^{-8} W m^{-2} K^{-4}$, Eq. 1.13, p 8
ψ_w	general symbol for water potential, p 3, various units
$\psi_m, \psi_v, \psi_f, \psi_n$	water potential expressed per unit mass, volume, weight or amount of substance respectively, p 3, J/kg, J/m^3 , J/N, J/mol
Ω	wire resistivity, Eq. 1.18, p 10, Ωm
ΔT	$T - T_j$, Eq. 1.11, p 7, $^{\circ}C$

Chapter 2

Symbols used in this chapter but not listed here are to be found in the list for Chapter 1 or defined more fully in the text.

a, b, c,....	exponent values, Eq. 2.24, p 44
a_{th}, b_{th}	as for a and b, but theoretically calculated values, Section 2.4.2, p 38
c	defined by Eq. 7 of Campbell (1979), p 50
dV	zero offset voltage, Eq. 2.30, p 50, μV
D	deviation of calculated from measured quantity relative to the measured, Table 2.2, p 32, %
E_p	total error in measured psychrometric water potential, Eq. 2.29, p 45, %
$E_{p1}, E_{p2}, E_{p3}, E_{p4}$	subcomponent error in measured water potential where $E_p = (E_{p1}^2 + E_{p2}^2 + E_{p3}^2 + E_{p4}^2)^{\frac{1}{2}}$, Eq. 2.27, p 44

NOTATION (continued)

E_{p31}, E_{p32}	$E_{p3} = (E_{p31}^2 + E_{p32}^2)^{\frac{1}{2}}$, Eq. 2.30, p 50
f	$f = f(X^a, Y^b, Z^c, \dots)$ where X, Y, Z, \dots are quantities determining f and a, b, c, \dots are exponent values, Eq. 2.24, p 44
I	intercept of the linear regression of T vs $1/k_T$, Eq. 2.10, p 30, $^{\circ}\text{C}$
$k_T(c)$	calculated k_T value, Eq. 2.19, p 39, $\text{kPa}/\mu\text{V}$
$k_T(1), k_T(2), k_T(3), k_T(4)$	calculated k_T value according to models 1, 2, 3 and 4, p 33, $\text{kPa}/\mu\text{V}$
$k_{T_0}, k_{T_0(1)}, k_{T_0(2)}$	k_T value for $T = T_0, T_0(1), T_0(2)$ respectively, Section 2.4.2, $\text{kPa}/\mu\text{V}$
$k_{T_0}(\text{theory})$	theoretically calculated k_T value for $T = T_0$, Section 2.4.2, $\text{kPa}/\mu\text{V}$
M	a temperature dependent quantity, p 50
n	number of points
r	sample correlation coefficient; $r = 10^6 \times r_j$, Table 2.1, p 31, μm
\bar{R}	mean effective sensing thermojunction radius, Table 2.9, p 39, μm
S	slope of the linear regression of T vs $1/k_T$, Eq. 2.10, p 30, $^{\circ}\text{C} \mu\text{V}/\text{kPa}$
$SE, S_{y.x}$	standard error, standard error estimate of y on x
$t(n-1; 95\%)$	Students' t value for $n-1$ degrees of freedom and 95% level of confidence, Eq. 2.28, p 45
$\bar{T}, T_{\min}, T_{\max}$	average, minimum and maximum temperatures, p 42, $^{\circ}\text{C}$
$T_0, T_0(1), T_0(2)$	standard temperatures, $T_0 \approx 25^{\circ}\text{C}$, $T_0(1) < T_0 < T_0(2)$, p 42, $^{\circ}\text{C}$
V_{\max}	maximum voltage attained during sensing thermojunction cooling, Eq. 2.2, p 20, μV
V_T	$V(T_w)$, Eq. 2.2, p 20, μV
V_T'	V_T corrected for the voltage corresponding to $\psi_T = 0$ kPa , p 45, μV

NOTATION (continued)

X, Y	major and minor axis dimension for an elliptically shaped sensing thermojunction, p 38, μm
X, Y, Z, \dots	quantities determining f , p 44
$\sigma^2(f)$	variance of the mean value f , Eq. 2.24, p 44, where f may assume the value X, Y, Z, \dots (Eq. 2.24, p 44), ψ_T, S, I, V_T and T (Eq. 2.27, p 44)

Chapter 3

Symbols used in this chapter but not listed here are to be found in the list for Chapters 1 or 2 or are defined more fully in the text.

A, B	empirically determined constants, Eq. 3.14, p 65
E_d	total error in measured dewpoint water potential, Eq. 3.13, p 63, %
$E_{d1}, E_{d2}, E_{d3}, E_{d4}, E_{d5}$	subcomponent error in measured water potential where $E_d = (E_{d1}^2 + E_{d2}^2 + E_{d3}^2 + E_{d4}^2 + E_{d5}^2)^{\frac{1}{2}}$, Eq. 3.13, p 63
$E_{d31}, E_{d32}, E_{d33}$	$E_{d3} = (E_{d31}^2 + E_{d32}^2 + E_{d33}^2)^{\frac{1}{2}}$, Eq. 3.16, p 67
$R1, R2$	0 to 100 μV and 0 to 30 μV microvoltmeter range, Table 3.1, p 56
$S_d(c)$	calculated S_d value, Eq. 3.5, p 59, $\text{kPa}/\mu\text{V}$
$S_d(\text{theory}; T_0)$	theoretically calculated S_d value for $T = T_0$, Eq. 3.3, p 59
$V(T_{dp}); V_d$	dewpoint voltage, p 55, μV
$\Pi_0(T)$	dewpoint cooling coefficient Π at T_0 , Eq. 3.1, p 57, μV
$\sigma^2(V_d)$	variance of mean value $V_d (= V(T_{dp}))$, Eq. 3.11, p 64

Chapter 4

Symbols used in this chapter but not listed here are to be found in the list for Chapters 1, 2 and 3 or defined more fully in the text.

$f(V), f(x), f(\bar{x})$	a function of volume V , quantity x and mean value \bar{x}
--------------------------	--

NOTATION (continued)

n_s	total amount of solute substance, Eq. 4.2, p 72
P	balancing pressure, Eq. 4.2, p 72
RSD	relative saturation deficit, Eq. 4.4, p 72, %
V_o, V_e	original symplastic volume and total volume of sap expressed, respectively, Eq. 4.3, p 72
$\sigma^2(x)$	variance of quantity x , Table 4.2, p 79
$\psi(\text{osmotic})$	osmotic water potential, Eq. 4.1, p 72
Chapter 5	
R	volume ratio of lanolin to beeswax, p 99
SPC	Scholander pressure chamber measurement, Fig. 5.14, p 118, kPa
T_s	softening temperature of lanolin-beeswax mixture, p 99, °C
ψ_{PC}	pressure chamber water potential, Table 5.4, p 106, kPa
$\psi_{PSY}^{(CA)}$; $\psi_{PSY}^{(LA)}$; $\psi_{PSY}^W(CA)$; $\psi_{PSY}^W(LA)$	psychrometer water potential as measured using coarse abrasion, intensive light abrasion, coarse abrasion (but corrected for apparent "xylem tension relaxation"), and intensive light abrasion (corrected for "xylem tension relaxation") respectively, Table 5.4, p 106, kPa
ψ_{tot}	total leaf water potential, as calculated for pressure chamber measurements corrected for xylem sap water potential, Table 5.4, p 106, kPa

LIST OF TABLES

Table	Page
1.1 Values of some of the temperature dependent quantities of Eq. 1.22	11
1.2 The values of the temperature dependent terms defined in Eq. 1.23	12
1.3 Dewpoint hygrometer sensitivity $S_d(\text{theory})^{-1}$ as a function of temperature, as calculated from Eq. 1.25	15
2.1 Statistical data for the calibration curves of psychrometer no. 4 (where $1/k_T$ is the slope of the line)	31
2.2 Comparison between measured (for the calibration temperatures shown) and the values of k_T (kPa/ μ V) predicted from the four temperature correction models. The percentage deviations D(%) of calculated from measured values are shown	32
2.3 Statistical data for the T vs $1/k_T$ linear relationship and the associated a, b, k_{25} values for the various data sources (Table 2.2)	34
2.4 Measured k_T values (all with units kPa/ μ V) as a function of block temperature T ($^{\circ}$ C) for the four leaf psychrometers. The $k_T(\text{theory})$ values (kPa/ μ V) are presented for comparison and discussed in Section 2.4.2	34
2.5 Comparison between measured (for the calibration temperatures) and predicted k_T (kPa/ μ V) values for psychrometer no.4 using models 1, 2 and 3. The percentage D (%) of the calculated from the measured value (relative to the measured) is indicated. The data for the last four columns are discussed later (Section 2.4.2)	35
2.6 Mean and standard deviations of the percentage deviation between the measured reciprocal slope k_T and the predicted value, relative to k_T , for psychrometers nos 1 to 4, for the various models	35
2.7 $\sqrt{\sum D^2 / (n-1)}$ for the various data sets indicated and for the various models. Models 5 and 6 will be discussed later (Section 2.4.2)	37

LIST OF TABLES (continued)

Table		Page
2.8	The statistical data for the T vs $1/k_T$ linear relationship and the associated a , b , k_{25} values for the four leaf psychrometers	37
2.9	Measured (X , Y and r_w) and calculated mean effective (\bar{R}) dimensions for four leaf psychrometers	39
2.10	The theoretical $1/k_T$ (theory) ($dV/d\psi_V$) values as a function of temperature T (calculated using Eq. 1.22) for the four leaf psychrometers ($r_c = 2\,500\ \mu\text{m}$; $r_w = 12,5\ \mu\text{m}$ and $\lambda = 1\,000\ \mu\text{m}$), with $r_j = Y$ (Table 2.9)	40
2.11	The statistical data for the T vs $1/k_T$ (theory) linear relationship (where $15\ ^\circ\text{C} \leq T \leq 40\ ^\circ\text{C}$) and the associated a_{th} , b_{th} and k_{25} (theory) values for the four leaf hygrometers. The k_T (theory) values were calculated using Eq. 1.22 where $r_j = Y$ (Table 2.9)	40
2.12	Parameters associated with psychrometric error calculation, for a few psychrometers. The total error is calculated from 0 to $45\ ^\circ\text{C}$ for a zero offset of $0,5\ \mu\text{V}$ and a water potential of $-1\,250\ \text{kPa}$	47
2.13	Psychrometric error components (and subcomponents) for a few psychrometers, as a function of temperature (Eq. 2.27). A gap in the table implies a temperature independent error. A zero offset of $0,5\ \mu\text{V}$ is assumed	51
3.1	Comparison between the mean of four Π_0 values (in the body of the table with standard error values in brackets), measured at $25\ ^\circ\text{C}$, as a function of the 0 to 100 (R1) and 0 to 30 μV (R2) ranges and the stationary voltage output, for various hygrometers	56
3.2	Statistical data for the Π_0 vs T relationship for four leaf hygrometers	58
3.3	Statistical data for three leaf hygrometers. The calibration slopes for an ideal hygrometer is also shown together with the $k_T/S_d(T)$ ratio for each hygrometer, as a function of temperature	61
3.4	Comparison of the measured ($1/S_d(T)$) and the calculated ($1/S_d(c)$) calibration slopes at various temperatures for	

LIST OF TABLES (continued)

Table		Page
3.4 (cont)	three dewpoint hygrometers. Values of $S_d(c)$ are based on the measured slope at 24,8 °C. The error between the measured and calculated slopes (D) is relative to $S_d(T)$ at the particular temperature	61
3.5	Dewpoint hygrometer error components, subcomponents and k_T/S_d as a function of temperature (Eqs 3.9 to 3.16). A gap in the table implies a temperature independent error. A zero offset of 0,5 μV is assumed	64
3.6	Parameters associated with dewpoint error calculation, for a few hygrometers (Table 3.5)	66
4.1	Statistical data for the various psychrometer, pressure chamber and press water potential comparisons (Figs 4.2 to 4.4)	77
4.2	Statistical data for linear regressions of reciprocal total leaf water potential measurements (from the three instruments) on relative saturation deficit, RSD (> 25 %)	79
5.1	Relevant details from various literature sources on the use of <i>in situ</i> thermocouple leaf hygrometers for non-destructive measurement of water potential (X \equiv no; \checkmark \equiv yes). Some of the early workers enclosed entire leaves	84
5.2	Abrasion treatments used in this investigation	88
5.3	Comparison of citrus leaf water potential using thermocouple psychrometers (various abrasion treatments for units on the same leaf) and pressure chamber (mean values only from adjacent leaves)	91
5.4	Associated statistical parameters for the linear regression curves shown in Figs 5.8 and 5.9 (psychrometric vs pressure chamber measurements) and Fig. 5.10 (narrow aperture psychrometer measurements vs wide aperture) over leaf areas that were pretreated (light abrasion)	106
5.5	Comparison of total leaf water potential ψ_{tot} (kPa) and psychrometric measurements using the slope and intercept parameters of Table 5.4	106
5.6	Leaf excision details for the field measurements and the prevailing environmental climatic conditions	111

LIST OF TABLES (continued)

Table		Page
5.7	Associated statistical data for the pressure chamber-psychrometer curves shown in Figs 5.12 and 5.13	114
5.8	Water potential values (kPa) measured using psychrometric and pressure chamber methods and also values corrected for the time lapse (1 min) between psychrometer and pressure chamber measurements. Measurements were performed in the field under high atmospheric demand conditions using citrus plants	116

LIST OF FIGURES

Figure		Page
1.1	Cross-sectional view of a typical psychrometer. The block of the unit is usually of aluminium or teflon, in the case of leaf and soil psychrometers, respectively. The block temperature is measured in or close to the block	7
1.2	Diagram depicting the energy balance of a thermocouple psychrometer (Eq. 1.12)	9
2.1	Voltage output for an ideal thermocouple psychrometer for a cooling time of 20 s and $\psi_V = -1\ 757$ kPa ($T = 25\ ^\circ\text{C}$)	21
2.2	Chamber used by Brown & Collins (1980) for the calibration of soil psychrometers (also referred to as screen-caged psychrometers)	22
2.3	Actual thermocouple psychrometer output voltage as a function of time (20 s cooling time) and $\psi_V = -1\ 757$ kPa ($T = 25\ ^\circ\text{C}$)	24
2.4	Voltage output curves for psychrometer no. 1 for a cooling time of 20 s, $T = 25\ ^\circ\text{C}$ and (a) $\psi_V = -1\ 364$ kPa; (b) $\psi_V = -2\ 274$ kPa; (c) $\psi_V = -4\ 626$ kPa	26
2.5	Voltage output as a function of time for a wire mesh soil psychrometer (20 s cooling time) sealed above a salt solution with $\psi_V = -922$ kPa (at $25\ ^\circ\text{C}$)	27
2.6	Idealized relationship between V_T and ψ_T for $25\ ^\circ\text{C}$ and temperature T . A given ψ_T can result in a voltage V_T at temperature T and a voltage V_{25} at $25\ ^\circ\text{C}$	30
2.7	a_{th} , b_{th} ($^\circ\text{C}^{-1}$), and k_{25} (theory) ($\text{kPa}/\mu\text{V}$) as a function of the sensing thermocouple radius r_j (μm) over the temperature range 15 to $40\ ^\circ\text{C}$. In the indicated equations, $r = 10^6 \times r_j$, and R is the sample correlation coefficient	41
2.8	Block temperature T plotted against $-10^3 V_T'/\psi_T$ for psychrometer number 11 (which had the largest associated errors)	47
2.9	Calculated error, E_p , in measured water potential for the best (no. 7) and the worst (no. 1) psychrometers, as a function of temperature	49

LIST OF FIGURES (continued)

Figure		Page
3.1	Calculated error, E_d , in measured water potential for the best (no. 5A) and the worst (no. 2A) dewpoint hygrometers, as a function of temperature (cf. Fig. 2.9, p 49)	65
3.2	$k_T/S_d(T)$ as a function of $T - I$ for hygrometer no. 2	66
4.1	Diagrammatic representation of a soybean trifoliolate. The procedure for the leaf subsampling is indicated	74
4.2	Relationship between total leaf water potential measured using the pressure chamber against that measured using the thermocouple psychrometric technique	76
4.3	Relationship between total leaf water potential measured using the hydraulic press against that measured using the psychrometric technique	76
4.4	Relationship between total leaf water potential measured using the hydraulic press against that measured using the pressure chamber	77
4.5	Linear portion of a pressure volume curve as obtained using thermocouple psychrometers	79
4.6	Linear portion of a pressure volume curve as obtained using the pressure chamber	80
4.7	Linear portion of a pressure volume curve as obtained using the J-14 hydraulic press	80
5.1	Measured water potentials as a function of time after sealing for the no abrasion and intensive light abrasion treatments. Both psychrometers were mounted on the same leaf for these laboratory measurements	89
5.2	Voltage output curves for two psychrometers sealed on the same leaf. The output for (a) is for a no abrasion treatment and that for (b) a light abrasion	90
5.3	Voltage output curves for two psychrometers sealed on the same leaf. The output for (a) is for a light abrasion treatment and that for (b) a coarse abrasion	90
5.4	Voltage output curves for two psychrometers sealed on different leaves of the same citrus plant. Treatments used in both cases was an intensive light abrasion	90

LIST OF FIGURES (continued)

Plate		Page
5.1	Scanning electron micrographs for the various abrasion treatments (Table 5.2): (a) 500X, control treatment; (b) 2 000X, control treatment; (c) 500X, bud abrasion (30 s); (d) 2 000X, bud abrasion (30 s); (e) 500X, light abrasion (30 s); (f) 2 000X light abrasion (30 s); (g) 500X, light abrasion (60 s); (h) 2 000X, light abrasion (60 s); (i) 500X, coarse abrasion (30 s); (j) 2 000X, coarse abrasion (30 s)	92, 93
Figure		
5.5	(a) A partial cut-away of an <i>in situ</i> leaf psychrometer with thermal insulation and aluminium foil covering but without the aluminium foil covering the lead wire at the piston top (b) As in Fig. 5.5a, but with aluminium foil covering the lead wire at the piston top (c) Microvoltmeter top is covered with aluminium foil tape and the inside filled with polystyrene, the port-connector side covered with polystyrene and the microvoltmeter top is only slightly opened for switching and connecting (d) The rechargeable battery unit covered with aluminium foil tape	97, 98
5.6	Histogram plot of the percentage occurrence of the various psychrometer temperature gradients occurring in the field situation where block temperatures varied between 12 and 29 °C	103
5.7	Comparison between psychrometer (no abrasion) and pressure chamber measurements of citrus leaf water potential. Each point represents an average of 2 to 3 psychrometer measurements from the same plant and 3 pressure chamber measurements using neighbouring leaves (+ indicates wide aperture psychrometer measurements and o narrow)	104
5.8	Comparison between psychrometer (coarse abrasion) and pressure chamber measurements of citrus leaf water potential (2 to 3 measurements in each case, from the same plant)	104
5.9	Comparison between psychrometer (light abrasion) and pressure chamber measurements of citrus leaf water potential (2 to 3 three measurements in each case, from the same plant)	105

LIST OF FIGURES (continued)

Figure		Page
5.10	Comparison between psychrometer measurements (intensive light abrasion) using wide aperture unit and those using narrow aperture unit. Individual measurements were performed using the same leaf	105
5.11	The decrease in citrus leaf water potential following excision in the laboratory, as measured by pressure chamber(—) and psychrometric (----) techniques. Only one leaf was used in the case of psychrometric measurements and a different leaf for each pressure chamber measurement. All leaves were of nearly equal area and age and generally of the same colour, for these measurements	112
5.12	The relationship between pressure chamber and leaf psychrometer measurement for citrus leaves excised in the laboratory. Measurements were performed 2 to 200 min after petiole excision	113
5.13	The relationship between pressure chamber and predicted leaf psychrometer measurements (extrapolated to the same time as the former) for various citrus leaves excised in the field. Field measurements were usually within the first two minutes after excision	117
5.14	Field measured leaf water potential as a function of time after petiole excision for two leaves from the same citrus plant. The Scholander pressure chamber measurements (SPC) at 90 and 120 s are shown as well as the time predicted psychrometer measurements for these times, respectively	118
5.15	The decrease in citrus leaf water potential following field excision for leaf F and G (low evaporative demand conditions and from the same plant), leaf C (high evaporation) and leaf D and E (low evaporation and from the same plant)	119
5.16	The effect of continuously condensing and evaporating psychrometer chamber water on the measured water potential	121
5.17	Measured water potential as a function of time for three uncovered leaves excised under dark conditions. P indicates a petiole excision and M a midrib excision	122

Measurement of Water Potential Using Thermocouple Hygrometers

by

Michael J Savage

Supervisor: Dr Alfred Cass

Department of Soil Science and Agrometeorology, University of
Natal, Pietermaritzburg, South Africa 3201

Co-supervisor: Professor James M de Jager

Department of Agrometeorology, University of Orange Free State,
Bloemfontein, South Africa 9301

Theory predicts that the time dependent voltage curve of a thermocouple psychrometer where there is no change in output voltage with time during the evaporation cycle defines the wet bulb temperature T_w corresponding to the water potential. In practice, a change in voltage with time does occur and it is convenient to define the voltage corresponding to the water potential as the maximum point-of-inflection voltage.

A predictive model based on calibration data at a few temperatures is used to obtain the psychrometer calibration slope at any temperature. Use of this model indicates that psychrometers differ from each other and therefore must be individually calibrated if accuracy better than $\pm 5\%$ in the measurement of water potential is required. Dewpoint hygrometers are shown to be less temperature sensitive than psychrometers and have the added advantage of a voltage sensitivity nearly twice that of psychrometers, typically $-7,0 \times 10^{-3} \mu\text{V/kPa}$ compared to $-3,7 \times 10^{-3} \mu\text{V/kPa}$ at 25°C .

The accurate temperature correction of hygrometer calibration curve slopes is a necessity if field measurements are undertaken using either psychrometric or dewpoint techniques. In the case of thermocouple psychrometers, two temperature correction models are proposed, each based on measurement of the thermojunction radius and calculation of the theoretical voltage sensitivity to changes in water potential. The first model relies on calibration at a single temperature and

the second at two temperatures. Both these models were more accurate than the temperature correction models currently in use for four leaf psychrometers calibrated over a range of temperatures (15 to 38 °C). The model based on calibration at two temperatures is superior to that based on only one calibration. The model proposed for dewpoint hygrometers is similar to that for psychrometers. It is based on the theoretical voltage sensitivity to changes in water potential. Comparison with empirical data from three dewpoint hygrometers calibrated at four different temperatures indicates that these instruments need only be calibrated at, say 25 °C, if the calibration slopes are corrected for temperature.

A model is presented for the calculation of the error in measured thermocouple hygrometric water potential for individual hygrometers used in the dewpoint or psychrometric mode. The model is based on calculation of the relative standard error in measured thermocouple psychrometric water potential as a function of temperature. Sources of error in the psychrometric mode were in calibration of the instrument as a function of water potential and temperature and in voltage (due to electronic noise and zero offsets) and temperature measurement in the field. Total error increased as temperature decreased, approaching a value usually determined by the shape of the thermocouple junction, electronic noise (at low voltages less than 1 μV) and errors in temperature measurement. At higher temperatures, error was a combination of calibration errors, electronic noise and zero offset voltage. Field calibration data for a number of leaf psychrometers contained total errors that ranged between 6 (at 0 °C) and 2 % (at 45 °C) for the better psychrometers and between 11 (at 0 °C) and 5 % (at 45 °C) for the worst assuming that the zero offset was 0,5 μV . Zero offset values were less than 0,7 μV at all times. The dewpoint errors arose from calibration of the dewpoint hygrometer as a function of water potential, extrapolation of the calibration slope to other temperatures, setting the dewpoint coefficient and errors in voltage and temperature measurement. The total error also increased as temperature decreased, because of the differences in temperature sensitivity between dewpoint and psychrometric calibration constants. Consequently, the major source of error in the dewpoint mode arose from the difficulty in determining the dewpoint coefficient. This error, which is temperature dependent, contains three subcomponent

errors; the temperature dependence, random variation associated with determining the temperature dependence and error in setting the correct value. Calibration and extrapolation errors were smaller than those of the psychrometric technique. Typically, the error in a dewpoint measurement varied between about 6 and 2 % for the best hygrometer and between 10 and 3 % for the worst for temperatures between 0 and 45 °C respectively. At low temperatures, the dewpoint technique often has no advantage over the psychrometric technique, in terms of measurement errors.

In a comparative laboratory study, leaf water potentials were measured using the Scholander pressure chamber, psychrometers and hydraulic press. Newly mature trifoliates cut from field grown soybean (*Glycine max* (L) Merr. cv. Oribi) were turgidified and, after different degrees of dehydration, leaf water potential measured. One leaflet from the trifoliolate was used for the thermocouple psychrometer and another for the press while the central leaflet with its petiolule was retained for use in the pressure chamber. Significant correlations between measurements using these instruments were obtained but the slopes for hydraulic press vs psychrometer measurement curve and hydraulic press vs pressure chamber were 0,742 and 0,775 respectively. Plots of pressure-volume curves indicate that the point of incipient plasmolysis was the same (statistically) for the thermocouple psychrometer and the pressure chamber, but much larger for the hydraulic press. The above-mentioned differences between the three instruments emphasize the need for calibrating the endpoint defined using the press against one or more of the standard techniques, and, limiting the use of the press to one person.

Cuticular resistance to water vapour diffusion between the substomatal cavity and the sensing psychrometer junction is a problem unique to leaf psychrometry and dewpoint hygrometry; this resistance is not encountered in soil or solution psychrometry. The cuticular resistance may introduce error in the leaf water potential measurement. The effect of abraiding the cuticle of *Citrus jambhiri* to reduce its resistance, on the measured leaf water potential was investigated. Psychrometric measurements of leaf water potential were compared with simultaneous measurements on nearby leaves using the Scholander pressure chamber, in a field situation. Leaf surface damage, due to abrasion, was investigated using scanning electron microscopy.

Thermocouple psychrometers are the only instruments which can measure the *in situ* water potential of intact leaves, and which may be suitable for continuous, non-destructive monitoring of water potential. Unfortunately, their usefulness is limited by a number of difficulties, among them fluctuating temperatures and temperature gradients within the psychrometer, sealing of the psychrometer chamber to the leaf, shading of the leaf by the psychrometer and resistance to water vapour diffusion by the cuticle when the stomates are closed. Using *Citrus jambhiri*, several psychrometer designs and operational modifications were tested. *In situ* psychrometric measurements compared favourably with simultaneous Scholander pressure chamber measurements on neighbouring leaves, corrected for the osmotic potential and the apparent effect of "xylem tension relaxation" following petiole excision.

It is generally assumed that enclosure of a leaf by an *in situ* thermocouple psychrometer substantially modifies the leaf environment, possibly altering leaf water potential, the quantity to be measured. Furthermore, the time response of leaf psychrometers to sudden leaf water potential changes has not been tested under field conditions. In a laboratory investigation, we found good linear correlation between *in situ* leaf psychrometer (sealed over abraded area) and Scholander pressure chamber measurements (using adjacent leaves) of leaf water potential, 2 to 200 minutes after excision of citrus leaves. A field investigation involved psychrometric measurement prior to petiole excision, and 1 min after excision, simultaneous pressure chamber measurements on adjacent citrus leaves immediately prior to the time of excision and then on the psychrometer leaf about 2 min after excision. Statistical comparisons indicated that within the first two minutes after excision, psychrometer measurements compared favourably with pressure chamber measurements. There was no evidence for a psychrometer leaf water potential time lag. For the high evaporative demand conditions, water potential decreased after excision by as much as 700 kPa in the first minute. Psychrometer field measurements indicated that within the first 5 min of leaf petiole excision, the decrease in leaf water potential with time was linear but that within the first 15 s, there was a temporary increase of the order of a few tens of kilopascal.

The thermocouple psychrometer can be used to measure dynamic changes in leaf water potential non-destructively, with an accuracy that compares favourably with that of the pressure chamber.

Using *in situ* thermocouple leaf hygrometers (dewpoint and psychrometric techniques employed) attached to *Citrus jambhiri* leaves, an increase in measured water potential immediately following petiole excision was observed. The increase ranged between 20 to 80 kPa and occurred 30 s after petiole excision and 100 s after midrib excisions. No relationship between the actual leaf water potential and the increase in water potential due to excision, was found.

INTRODUCTION

During the past decade, water potential has gained wide acceptance as a fundamental measure of plant water status (Hsiao, 1973). This wide acceptance is of theoretical and practical nature. Under isothermal conditions, water potential measurements can be used to predict the direction of water movement in the soil, plant or atmosphere. If liquid and vapour conductivities in this system are known, rates of water movement can be predicted and *vice versa* (Milburn, 1979). Water stress of plants may be inferred from measurements of water potential, as it appears to be most closely related to physiological and biochemical processes which control plant growth (Kramer, 1969; Begg & Turner, 1976; Milburn, 1979; Turner & Begg, 1981). Other methods of inferring plant water potentials are possible. However, as Kramer (1972) points out, assumptions concerning plant water stress based on measurements of soil water stress or rate of evaporation can sometimes be very misleading. He maintains that the only reliable indicators of plant water stress are measurements on the plants themselves, as they integrate all internal and external factors determining the amount of stress at a particular time. Such a measure is plant or leaf water potential.

The water relations of pasture plants have been discussed by Brown (1977) and Redmann (1976) and their responses to water deficits by Turner & Begg (1978) and Hsiao (1973). Water relations are affected by and affect many agricultural practices and occurrences: influence of water on microbial decomposition of crop residues (Myrold, Elliott, Papendick & Campbell, 1981); microbial growth and development of plant disease (Cook & Papendick, 1978); movement of soil organisms, effects of soil water relations on gaseous and solute diffusion (Papendick & Campbell, 1980); the effect of fire and the fire regime on grassland plant water relations (Savage, 1980; Savage & Vermeulen, 1983); drought responses of crops (Sojka, Stolzy & Fischer, 1979) being a few examples.

The principle of thermocouple psychrometry was described by Hill (1930) and Spanner (1951) showed that it was possible to measure water potential using a thermocouple in vapour pressure equilibrium with a leaf sample (psychrometric method). The use of an alternative technique that uses the same thermocouple hygrometer, the dew-point technique, is relatively new, being first proposed by Neumann &

Thurtell (1972), and modified by Campbell, Campbell & Barlow (1973). The psychrometric and dewpoint methods appear to compare although no field use comparisons have apparently been attempted. There is some evidence indicating that the dewpoint method results in water potential measured under isopiestic conditions (Durand-Campero, 1981).

Thermocouple hygrometers have been used for many applications: the inflammability of pasture material may be measured using psychrometers (Brown, 1970); Wiebe (1981) and Wiebe, Kidambi, Richardson & Ernstrom (1981) measured water potentials ranging from free water to oven dryness; Brown (1972) determined leaf osmotic potential using psychrometers and Oosterhuis (1981) used these instruments to investigate osmotic adjustment (Turner & Jones, 1980) in cotton roots and leaves; water relations of mine dumps and snow packs (van Haveren, 1972) have been investigated; Walker, Oosterhuis & Savage (1983) used these instruments in a field program to measure total and osmotic water potential of winter wheat; they have also been used to measure water potential in trees (Wiebe, Brown, Daniel & Campbell, 1970; Wiebe, Campbell, Gardner, Rawlins, Cary & Brown, 1971), stems (Michel, 1977), roots (Nnyamah & Black, 1977; Nnyamah, Black & Tan, 1978), and leaves (Campbell & Campbell, 1974).

The objectives of this study are:

1. to investigate the proper calibration, measurement accuracy and use of thermocouple hygrometers;
2. to compare the measurement of water potential using the psychrometric technique against other commonly accepted methods;
3. to investigate the use (accuracy and time response) of thermocouple psychrometers for the measurement of leaf potential non-destructively in a field situation.

CHAPTER 1

THEORY OF THERMOCOUPLE HYGROMETERS

1.1 WATER POTENTIAL

1.1.1 Introduction

The term "water potential" is often used ambiguously in the international literature. The potential of water is the amount of useful work per unit quantity of water done by means of externally applied forces in transferring, reversibly and isothermally, an infinitesimal amount of water from a standard reference state to the soil, plant or atmosphere system under consideration. The reference state chosen is usually pure free water at the same temperature as the water in the system and at a pressure of one standard atmosphere; that is, 101,3 kPa (adapted from Taylor & Ashcroft, 1972, p 153 and Bolt *et al.*, 1975). The unit of work in the International System of Units (SI) is the joule, abbreviated J. The general symbol ψ_w is often used for water potential. However, because the quantity of water may be expressed as mass, volume, weight or amount of substance, it follows that the units of water potential may be J/kg, J/m³, J/N or J/mol, distinguished by the symbols ψ_m , ψ_v , ψ_f or ψ_n respectively (Savage 1978, 1979; Rose, 1979). These quantities may be converted as follows:

$$\rho_w \psi_m = \psi_v = \rho_w g \psi_f = \psi_n / \bar{V}_w, \quad 1.1$$

where ρ_w (kg/m³) is the density of liquid water where $\rho_w = \rho_w(T)$, T (°C) being the water temperature, g (m/s²) the acceleration of gravity, and \bar{V}_w (m³/mol) the partial molar volume of water. A more detailed analysis of the relationships between ψ_m , ψ_v and ψ_f is given by Rose (1979) (who omitted ψ_n). For present purposes, only ψ_m and ψ_v will be used.

In the obsolete centimetre, gram and second system of units (cgs), it was often assumed that $\rho_w = 1$ g/cm³ irrespective of temperature so that ψ_m and ψ_v were often assumed to be one and the same quantity. For example, Meidner & Sheriff (1976, p 10, 138) use the unit J/kg and 10⁻² bar interchangeably; Taylor & Ashcroft

(1972, p 159) add ψ_m and ψ_v terms. It is essential to adopt a more disciplined approach to the use of units and to pay attention to the effect of temperature on certain so-called "constants".

1.1.2 Thermodynamic theory of water potential

In essence, hygrometers may be regarded as systems containing solutes, liquid and vapour enclosed in a sealed cavity that can be maintained at constant temperature and pressure. The chemical potential μ_w (J/mol) of water in a biological system containing liquid water, water vapour and solutes, relative to that at a reference position, $\mu_w(0)$, is given by (Babcock, 1963):

$$\begin{aligned} \mu_w - \mu_w(0) = d\mu_w = & -\bar{S}_w dT + \bar{V}_w dP + \sum_j \bar{Y}_j dX_j \\ & + \sum_k \left(\frac{\partial \mu_w}{\partial n_k} \right)_{T, P, X_j, n_{\ell} (\ell \neq k)} dn_k, \end{aligned} \quad 1.2$$

where $\mu_w(0)$ is defined as the chemical potential of pure free water at a pressure of 101,3 kPa and at the same temperature as the water in the biological system. Symbols are defined in the NOTATION. For these isothermal conditions, Eq. 1.2 becomes

$$\mu_w - \mu_w(0) = \bar{V}_w dP + \sum_j \bar{Y}_j dX_j + \sum_k \left(\frac{\partial \mu_w}{\partial n_k} \right)_{T, P, X_j, n_{\ell} (\ell \neq k)} dn_k, \quad 1.3$$

$$\psi_m = \{ \mu_w - \mu_w(0) \} / \bar{M}_w, \quad 1.4$$

$$\psi_v = \{ \mu_w - \mu_w(0) \} / \bar{V}_w, \quad 1.5$$

$$\psi_f = \{ \mu_w - \mu_w(0) \} / \bar{M}_w g, \quad 1.6$$

and $\psi_n = \mu_w - \mu_w(0)$,

where \bar{M}_w (kg/mol) is the molecular mass of water, $\rho_w = \bar{M}_w / \bar{V}_w$, X is an extensive parameter and Y an intensive parameter that account for forms of work other than that due to changes of pressure, temperature and chemical composition, where $Y_j dX_j$ is the j th

work term (Bolt & Frissel, 1960).

Consider water vapour (which is one component of a vapour phase) behaving as an ideal gas. Combining the universal gas law equation ($e\bar{V}_w = RT$), Eqs 1.3 and 1.5, and integrating, we get the Kelvin equation:

$$\psi_v = (RT/\bar{V}_w) \ln e/e_0. \quad 1.7$$

It has been assumed that isothermal conditions prevail during the change in pressure from e_0 to e and that $e > 0$ kPa.

1.1.3 Components of water potential

Under isothermal conditions, three terms emerge from the thermodynamic theory as being components of $\psi_v \bar{V}_w$ (Eqs 1.1 and 1.3):

$$\psi_v \bar{V}_w = \bar{V}_w dP + \sum_j Y_j dX_j + \sum_k \left(\frac{\partial \mu_w}{\partial n_k} \right)_{T,P,X_j,n_\ell(\ell \neq k)} dn_k. \quad 1.8$$

Applying Eq. 1.8 under conditions of constant pressure and in the absence of any work fields, ψ_v becomes a function of composition and concentration only:

$$\psi_v \bar{V}_w = \sum_k \left(\frac{\partial \mu_w}{\partial n_k} \right)_{T,P,X_j,n_\ell(\ell \neq k)} dn_k. \quad 1.9$$

Combining Eqs 1.7 and 1.9 and considering a solution containing only one solute, say NaCl, we get:

$$\psi_v = (RT/\bar{V}_w) \ln e/e_0 = \frac{1}{\bar{V}_w} \left(\frac{\partial \mu_w}{\partial n_{\text{NaCl}}} \right)_{T,P,X_j}. \quad 1.10$$

Thermocouple hygrometers are instruments capable of measuring T and either the wet bulb temperature T_w or the dewpoint temperature T_{dp} , enabling e/e_0 to be calculated. Hence Eq. 1.10 provides a convenient method of calibrating these instruments with respect to ψ_v for a closed system containing only a solution of NaCl or some other strong electrolyte. A range of ψ_v is obtained

by varying dn_{NaCl} . The ψ_m (J/kg) values for NaCl and KCl solutions have been published by Lang (1967) and Campbell & Gardner (1971) respectively. Conversion to other units is possible (Eqs 1.3 to 1.6).

1.2 THERMOCOUPLE HYGROMETERS

1.2.1 Introduction

A thermocouple hygrometer operating in the psychrometric mode enables measurement of the dry (T) and wet bulb (T_w) temperature difference while the dewpoint mode enables measurement of the dry bulb and dewpoint (T_{dp}) temperature difference. These operational modes use the same sensor but different voltmeter circuitry. Both modes allow measurement of the water potential of solutions, soils and biological materials by applying the theory discussed in Section 1.1.

1.2.2 Thermocouple psychrometers

1.2.2.1 *Mechanics of the psychrometric technique*

Spanner (1951) developed a vapour phase method for measuring water potential using a Peltier-cooled thermocouple psychrometer that senses the relative humidity (e/e_0) of a chamber containing leaf tissue. Applying the Kelvin equation (Eq. 1.7), ψ_v for the leaf may then be determined.

According to the Peltier effect, when a current is passed through a thermocouple circuit, one junction liberates heat energy to the surroundings while the other absorbs heat energy. Reversal of the current direction results in a reversal of the heating and cooling effects. The sensing junction shown in Fig. 1.1 is cooled, and the reference junctions are heated by the passage of an electric current of 4 to 8 mA in a certain current direction. The heat absorbed by the reference junctions is rapidly dissipated because of the relatively large mass and high thermal conductivity of the copper pins (Campbell & Campbell, 1974) contained within the relatively massive block of the thermocouple hygrometer (Fig. 1.1).

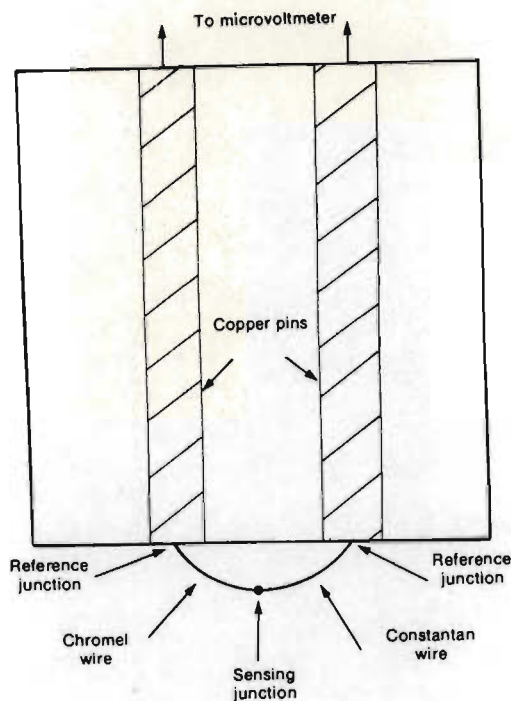


FIG. 1.1 Cross-sectional view of a typical psychrometer. The block of the unit is usually aluminium or teflon, in the case of leaf and soil psychrometers, respectively. The block temperature is measured in or close to the block

The sensing thermocouple junction is located immediately above the leaf, soil or moisture sample enclosed in a cavity of dimensions that depend on hygrometer type. Water vapour in the sealed cavity rapidly reaches energy equilibrium with the sample (Millar, 1974). When the sensing junction is cooled to below the dewpoint temperature of the air, water will condense onto the sensing junction. If the cooling current is terminated, the enclosed air and thermojunction will return to the temperature of the metal block. When the wet bulb temperature is reached, water will evaporate causing slight cooling of the sensing junction during return to the temperature of the metal block. The difference between the reference temperature (T) and sensing junction temperature (T_j), ΔT , results in an output voltage V (μV) (the Seebeck effect) given by

$$V = S(T - T_j) = S \cdot \Delta T, \quad 1.11$$

where S ($\mu V/K$), the chromel-constantan thermocouple voltage sensi-

tivity to temperature, is temperature dependent (Table 1.1, p 11). In this discussion, it has been assumed that the block temperature T is the same as the reference junction temperature (Fig. 1.1).

1.2.2.2 Energy balance of a thermocouple psychrometer

The relationship between the thermojunction temperature relative to the psychrometer, ΔT , and the Peltier cooling current I can be obtained by invoking a thermal energy balance for the junction and solving for ΔT . Following Rawlins (1966) and Peck (1968), the energy balance is expressed by the equation {influx of junction heat energy = outflux of junction heat energy} (Fig. 1.2) with unit J/s or W:

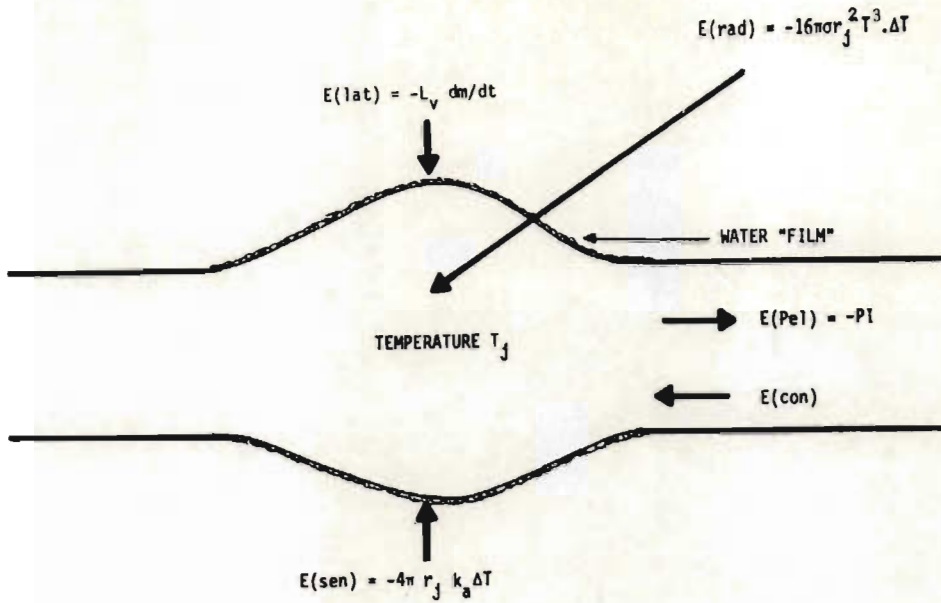
$$E(\text{rad}) + E(\text{sen}) + E(\text{con}) + E(\text{lat}) + E(\text{Pel}) = C d(\Delta T)/dt \quad 1.12$$

where $E(\text{rad})$ is the rate of energy transfer to the junction by radiation from the walls of the chamber, $E(\text{sen})$ is the rate of sensible heat energy transfer from the air to the thermojunction, $E(\text{con})$ is the rate at which heat energy (W) is conducted to the thermojunction along the wires, $E(\text{lat})$ is the rate at which latent heat energy is transferred to the junction, and $E(\text{Pel}) = -PI$ where P is the Peltier coefficient (V) for the thermojunction and I is the Peltier cooling current (A). The negative sign is present because for a certain current direction, the thermojunction is being cooled by the Peltier effect. That is, during condensation $E(\text{lat}) < 0$ and during evaporation $E(\text{lat}) > 0$ and $I = 0$ mA. C (J/K) is the junction heat capacity and t is time (s). Each of the terms of Eq. 1.12 will be discussed.

Radiant heat energy transfer to the junction, $E(\text{rad})$: Assuming that the chamber walls are concentric with the assumed spherical thermojunction and that the emissivities of the junction surface and the chamber walls are equal, we obtain

$$E(\text{rad}) = -16\pi\sigma r_j^2 T^3 \Delta T \quad 1.13$$

where σ is the Stefan-Boltzmann constant, ($5,6697 \times 10^{-8} \text{ W m}^{-2} \text{ K}^{-4}$) and r_j is the radius of the spherical thermojunction (Rawlins, 1966).



$$E(\text{rad}) + E(\text{sen}) + E(\text{con}) + E(\text{lat}) + E(\text{Pel}) = C \frac{d(\Delta T)}{dt}$$

FIG. 1.2 Diagram depicting the energy balance of a thermocouple psychrometer (Eq. 1.12)

Since the thermojunction will have a much smaller emissivity when dry compared to when wet, Eq. 1.13 is oversimplified. In all cases though, $E(\text{rad})$ is less than 1% of any of the other energy balance terms (Baughn, 1974).

Sensible heat energy transfer from the air to the junction, $E(\text{sen})$: Following Rawlins (1966) and Peck (1968), we assume that $E(\text{sen})$ consists entirely of molecular conduction between the assumed spherical chamber and concentric spherical junction:

$$E(\text{sen}) = -4\pi r_j k_a \Delta T, \quad 1.14$$

where k_a is the thermal conductivity of air ($\text{W m}^{-1} \text{K}^{-1}$). Spanner (1951) assumed that both $E(\text{sen})$ and $E(\text{rad})$ were negligibly small.

Heat energy transfer by conduction through the wires, $E(\text{con})$: Peck (1968) determined the temperature distribution as a function of distance x away from the thermojunction. It is possible to determine the temperature gradient for $x = 0$:

$$E(\text{con}) = \frac{-2B}{\gamma \sinh \gamma \lambda} \{(\Delta T - G/\gamma^2) \cosh \gamma \lambda + G/\gamma^2\}, \quad 1.15$$

$$\text{where } B = 8\pi r_w \sigma T^3 + 2\pi k_a / (\ln r_c - \ln r_w), \quad 1.16$$

$$\gamma = (B/\pi r_w^2 k_w)^{\frac{1}{2}}, \quad 1.17$$

$$G = \Omega I^2 / \pi^2 r_w^4 k_w, \quad 1.18$$

λ is the length of wire (m) from the junction to the wall, r_w the radius of the wire (m), r_c the radius of the thermocouple chamber (m), k_w the thermal conductivity of the wire ($\text{W m}^{-1}\text{K}^{-1}$), and Ω the resistivity of the wire ($\Omega \text{ m}$) (Rawlins, 1966).

It has been assumed that Ω , r_w , k_w and λ are the same on either side of the thermojunction and that at the chamber wall $\Delta T = 0$ °C but at the junction $\Delta T = T - T_j$ (Peck, 1969).

Latent heat energy transfer, $E(\text{lat})$: This component of the energy balance equation is a function of the evaporation rate, dm/dt (kg/s) where $E(\text{lat}) = -L_v dm/dt$ and L_v is the specific latent heat of vapourization (J/kg). Peck (1968) provides a theoretical base for expressing latent heat energy transfer:

$$E(\text{lat}) = - \frac{4\pi r_j L_v D_v \rho_v}{e_o} (e_o \bar{v}_w \psi_v / RT + \beta \Delta T), \quad 1.19$$

where the symbols are defined in the NOTATION.

Energy transfer due to Peltier cooling, $E(\text{Pel})$: It can be shown that (Zemansky, 1957, p 301):

$$E(\text{Pel}) = -PI, \quad 1.20$$

where I is the cooling current (A) and P is the Peltier cooling coefficient (V), given by $P = T dV/dT$.

Derivation of junction temperature: Combining Eqs 1.12, 1.13, 1.14, 1.15, 1.19 and 1.20 and assuming that the junction temperature responds extremely rapidly to changes in any of the energy balance components (so that $d(\Delta T)/dt = 0$), we get:

$$-16\pi\sigma_j^2 T^3 \cdot \Delta T - 4\pi r_j k_a \cdot \Delta T - \frac{2B}{\gamma \sinh \gamma\lambda} \{(\Delta T - G/\gamma^2) \cosh \gamma\lambda + G/\gamma^2\} \\ - \frac{4\pi r_j L_v D_v \rho_v}{e_0} \{e_0 \bar{V}_w \psi_v / RT + \beta \cdot \Delta T\} - PI = 0.$$

Therefore, solving for ΔT :

$$\Delta T = \frac{\frac{2BG}{\gamma^3} \{\coth \gamma\lambda - \operatorname{cosec} \gamma\lambda\} - 4\pi r_j L_v D_v \rho_v \bar{V}_w \psi_v / RT - PI}{16\pi\sigma_j^2 T^3 + 4\pi r_j k_a + \frac{2B}{\gamma} \coth \gamma\lambda + 4\pi r_j L_v D_v \rho_v \beta / e_0} \quad 1.21$$

During the condensation phase the above expression holds but during the evaporation phase $I = 0$ and $\Delta T = T_j - T < 0$ °C.

Junction temperature as a function of ψ_v : During the evaporation phase, $G = I = 0$ (numerically) and since $V = S \cdot \Delta T$ (Eq. 1.11), we obtain an expression for the theoretical psychrometric calibration constant, $1/k_T(\text{theory}) = dV(T_w)/d\psi_v$, where

$$dV(T_w)/d\psi_v = \frac{-4\pi r_j S L_v D_v \rho_v \bar{V}_w / RT}{16\pi\sigma_j^2 T^3 + 4\pi r_j k_a + \frac{2B}{\gamma} \coth \gamma\lambda + 4\pi r_j L_v D_v \rho_v \beta / e_0} \quad 1.22$$

The quantities $S, L_v, D_v, \rho_v, \bar{V}_w, k_a, B, \gamma, \beta$ and e_0 are all temperature dependent and for this reason it is necessary to evaluate the right hand side of Eq. 1.22 as a function of temperature (Table 1.1).

TABLE 1.1 Values of some of the temperature dependent quantities of Eq. 1.22

Quantity	T	T	S	L_v	$\rho_v \times 10^5$	ρ_v	$\bar{V}_w \times 10^6$	k_a	B	e_0
Unit	°C	K	$\mu\text{V/K}$	kJ/kg	m^2/s	g/m^3	m^3/mol	$\text{mW m}^{-1} \text{K}^{-1}$	Pa/K	kPa
Reference †:	5	2	2	3	4	2	2	1
	0	273,15	58,62	2501	2,12	4,85	18,02	24,3	45	0,611
	5	278,15	59,06	2489	2,20	6,80	18,02	24,6	61	0,872
	10	283,15	59,49	2477	2,27	9,41	18,02	25,0	83	1,227
	15	288,15	59,91	2465	2,34	12,83	18,03	25,3	110	1,704
	20	293,15	60,34	2454	2,42	17,30	18,05	25,7	145	2,337
	25	298,15	60,77	2442	2,49	23,04	18,07	26,0	189	3,167
	30	303,15	61,20	2430	2,57	30,35	18,09	26,4	244	4,243
	35	308,15	61,63	2418	2,64	39,6	18,12	26,7	312	5,624
	40	313,15	62,06	2406	2,72	51,1	18,16	27,0	394	7,378
	45	318,15	62,48	2394	2,80	65,6	18,19	27,4	494	9,585

† Reference : 1. List (1951) 2. Monteith (1973) 3. Rawlins (1966) 4. van Kaveren & Brown (1972)
5. Weast (1978) (adapted from)

1.2.2.3 Temperature dependence of $k_T(\text{theory})$

Most of the parameters on the right hand side of Eq. 1.22 are temperature dependent and hence $k_T(\text{theory})$ will be dependent on the block temperature T . Also, each term of the right hand side of Eq. 1.22 contains at least one quantity which is dependent on the geometry of the thermojunction and cavity. Eq. 1.22 may be written in the simplified form:

$$1/k_T(\text{theory}) = dV(T_w)/d\psi_V = \frac{\text{Term}(1)}{\text{Term}(2) + \text{Term}(3) + \text{Term}(4) + \text{Term}(5)} \quad 1.23$$

Using values from Table 1.1 and r_j , r_c , r_w and λ values of 95; 2 500; 12,5 and 4 300 μm respectively (Scotter, 1972), each of the terms of Eq. 1.23 were evaluated and $k_T(\text{theory})^{-1}$ determined as a function of temperature (Table 1.2). In performing these calculations, spherical symmetry has been assumed for both thermojunction and its cavity. Generally the lack of spherical symmetry can be expected to introduce deviation between theoretical and measured performance (Baughn, 1974).

Wiebe *et al.* (1970) used an empirical equation for correcting V (μV) corresponding to a particular ψ_V and block temperature T ($^{\circ}\text{C}$) to V_{25} , the output voltage at 25 $^{\circ}\text{C}$:

$$V_{25} = V/(a + bT) \quad 1.24$$

where the basic assumption was that V is linearly related to T for

TABLE 1.2 The values[†] of the temperature dependent terms defined in Eq. 1.23

Temperature T ($^{\circ}\text{C}$)	Term(1) $\times 10^{10}$ ($\mu\text{V K}^{-1}\text{m}^{-3}\text{s}^{-1}$)	Term(2) $\times 10^5$ (W/K)	Term(3) $\times 10^5$ (W/K)	Term(4) $\times 10^5$ (W/K)	Term(5) $\times 10^5$ (W/K)	$10^3/k_T(\text{theory})$ ($\mu\text{V/kPa}$)
0	-1,42790	0,05242	2,90095	3,46325	2,26098	-1,646
5	-2,04566	0,05535	2,93676	3,48550	3,10959	-2,134
10	-2,87628	0,05839	2,98451	3,51458	4,27276	-2,656
15	-3,98331	0,06154	3,02033	3,53659	5,70317	-3,233
20	-5,48070	0,06480	3,06808	3,56535	7,60990	-3,830
25	-7,40880	0,06817	3,10389	3,58714	9,98101	-4,426
30	-9,93890	0,07166	3,15165	3,61559	13,01213	-5,007
35	-13,15380	0,07526	3,18746	3,63717	16,74165	-5,564
40	-17,28098	0,07898	3,22327	3,65866	21,31947	-6,111
45	-22,54623	0,08283	3,27103	3,68670	27,05542	-6,613

[†] The calculated values have been rounded off

a given ψ_v . The a and b values were determined by measuring the corresponding output voltage of a 0,5 mol/kg KCl solution (Meyn & White, 1972) at several temperatures between 4 and 25 °C (Wiebe *et al.*, 1970). Brown (1970) found $a = 0,325$ and $b = 0,027$ (°C)⁻¹. At present, the most common procedure is to calibrate the psychrometer at a temperature near 25 °C and then convert measured voltages at field temperatures to the value at 25 °C using Eq. 1.24 with $a = 0,350$ and $b = 0,026$ (°C)⁻¹ (Wiebe *et al.*, 1970). The (near) 25 °C calibration curve is then used to obtain ψ_{25} , the volumetric water potential at 25 °C. From the data of Meyn & White (1972), k_T is a linear function of temperature T but Wheeler (1972) found that this was not the case for his empirical data. Extensive regression analysis of Wheeler's data was avoided through the use of graphical calibration curves. Wheeler, Qashu & Evans (1972) further state: "the temperature dependence of the psychrometers are themselves temperature dependent and a single bivariate equation could not be fitted to the calibration data". This aspect will be discussed in more detail in Chapter 2.

1.2.3 Dewpoint hygrometers

1.2.3.1 *Mechanics of dewpoint hygrometers*

Neumann & Thurtell (1972) were the first to introduce a technique for measuring the dewpoint temperature depression in a small sealed cavity adjacent to a leaf surface. These authors showed that e/e_0 can be calculated by measurement of the dewpoint temperature T_{dp} and the system temperature T ; hence the Kelvin equation (Eq. 1.7) may be applied to determine ψ_v .

Consider a hypothetical thermojunction whose temperature is determined only by latent heat energy transfer; that is, only by evaporation and condensation. If the junction is covered with water and at a temperature $T_j > T_{dp}$, then water will evaporate from the junction until $T_j = T_{dp}$. If $T_j < T_{dp}$, then water will condense onto the junction, again until $T_j = T_{dp}$. If heat energy transfer is via latent heat only, then the junction temperature will always converge on T_{dp} (Campbell *et al.*, 1973). Measurements by this technique are relatively independent of the wetting characteristics of the junction, and the size and shape of the

water droplet formed on the junction (Nnyamah & Black, 1977).

Campbell *et al.* (1973) point out: "under practical conditions, it is not possible for a thermocouple junction to be independent of heat transfer mechanisms which exist in ordinary environments ... During the measurement the wet junction temperature will always be below the temperature of its surroundings so heat (energy) will flow from the surroundings to the junction. Using Peltier cooling, a counter flow can be created and adjusted electrically to exactly balance the heat inflow for a net transfer of zero. If this condition is set up on a dry thermocouple to balance all heat transfer other than condensing or evaporating water, then when the junction is wet its temperature will converge on the dewpoint just as in the hypothetical example".

For a small current I flowing through a thermoelectric circuit, the rate of energy transfer is $-PI$, namely $E(PeI)$. For a larger current, Joule heating becomes significant so that the rate of heat energy transfer is now $-PI + I^2R$ where R is the electrical resistance of the thermojunction and neighbouring thermocouple lead wires. The Joule heating offsets the Peltier cooling and the temperature depression via Peltier cooling alone will be reduced. The cooling coefficient Π of a given hygrometer is defined then as the differential voltage which results from a specified cooling current passing through the thermojunction.

1.2.3.2 Energy balance of dewpoint hygrometers

If the thermojunction is held at the dewpoint temperature then the energy balance equation (Eq. 1.12) reduces to $E(lat) = 0$ and hence from Eq. 1.19, where now $\Delta T = T - T_{dp}$,

$$-\frac{4\pi r_j L_v D_v \rho_v}{e_0} (e_0 \bar{V}_w \psi_v / RT + \beta \Delta T) = 0.$$

This equation provides an expression for the theoretical dewpoint calibration constant $S_d(\text{theory})$ where:

$$1/S_d(\text{theory}) = dV(T_{dp})/d\psi_v = -Se_0 \bar{V}_w / RT\beta. \quad 1.25$$

Theory therefore predicts that $S_d(\text{theory})$ is independent of the wetting characteristics of the junction, and the size and shape of the water droplet formed on the junction but is temperature dependent. Using values from Table 1.1, $S_d(\text{theory})^{-1}$ was calculated as a function of temperature (Table 1.3). One advantage of using dewpoint hygrometers is the greater voltage sensitivity for a given water potential compared to the psychrometer (Tables 1.2 and 1.3). For example, $S_d(\text{theory})^{-1}$ is more than double $k_T(\text{theory})^{-1}$ at 15 °C.

TABLE 1.3 Dewpoint hygrometer sensitivity $S_d(\text{theory})^{-1}$ as a function of temperature, as calculated from Eq. 1.25

$T(^{\circ}\text{C})$	0	5	10	15	20	25
$10^3/S_d(\text{theory})$ ($\mu\text{V}/\text{kPa}$)	-6,315	-6,579	-6,732	-6,984	-7,202	-7,423
$T(^{\circ}\text{C})$	30	35	40	45		
$10^3/S_d(\text{theory})$ ($\mu\text{V}/\text{kPa}$)	-7,638	-7,857	-8,106	-8,336		

Campbell *et al.* (1973) showed that, for a wet thermojunction being cooled by the passage of a cooling current with $V = V(T_{dp})$,

$$\frac{dV}{d\psi_V} = \frac{-4\pi r_j S L_V D_V \rho_V \bar{V}_W / RT}{(1-D\Pi)(16\pi\sigma r_j^2 T^3 + 4\pi r_j k_a + \frac{2B}{\gamma} \coth \gamma\lambda) + 4\pi r_j L_V D_V \rho_V \beta / e_0}, \quad 1.26$$

where Π is the cooling coefficient (μV) of the thermocouple, and D is the dewpoint gain (μV^{-1}) of the microvoltmeter. D , a property of the microvoltmeter setting, determines the mode of operation of the hygrometer. When $D = 0 \mu\text{V}^{-1}$, Eq. 1.26 is identical to Eq. 1.22 and the hygrometer then behaves as a thermocouple psychrometer. In order for the temperature of the thermojunction to be determined only by latent heat energy transfer, $1-D\Pi$ must be zero so that $D = 1/\Pi$ and Eq. 1.26 reduces to Eq. 1.25.

Baughn (1974) used Eq. 1.12 with $E(\text{sen}) = 0$ and the right hand side zero. He found, as did Neumann & Thurtell (1972), that the hygrometer calibrations agreed with the theory to within 1 % if

r_j were set to zero. Setting $r_j = 0$, however, is not justified as the lower limit for the effective junction size would be the wire radius r_w . The disagreement between theory and experiment must result from the fact that Eqs 1.14 and 1.15 cannot hold simultaneously (Baughn, 1974) due to the physical constraints of the hygrometer system. In the former case (sensible heat) energy flow is treated as that between concentric spheres; in the latter case (conduction) energy flow is treated as that cylindrically symmetric to the thermojunction. Baughn (1974) points out that the excellent agreement between theory and experiment, as found by Neumann & Thurtell (1972), must be regarded as fortuitous. For this reason, calculation of calibration constants from the theory presented here does not offer itself as an acceptably accurate alternative to empirical calibration.

1.2.3.3 *Temperature dependence of dewpoint hygrometers*

The theoretical calibration constant for dewpoint hygrometers is not as temperature sensitive as that of thermocouple psychrometers (Table 1.3). However, the equation used to calculate $dV/d\psi_v$ (Eq. 1.25) assumes that $D = 1/\Pi$ is set correctly. Hence Π , a temperature dependent quantity, must be accurately known as a function of temperature in order to accommodate temperature variation.

1.3 SUMMARY

Thermodynamic theory is used to derive a calibration equation for thermocouple hygrometers (Eq. 1.10) for a closed system containing a single strong electrolyte solution only. The influence of temperature is accounted for by measurement and use of the correct temperature dependent constants.

The energy balance of a cooled thermocouple psychrometer is described (Fig. 1.2). An expression for the relationship between the thermojunction temperature T_j relative to the block temperature T (Fig. 1.1) shows that at a given temperature, T , the voltage output is directly proportional to the water potential ψ_v (Eq. 1.22). Any accurate measurement of ψ_v is contingent upon the temperature dependence of psychrometers and in order to ade-

quately describe their behaviour, this dependence will have to be investigated further (Chapter 2).

The dewpoint hygrometer senses the dewpoint temperature T_{dp} provided that all other forms of heat energy transfer except latent heat energy are compensated for (Eq. 1.25). Provided that in this mode the instrument senses T_{dp} , the output voltage is not as temperature dependent as when used in the psychrometric mode (Tables 1.2 and 1.3).

CALIBRATION OF THERMOCOUPLE HYGROMETERS USING THE PSYCHROMETRIC TECHNIQUE

2.1 INTRODUCTION

At present, much interest in the measurement of water potential using thermocouple hygrometers is evident (Peck, 1968, 1969; Millar, 1971a, b; Rawlins, 1972; Campbell & Campbell, 1974; Millar, 1974; Michel, 1977; Wiebe & Prosser, 1977; Brown & Tanner, 1981). Calibration procedures of *in situ* leaf psychrometers have not been adequately described, and the need for accurate calibration is self evident; field measurement of water potential can only be as accurate as the calibration of the hygrometer (Easter & Sosebee, 1974). This chapter reports on calibration procedures for thermocouple psychrometers, leaf psychrometers in particular, and discusses some of the major difficulties that might be experienced in the calibration of these instruments. Two new models (one empirical and one theoretical) for the temperature correction of a psychrometer calibration curve are proposed. Comparison of these models with the existing methods for temperature correction, indicates the superiority of the models proposed here.

2.2 DEFINITION OF THERMOJUNCTION STEADY STATE

2.2.1 Introduction

Peck (1968) showed that at steady state, the voltage following cooling uniquely determines the volumetric water potential ψ_v (Eq. 1.22). In theory, this steady state point appears easily determined; in practice, its definition has been one of the causes of the problems associated with thermocouple psychrometers (Bristow & de Jager, 1980). Some authors measured the output voltage one minute following the cessation of cooling; others read it "immediately" (Millar, 1971a, b).

2.2.2 Theory

Suppose that the sensing thermojunction (Fig. 1.1) is sealed in a chamber above a soil or leaf sample or salt solution

of volumetric water potential ψ_v . It is assumed that the vapour in the chamber is in vapour and temperature equilibrium with its surroundings. Heat energy is gained by the thermojunction by conduction along the wires, sensible heat transfer in air, and lost by radiative exchange with the chamber walls, evaporation of water and Peltier cooling:

$$S\{E(\text{rad}) + E(\text{sen}) + E(\text{con}) + E(\text{lat}) + E(\text{Pel})\} = C \, dV/dt.$$

Peck (1968) claims: "it is reasonable to suppose that the junction temperature, assumes a steady value within a typical period of about 1 s after the connection or disconnection of the cooling current."

If the sensing junction is cooled to below the dewpoint temperature of the air, water will condense onto this junction. When the cooling current is terminated, the enclosed air and thermojunction will return to the temperature, T , of the metal block. During this return, steady state ($dV/dt = 0$) is reached so that

$$E(\text{rad}) + E(\text{sen}) + E(\text{con}) + E(\text{lat}) = 0 \text{ or } dE/dt = 0 \quad 2.1$$

where E is the net energy exchange at the sensing thermojunction. The temperature of the junction, T_j , corresponding to this steady state condition is defined as the wet bulb temperature T_w .

The idealized time dependent psychrometer output voltage curve is shown in Fig 2.1, p 21). This curve indicates the temperature difference between the sensing and reference junctions (Fig. 1.1) as a function of time, due to the sensing junction being cooled for a specified time. The output voltage V resulting from this temperature difference is given by Eq. 1.11, $V \approx S(T - T_j)$. The curve AB of Fig. 2.1 represents the cooling cycle, as the slope at any time t , is positive ($dV/dt > 0$). During cooling, water condenses onto the thermojunction releasing latent heat energy and hence cooling is offset to a certain extent. Samples with high water potentials (near zero) will offset cooling to a larger extent than samples with low water potentials due to the greater mass of water releasing latent heat of condensation to the junction. At the cessation of the cooling cycle, the junction temperature T_j

changes abruptly (indicated by curve BC of Fig. 2.1). Evaporation of the water film on the thermojunction slows the rate of approach of the junction temperature T_j to the block temperature T , as a result of the evaporating water absorbing latent heat energy from the thermojunction. If it is assumed that the evaporation of water causes no net loss of energy (Eq. 2.1) at the thermojunction, then $dT_j/dt = 0$ and during this time the junction temperature is defined to be T_w , the wet bulb temperature. Hence $dV(T_w)/dt = 0$ and the plateau or curve EF then indicates attainment of steady state energy conditions and the voltage $V(T_w)$ uniquely defines ψ_v for a given psychrometer at a specified temperature (Eq. 1.22).

The maximum voltage attained during cooling, V_{\max}^\dagger , can be obtained using Eq. 1.21, assuming steady state ($dV/dt = 0$), and the output voltage $V(T_w)$ at which steady state occurs during evaporation obtained using Eq. 1.22. Hence, for a given psychrometer,

$$V_{\max} - V(T_w) = \frac{\frac{2BGS}{\gamma^3} \{\coth \gamma\lambda - \operatorname{cosec} \gamma\lambda\} - SPI}{16\pi\sigma r_j^2 T^3 + 4\pi r_j k_a + \frac{2B}{\gamma} \coth \gamma\lambda + 4\pi r_j L_v D_v \rho_v \beta / e_0}, \quad 2.2$$

an expression that is independent of the water potential ψ_v and constant for a given temperature and cooling current. Calculations indicate that $V_{\max} > V(T_w)$ (for $3 \text{ mA} < I < 8 \text{ mA}$) and that $V_{\max} - V(T_w)$ is temperature dependent and greatly influenced by the magnitude of the cooling current I .

Therefore, provided there is no resistance to water vapour movement, V_{\max} as a function of ψ_v (Eq. 1.21) and $V(T_w)$ as a function of ψ_v (Eq. 1.22) are parallel lines, for a given psychrometer at a specified temperature. This theoretical development can be used to determine whether or not leaf material offers a resistance to water vapour movement into the psychrometer cavity (Wiebe, 1982, personal communication; Chapter 5).

[†] The V_{\max} concept was suggested by Wiebe (1982, personal communication) but was originally discussed by Spanner (1951)

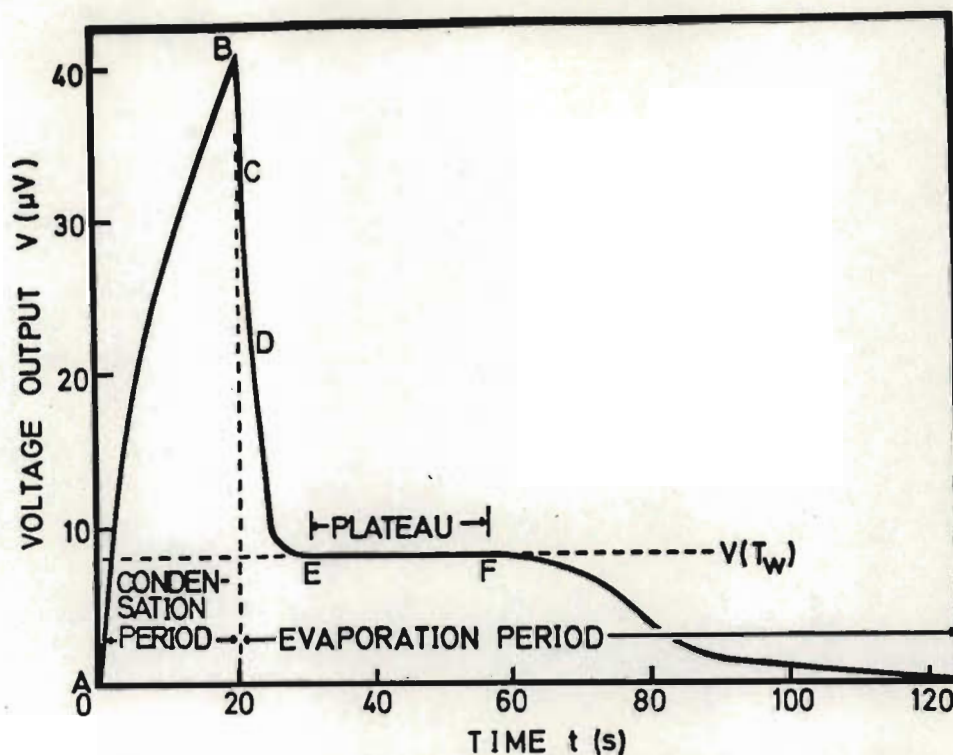


FIG. 2.1 Voltage output for an ideal thermocouple psychrometer for a cooling time of 20 s and $\psi_v = -1.757$ kPa ($T=25$ °C)

2.2.3 Materials and methods

The leaf psychrometers used in this study have been described by Campbell & Campbell (1974). It is assumed that the air in the chamber and all parts of the psychrometer remain at the same temperature. As a further precaution against temperature fluctuations, the microvoltmeter was insulated with polystyrene. Metal screen soil psychrometers (J.R.D. Merrill Speciality Equipment[†]) were calibrated in metal chambers (Brown & Collins, 1980) equipped with rubber O-ring seals (Fig. 2.2). The chambers were placed in a water bath with about 600 mm of submerged lead wire to avoid temperature gradients, due to conduction along the wire.

In the case of the leaf psychrometers, filter paper discs (Whatman no. 4) of diameter 17 mm were enclosed in small aluminium

[†] The mention of proprietary products is for the convenience of the reader and does not imply endorsement or otherwise by the author, the University of Natal or the Department of Agriculture

foil envelopes. Two or three drops of calibrating solution were used to saturate the filter paper in the envelope. This was inserted into the slit of the psychrometer and the aluminium cylinder firmly secured against the aluminium foil envelope by means of the set screw, thereby sealing the system. The assembly was then allowed to reach vapour and thermal equilibrium (generally less than 20 min). In the case of metal screen soil psychrometers, filter paper of width 20 mm was rolled around a 5 mm diameter rod, inserted into the chamber (Fig. 2.2) and saturated using a few drops of NaCl solution.

No deflection, ignoring transient spikes, when the function switch is rotated from "READ" to "INPUT SHORT"[†] indicates thermal equilibrium in the case of soil and leaf psychrometers. It is

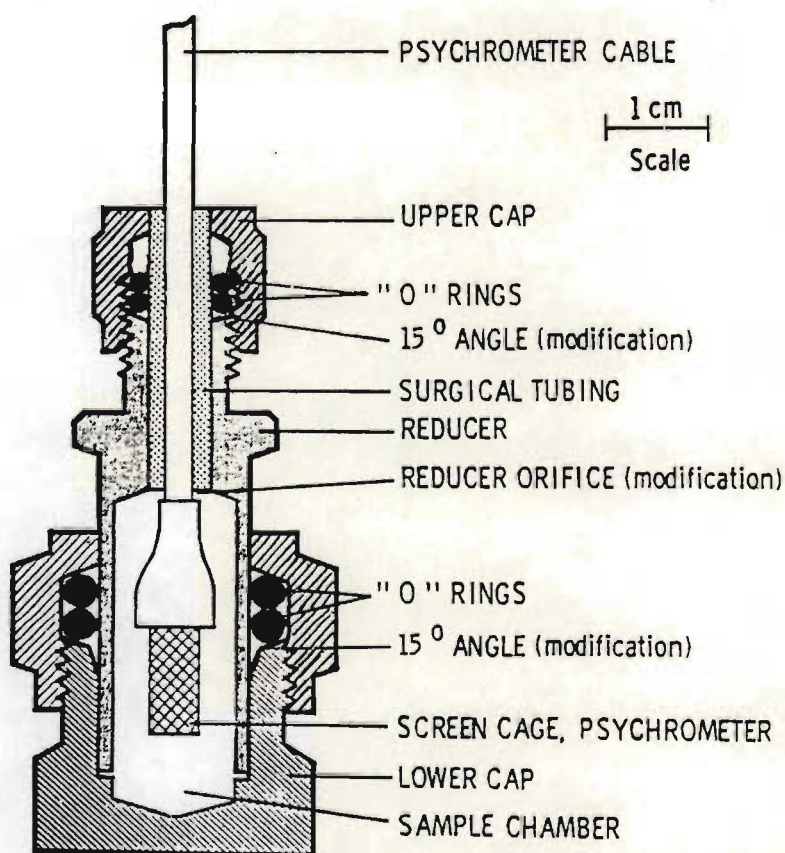


FIG. 2.2 Chamber used by Brown & Collins (1980) for the calibration of soil psychrometers (also referred to as screen-caged psychrometers)

[†] In this study, a Wescor HR-33T microvoltmeter was used but the meter of this unit was inadequate and replaced by a digital voltmeter

suggested that the test for temperature equilibrium be performed prior to each measurement rather than using a fixed time interval. The test for vapour equilibrium is to repeat a set of measurements; if $V(T_w)$ (see Section 2.2.4) remains constant in time, then vapour equilibrium exists.

At the end of a series of measurements the leaf psychrometer chamber was soaked in near boiling ammonium hydroxide (4 mol/kg) and steam cleaned, care being taken not to damage the delicate thermocouple. When steam cleaning the thermojunction, it is important that all water be removed before it can evaporate and leave unwanted crystal deposits. Soil psychrometers were steam cleaned and rinsed in ammonium hydroxide. The Wescor leaf psychrometers were calibrated at nine temperatures using a cooling time of 20 s, a voltage range of 0 to 100 μ V and standard sodium chloride (AR) solutions of 0 to 1,0 mol/kg (including 0,05 mol/kg) in increments of 0,1 mol/kg. The specific water potential of each molality NaCl was obtained from the table of Lang (1967) and converted to volumetric water potential (ψ_v). The psychrometer output voltage V was monitored using a chart recorder with a chart speed of 30 mm/min.

2.2.4 Results and discussion

During condensation, steady state is not reached within about 1 s as claimed by Peck (1968) (Fig. 2.3); the time for a constant voltage output to be achieved during cooling is greater than 60 s. In practice, this time period is too long and most workers have terminated cooling prior to steady state (during condensation) being attained. A non-equilibrium situation during evaporation therefore also occurs, with $V(T_w)$ dependent on the duration of cooling. It is therefore necessary to standardize procedures and use a cooling time of say 20 s if $\psi_v > -3\ 500$ kPa and 60 s if $\psi_v \leq -3\ 500$ kPa to eliminate the effect of cooling time on $V(T_w)$. Many workers have used variable cooling times.

Non-equilibrium is also the case during evaporation. The time dependent output voltage from a typical leaf psychrometer (Fig. 2.3) shows that $dT_j/dt \neq 0$ except at the beginning and end of measurement. Theory also predicts that steady state must be

reached (that is, $dE/dt = 0$ or $dT_j/dt = 0$) but in practice this does not occur during evaporation. Consider Fig. 2.3 where portion EF of the trace is a non-horizontal line (hereinafter referred to as the plateau). Each point of EF is in fact a point of inflection ($d^2V(T_j)/dt^2 = 0$) with the junction temperature T_j increasing in time t . This increase is due to a combination of the following:

1. the evaporating surface (the "outside" of the water film) and the surface exchanging sensible heat energy (the thermojunction surface) have different areas;
2. the diffusion equation for concentric spheres was applied (Eq. 1.19) in spite of the lack of spherical symmetry of the system;
3. during condensation, water probably condenses not only on the sensing thermojunction, but also on adjacent sections of the thermocouple wire;
4. for lower water potentials, longer cooling times are necessary for the same amount of water to be condensed;
5. steady state ($dT_j/dt = 0$) is not normally attained during condensation.

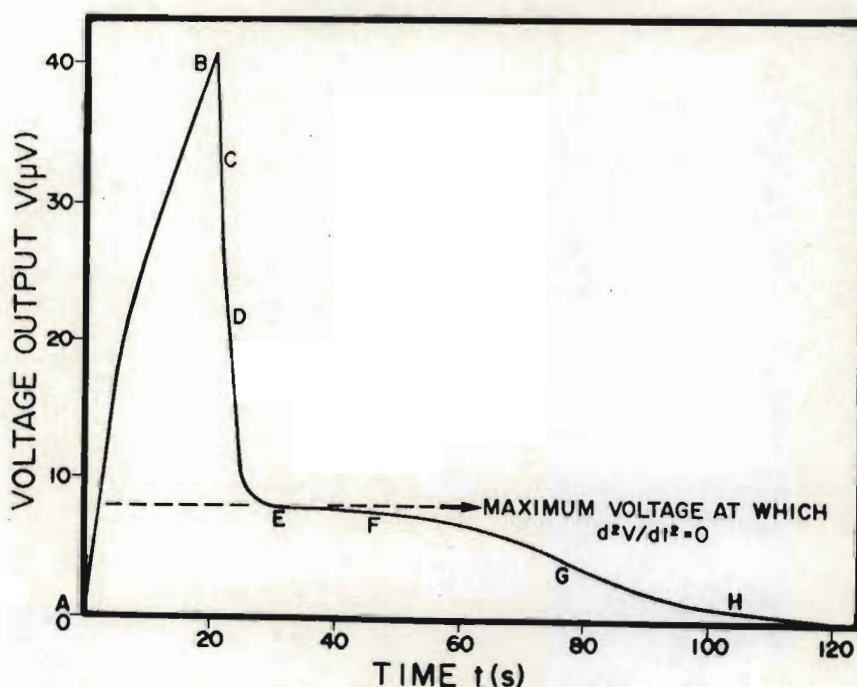


FIG. 2.3 Measured thermocouple psychrometer output voltage as a function of time (20 s cooling time) and $\psi_v = -1.757$ kPa ($T = 25^\circ C$)

Peck (1968) calculated that $dT_j/dt = 10^{-5} \text{ }^\circ\text{C/s}$ (for $\psi_v = -864 \text{ kPa}$) along the plateau EF (Fig. 2.3). Similar calculations were performed for psychrometer no. 1. Some of the complete voltage output curves are shown in Fig. 2.4. For $\psi_v = -1\,364 \text{ kPa}$ (Fig. 2.4a), $dT_j/dt = 0,23 \times 10^{-3} \text{ }^\circ\text{C/s}$, for $\psi_v = -2\,274 \text{ kPa}$ (Fig. 2.4b), $dT_j/dt = 0,47 \times 10^{-3} \text{ }^\circ\text{C/s}$ and for $\psi_v = -4\,626 \text{ kPa}$ (Fig. 2.4c), $dT_j/dt = 3,3 \times 10^{-3} \text{ }^\circ\text{C/s}$. In general then, $(dT_j/dt)_{EF}$ is affected by ψ_v (and the cooling time). Typically, if $T = 30 \text{ }^\circ\text{C}$, $dV(T_j) = -1,5 \text{ } \mu\text{V}$ for $\psi_v = -3\,735 \text{ kPa}$ along EF. At the high water potential, this voltage difference represents 20 % of the voltage corresponding to point E; at the low water potential, it is 9 %. If ψ_v decreases from 0 to $-4\,500 \text{ kPa}$, $-dV(T_j)/dt$ increases exponentially, depending on the block temperature T . The greater the temperature, the greater $-dV(T_j)/dt$, for a given ψ_v .

It is therefore necessary to define a point at which the voltage corresponding to ψ_v is to be measured. Using a chart speed of 30 mm/min and a 20 s cooling time, the point E of Fig. 2.3 is clearly definable for all water potentials as the voltage $V(T_w)$ corresponding to water potential ψ_v , and, the greatest voltage at which $d^2V(T_j)/dt^2 = 0$ for a junction temperature of T_j . The voltage corresponding to point E has been found to be slightly dependent on cooling, but independent of chart speed. The advantages of using point E as opposed to other points of the output curve are as follows:

1. easily definable (Fig 2.3);
2. corresponds to the same physical condition irrespective of water potential;
3. provides a better voltage sensitivity to water potential compared to any other point along EF;
4. independent of chart speed.

The time dependent output voltage from a metal screen soil psychrometer (Fig. 2.5) has a different characteristic shape from the curves of Fig. 2.4 for leaf psychrometers. The reference junctions (Fig. 1.1) for soil psychrometers are small copper pins embedded in teflon. During the evaporation cycle, the sensing junction is increasing in temperature (energy gain) and the reference junctions losing energy. It may be that the reference junctions are not sufficiently massive for heat energy dissipation

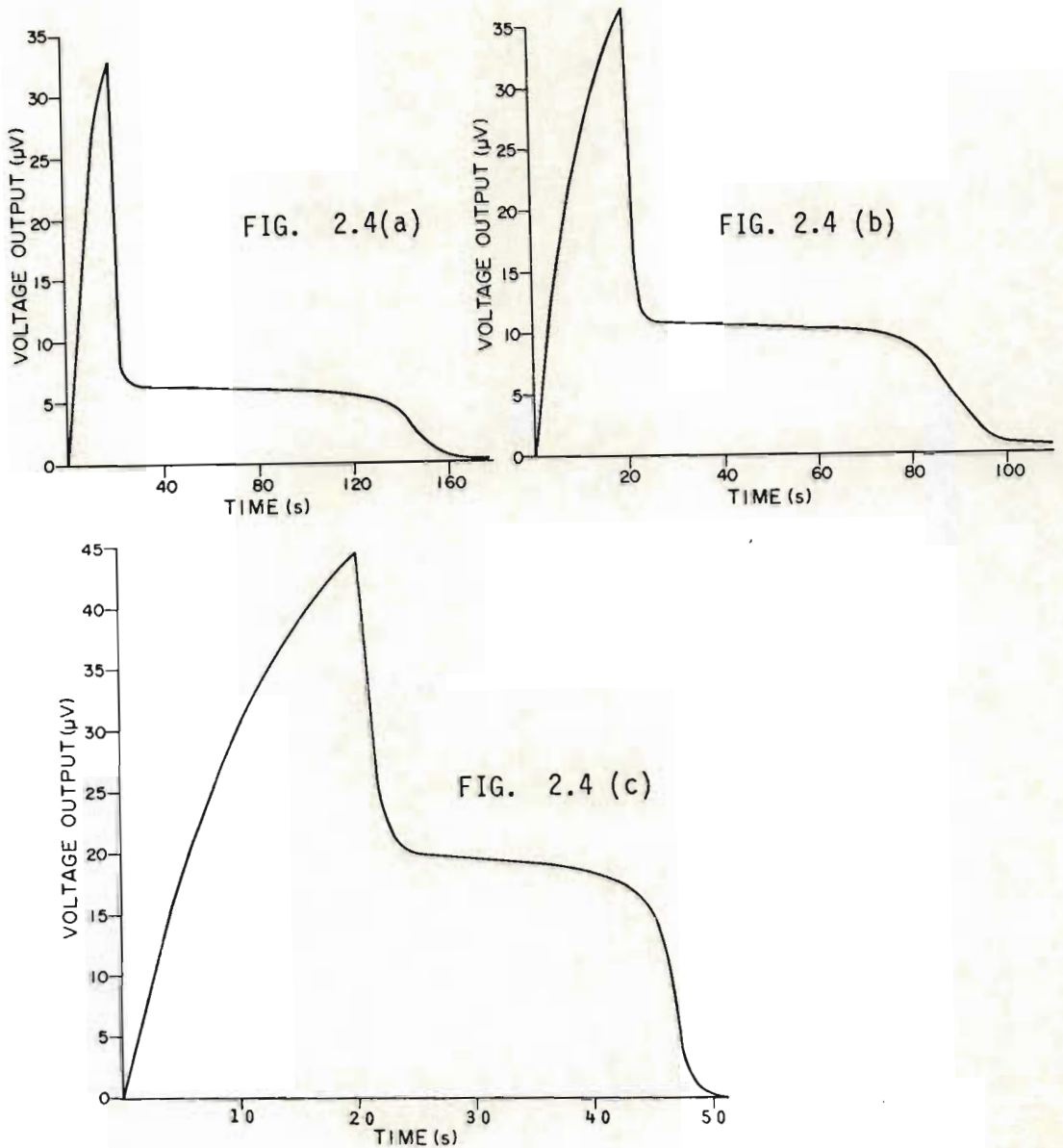


FIG. 2.4 Voltage output curves for psychrometer no. 1 for a cooling time of 20 s, $T = 25^{\circ}\text{C}$ and (a) $\psi_V = -1\,364$ kPa; (b) $\psi_V = -2\,274$ kPa; (c) $\psi_V = -4\,626$ kPa

and/or that Joule heating of the wires may occur, for a cooling current of roughly 7 mA. This energy lag or "overshoot" delays steady state and results in a slight voltage increase[†] (Fig. 2.5), for most soil psychrometers if $\psi_v > -3\ 000$ kPa. This overshoot was only occasionally observed when using leaf psychrometers (since the reference junction is sufficiently massive) or a Merrill switch box unit with $I = 5$ mA. In some cases, $I = 7$ mA resulted in negative voltages some 2 to 6 s after the cessation of cooling. Schimmelphennig (1972) and Briscoe & Tippets (1982) developed electronic switch systems that displayed or memory stored the voltage some short time after cessation of cooling, or continuously.^{††} Obviously then, it is not possible to use such systems or methods of determining output voltages for soil psychrometers placed in calibrating chambers if I is less than about 8 mA. Presumably it is possible to remove the overshoot by altering the value of I (Slack & Riggle, 1980).

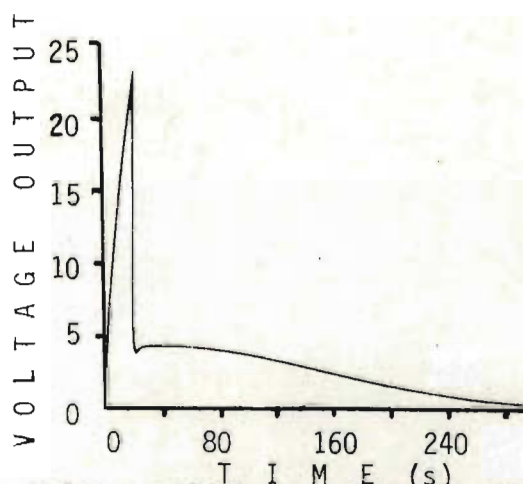


FIG. 2.5 Voltage output as a function of time for a wire mesh soil psychrometer (20 s cooling time) sealed above a salt solution with $\psi_v = -922$ kPa (at 25 °C)^{†††}

† The explanation provided here was provided by Wiebe (1981, personal communication)

†† A time of 2 s is equivalent to the chart distance of 1 mm after cooling (with a chart speed of 30 mm/min) used by Bristow & de Jager (1980)

††† Taken from the paper by Savage, Cass & de Jager (1981c)

2.3 TEMPERATURE DEPENDENCE OF PSYCHROMETER CALIBRATION

2.3.1 Introduction

A common procedure of correcting thermocouple output voltage V_T^\dagger at the block temperature, $T(^{\circ}\text{C})$ to that at 25°C (Brown, 1970; Bristow & de Jager, 1980) using the equation:

$$V_{25} = V_T / (0,325 + 0,027 T), \quad 2.3$$

suffers from a number of problems^{††}:

- (a) water potentials are corrected to exactly 25°C on the basis of a calibration curve determined near 25°C ;
- (b) there is no theoretical reason to substantiate the practice of correcting a measured water potential at temperature T to that at 25°C ;
- (c) Brown (1970) determined the constants $a = 0,325$ and $b = 0,027 (^{\circ}\text{C})^{-1}$ for a single water potential over a range of temperatures. These constants cannot be expected to apply to all psychrometers under all conditions (Wiebe *et al.*, 1971, p 26); in general, each psychrometer possesses a unique set of a and b values (Eq. 1.24).

In much of the published work using psychrometers, authors have relied on the above method of temperature correction claiming that ψ_V can be measured to within ± 10 kPa ($\pm 0,1$ bar).

2.3.2 Theory^{†††}

The objective of this section is to present a more comprehensive approach to the problem of temperature correction. Assuming that the voltage output V_T at temperature T can be expressed as a function of V_{25} , the output voltage at $T = 25^{\circ}\text{C}$, and the

[†] From hereon, V_T shall imply the voltage $V(T_w)$, defined in Section 2.2.4, corresponding to ψ_T

^{††} Based on the discussion by Savage, de Jager & Cass (1979)

^{†††} Based on the paper by Savage, Cass & de Jager (1981a)

block temperature T , where V_T is a linear function of T , then:

$$V_T = V_{25}(a + bT) \quad 2.4$$

$$\text{where } \{a + bT\}_T = 25 \text{ } ^\circ\text{C} = 1. \quad 2.5$$

If $1/k_T(\mu\text{V/kPa})$ is the slope of the psychrometers' voltage-water potential calibration curve at block temperature T , and assuming that the y-intercept is $0 \mu\text{V}^\dagger$ (see Section 2.4.1), with $1/k_{25}$ the slope at $25 \text{ } ^\circ\text{C}$, then

$$\psi_{25} = k_{25}V_{25} \quad 2.6$$

$$\text{and } \psi_T = k_TV_T \quad 2.7$$

defines the volumetric water potential at $25 \text{ } ^\circ\text{C}$ and temperature T respectively. Substituting Eq. 2.4 into 2.7:

$$\begin{aligned} \psi_T &= k_TV_{25}(a + bT) \\ &= \frac{k_T}{k_{25}} \cdot k_{25}V_{25}(a + bT), \end{aligned}$$

so that applying Eq. 2.6,

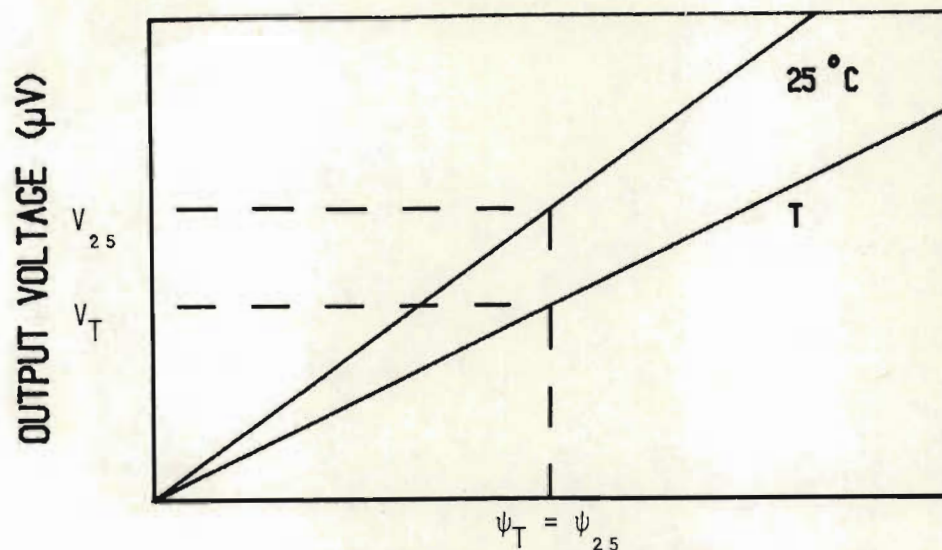
$$\psi_T = \frac{k_T}{k_{25}} \cdot \psi_{25}(a + bT)$$

$$\text{or } \frac{\psi_T}{\psi_{25}} = \frac{k_T}{k_{25}} (a + bT). \quad 2.8$$

A measured water potential is independent of temperature, as illustrated in Fig. 2.6, for two hypothetical calibration curves. That is,

$$\psi_T = \psi_{25}. \quad 2.9$$

[†] It is possible to correct for a non-zero intercept (Section 2.5)



VOLUMETRIC WATER POTENTIAL (kPa)

FIG. 2.6 Idealized relationship between V_T and ψ_T for 25°C and temperature T . A given ψ_T can result in a voltage V_T at temperature T and a voltage V_{25} at 25°C

Hence Eq. 2.8 reduces to

$$a + bT = k_{25}/k_T.$$

Rearranging and applying Eq. 2.5,

$$T = \frac{k_{25}}{b} \cdot \frac{1}{k_T} + \frac{25b - 1}{b}. \quad 2.10$$

Equation 2.10 can be used to determine k_{25} , a and b if the psychrometer has been calibrated at two or more temperatures. A plot of T as a function of $1/k_T$ ($\mu\text{V}/\text{kPa}$) yields a slope (S) of k_{25}/b and an intercept (I) of $(25b - 1)/b$. Hence

$$a = I/(I - 25), \quad 2.11$$

$$b = 1/(25 - I), \quad 2.12$$

$$k_{25} = S/(25 - I), \quad 2.13$$

$$k_T = k_{25}/(a + bT),$$

2.14

and $\psi_T = k_{25}V_T/(a + bT).$

2.15

2.3.3 Results and discussion

Four leaf psychrometers (two L-51A psychrometers for narrow leaf blades and two L-51 Wescor psychrometers, Logan, Utah, U.S.A.) were calibrated at nine temperatures ranging from 15 °C to 37,5 °C. A typical set of time dependent voltage output curves for psychrometer no. 1 is shown (Fig. 2.4). The statistical data for the V_T vs ψ_T linear calibration curves are presented (Table 2.1) for leaf psychrometer no. 4. Rauscher & Smith (1978) found that a non-linear predictor was often as good as a linear predictor. For the leaf psychrometers used in this study, this was never the case; the linear predictor was adequate for $\psi_T > -4\ 500$ kPa (Table 2.1).

Four temperature correction models are examined. The data test for these models are the corresponding k_T and T pairs obtained from various sources in the literature (Table 2.2) and empirical data from the four leaf psychrometers.

Model 1: This was proposed in Section 2.3.2; a plot of T vs $1/k_T$ ($\mu\text{V}/\text{kPa}$) may be used together with Eqs 2.11 to 2.15 inclusive to obtain an estimate of k_T (and hence ψ_T) at any temperature (Eqs 2.14 and 2.15), where $k_T = k_T(1)$.

TABLE 2.1 Statistical data for the calibration curves of psychrometer no. 4 (where $1/k_T$ is the slope of the line)

Temperature T (°C)	$\frac{1}{k_T} \times 10^3$ ($\mu\text{V}/\text{kPa}$)	SE(slope) $\times 10^3$ ($\mu\text{V}/\text{kPa}$)	y-intercept (μV)	SE(y-intercept) (μV)	r	SE(estimate of V_T on ψ_T) (μV)
15,0	-2,445	0,078	0,30	0,20	0,9950	0,3918
20,0	-3,169	0,052	0,35	0,13	0,9986	0,2677
23,3	-3,461	0,065	0,48	0,25	0,9968	0,4931
25,0	-3,683	0,121	0,71	0,32	0,9946	0,6332
27,0	-3,982	0,082	0,62	0,25	0,9986	0,4281
30,0	-4,267	0,069	0,24	0,18	0,9987	0,3679
35,0	-5,017	0,066	0,16	0,18	0,9991	0,3575
37,5	-5,451	0,101	0,11	0,27	0,9983	0,5475

TABLE 2.2 Comparison between measured (for the calibration temperatures shown) and the values of k_T (kPa/ μ V) predicted from four temperature correction models. The percentage deviations D(%) of calculated from measured values are shown

Data Source	MEASURED VALUES		CALCULATED VALUES ON THE BASIS OF THE VARIOUS MODELS							
	T	k_T	Model 1		Model 2		Model 3		Model 4	
			$k_T(1)$	D	$k_T(2)$	D	$k_T(3)$	D	$k_T(4)$	D
Campbell & Gardner (1971)	10	-416,7	-420	-0,8	-415	0,4	-405	2,8	-356	14,6
	25	-246,9	-245	0,8	-247	0,0	-247	0,0	-230	6,8
	40	-172,4	-173	-0,3	-176	-2,1	-178	-3,2	-104	39,7
Chow & de Vries (1973)	20	-333,3	-345	-3,6	-356	-6,8	-354	-6,2	-272	18,4
	25	-307,7	-296	3,8	-308	-0,1	-308	-0,1	-230	25,3
	30	-256,4	-259	-1,0	-271	-5,7	-272	-5,7	-188	26,7
	5	-334,6	-331	-1,1	-417-24,7		-400-19,5		-398	-18,9
Lang & Barrs (1965)	10	-281,3	-281	-0,3	-323-14,1		-315-11,8		-356	-26,5
	15	-240,0	-243	1,4	-263	-9,5	-259	-8,1	-314	-30,8
	20	-214,3	-214	0,0	-222	-3,5	-221	-2,9	-272	-26,9
	25	-191,9	-192	0,0	-192	0,0	-192	0,0	-230	-19,8
	30	-175,8	-176	-0,8	-169	-0,8	-170	3,4	-188	-6,9
Meyn & White (1972)	8	-420	-418	0,5	-407	3,1	-394	6,2	-373	11,2
	14	-320	-321	-0,3	-313	2,2	-308	3,8	-322	-0,6
	20	-260	-261	-0,4	-254	2,3	-253	2,7	-272	-4,6
	26	-220	-219	0,5	-214	2,7	-214	2,7	-222	-0,9
Scotter (1972)	15	-294,1	-293	0,4	-291	1,1	-288	2,1	-314	-6,8
	20	-243,9	-246	-0,9	-246	-0,9	-245	-0,5	-272	-11,5
	25	-212,8	-213	-0,1	-213	-0,1	-213	-0,1	-230	-8,1
	30	-188,7	-187	0,9	-187	0,9	-188	0,4	-188	0,4
	35	-166,7	-167	-0,2	-167	-0,2	-169	-1,4	-146	12,4
Wheeler (1972)	10	-300,0	-295	1,7	-342-14,0		-333-11,0		-356	-18,7
	20	-225,0	-227	-0,9	-235	-4,4	-234	-4,0	-272	-20,9
	30	-180,0	-184	-2,2	-179	0,6	-180	0,0	-188	-4,4
	40	-157,9	-155	1,8	-145	8,2	-146	7,5	-104	34,1

Model 2: According to Brown (1970),

$$k_T(2) = k_{25}/(0,325 + 0,027 T). \quad 2.16$$

Model 3: According to Wiebe *et al.* (1970),

$$k_T(3) = k_{25}/(0,350 + 0,026 T). \quad 2.17$$

Model 4: According to an equation adapted from Meyn & White (1972),

$$k_T(4) = -439,86 + 8,40 T. \quad 2.18$$

The parameters associated with model 1 (a, b and k_{25}) for the data referenced in Table 2.2 are shown in Table 2.3. The statistical data for these calculations are also shown in Table 2.3. Applying Eq. 2.14, it was possible to calculate $k_T(1)$, the predicted k_T value using model 1. Similarly, by applying Eqs 2.16, 2.17 and 2.18 it was possible to obtain $k_T(2)$, $k_T(3)$ and $k_T(4)$ respectively. These values are shown in Table 2.2 together with the measured k_T values. Model 1 is more accurate (smallest deviation) than any of the other models for these data, with model 2 marginally better than model 3, while model 4 shows the largest deviations for all data. Model 1 never has an error greater than 4 % while model 2, currently most popular, shows deviations of -14 to 8 %, for example (Table 2.2).

Other data have appeared in the literature for which the various calibration curves or associated data, were not given. Moore & Caldwell (1972) found that $a = 0,075$ and $b = 0,037 (^{\circ}\text{C})^{-1}$ (calibration at three temperatures) while Hoffman & Rawlins (1972) found that $\psi_T = V_T/(0,338 - 0,133 T)$ assuming $V_T = 0 \mu\text{V}$ if $\psi_T = 0 \text{ kPa}$.

The reciprocal calibration curve slopes (k_T), for the four psychrometers are listed in Table 2.4. A comparison between models 1, 2 and 3, for leaf psychrometer no. 4 is shown (Table 2.5,p35). Model 4 has been excluded because of its general inadequacy. The statistic $\sqrt{\Sigma D^2/(n - 1)}$ (where D has been previously defined (Table 2.5) and n is the number of calibrations over which the sum Σ is performed), indicates the superiority of model 1 (Table 2.6, p35), as

TABLE 2.3 Statistical data for the T vs $1/k_T$ linear relationship and the associated a , b , k_{25} values for the various data sources (Table 2.2)

Data Source	Slope		Intercept		r	SE(estimate of T on $1/k_T$)	a	b	k_{25}
	$(^{\circ}\text{C kPa}/\mu\text{V})$		$(^{\circ}\text{C})$						
Campbell & Gardner (1971)	- 8 820,9 \pm	149,8	-11,0 \pm 0,6		0,9999	0,36	0,3059	0,0278	-244,9
Chow & de Vries (1973) \dagger	-10 424,7 \pm 2 675,0		-10,3 \pm 9,1		0,9686	1,76	0,2900	0,0284	-296,1
Lang & Barrs (1965)	- 9 213,4 \pm	176,4	-22,9 \pm 0,8		0,9993	0,40	0,4774	0,0209	-192,6
Meyn & White (1972)	- 8 314,8 \pm	81,5	-11,9 \pm 0,3		0,9999	0,13	0,3225	0,0271	-225,4
Scotter (1972)	- 7 804,9 \pm	140,8	-11,7 \pm 0,7		0,9995	0,29	0,3175	0,0273	-212,8
Wheeler (1972)	- 9 826,0 \pm	561,1	-23,3 \pm 2,8		0,9968	1,27	0,4825	0,0207	-203,3

\dagger A double loop thermocouple psychrometer was used by these authors

TABLE 2.4 Measured k_T values (all with units $\text{kPa}/\mu\text{V}$) as a function of block temperature T ($^{\circ}\text{C}$) for the four leaf psychrometers. The $k_T(\text{theory})$ values ($\text{kPa}/\mu\text{V}$) are presented for comparison and discussed in Section 2.4.2

T	Psychrometer number							
	1		2		3		4	
	$k_T(\text{theory})$	k_T	$k_T(\text{theory})$	k_T	$k_T(\text{theory})$	k_T	$k_T(\text{theory})$	k_T
15,0	-371,1	-388,1	-399,4	-410,8	-407,4	-377,0	-393,5	-408,5
17,3	-337,4	-339,9	-	-	-367,3	-336,6	-	-
17,4	-	-	-359,2	-358,5	-	-	-	-
20,0	-304,9	-317,2	-	-	-329,3	-315,4	-319,9	-315,5
23,2	-273,6	-287,5	-	-	-293,2	-274,4	-	-
23,3	-	-	-323,9	-309,8	-	-	-284,8	-288,9
25,0	-258,7	-264,0	-272,4	-293,9	-276,2	-248,2	-269,5	-271,5
25,3	-	-	-	-	-273,6	-251,8	-	-
27,0	-	-	-	-	-	-	-253,5	-251,1
30,0	-224,6	-225,7	-235,0	-240,9	-237,9	-222,1	-232,8	-230,4
32,3	-211,8	-212,5	-221,1	-218,5	-	-	-	-
35,0	-198,5	-199,3	-206,7	-210,0	-209,0	-195,3	-205,0	-199,3
37,5	-187,6	-186,8	-194,9	-199,8	-197,0	-181,5	-193,4	-183,5

TABLE 2.5 Comparison between measured (for the calibration temperatures) and predicted k_T (kPa/ μ V) values for psychrometer no. 4 using models 1, 2 and 3. The percentage D (%) of the calculated from the measured value (relative to the measured) is indicated. The data for the last four columns are discussed later (Section 2.4.2)

T	k_T measured	$k_T(1)$	D	$k_T(2)$	D	$k_T(3)$	D	$k_T(5)$	D	$k_T(6)$	D
15,0	-408,5	-413	-1,0	-372	8,9	-367	0,2	-396	3,0	-388	5,0
20,0	-315,5	-325	-3,0	-314	0,5	-312	1,1	-322	-2,1	-316	0,0
23,3	-288,9	-285	-1,4	-285	1,3	-284	1,7	-287	0,7	-281	2,8
25,0	-271,5	-268	1,4	-272	-0,2	-272	-0,2	-272	0,0	-266	2,1
27,0	-251,1	-250	0,5	-258	-2,7	-258	-2,7	-255	-1,7	-251	0,1
30,0	-230,4	-228	1,1	-239	-3,7	-240	-4,2	-235	-1,8	-230	0,0
35,0	-199,3	-198	0,5	-214	-7,4	-215	-7,9	-207	-3,6	-203	-1,8
37,5	-183,5	-186	-1,4	-203	-10,6	-205	-1,7	-195	-6,2	-191	-4,3
Means of deviations D			-0,4		-1,74		-1,7		-1,46		0,49
Standard deviation of deviations D			1,52		5,92		6,64		2,79		2,86
$\sqrt{\sum D^2 / (n-1)}$			1,59		6,20		6,89		3,18		2,89

TABLE 2.6 Mean and standard deviation of the percentage deviation between the measured reciprocal slope k_T and the predicted value, relative to k_T , for psychrometers nos 1 to 4, for the various models[†]

Psychrometer number	Number of temperature calibrations	Model number				
		1	2	3	5	6
1	9	-0,17 \pm 1,52	-0,10 \pm 4,37	-0,11 \pm 5,14	-0,18 \pm 2,06	-0,47 \pm 1,33
2	8	-0,18 \pm 3,30	-5,11 \pm 5,63	-5,10 \pm 6,37	-4,91 \pm 3,29	3,56 \pm 3,00
3	9	-0,07 \pm 1,72	3,52 \pm 4,34	3,64 \pm 5,01	3,02 \pm 1,69	-2,02 \pm 2,42
4	8	-0,41 \pm 1,52	-1,74 \pm 5,92	-1,71 \pm 6,64	-1,46 \pm 2,79	0,49 \pm 2,86

[†] Model 1 is discussed in Section 2.3.2; model 2 that proposed by Brown (1970); model 3 that proposed by Wiebe *et al.* (1970); model 5 and 6 the single and double temperature calibration model (Section 2.4.2)

was the case for the literature data. Psychrometer no. 2 had the most irregular shape of the four psychrometers. This could account for the large $\sqrt{\sum D^2 / (n - 1)}$ value for this psychrometer (Table 2.7). It is interesting to note that in most cases, models 2 and 3 tend to underestimate k_T for $T < 25$ °C and overestimate for $T > 25$ °C (Table 2.2 and 2.5). The associated statistical data for a , b , k_{25} obtained by applying model 1, for the four leaf psychrometers is shown in Table 2.8.

2.4 COMPARISON BETWEEN THEORETICAL AND OBSERVED CALIBRATION CURVES

2.4.1 Intercept

Theoretically, $V_T = 0$ μ V if $\psi_T = 0$ kPa irrespective of the block temperature T (Eq. 1.22). In practice, the voltage output corresponding to deionized water is seldom zero (Table 2.1, p 31). Besides the problem of obtaining water that is absolutely pure and a thermojunction and cavity that is absolutely clean, water vapour may deviate from ideality and condensed water droplets may have small enough radii to yield positive potentials of a few tens of kPa.[†] For this reason, many workers (Meyn & White (1972) and Wheeler (1972), for example) do not use deionized water in the calibration process. One cannot then assume that the calibration curve does pass through the origin. Furthermore, the intercept value depends on the measurement techniques used to obtain the voltage output corresponding to the wet bulb depression ($T - T_w$). For example, the techniques used by Schimmelpfennig (1972) or Bristow & de Jager (1980) would result in a y-intercept statistically greater than 0 μ V in the case of leaf psychrometers, but less than 0 μ V for soil psychrometers (Section 2.2.4). Rauscher & Smith (1978) showed a calibration curve with a "psychrometer output" of ≈ 5 μ V corresponding to $\psi_T = 0$ kPa.

Campbell (1972) devised a simple procedure for assessing thermocouple contamination: if a sample of deionized water is inserted beneath the contaminated thermojunction without sealing, then water will condense onto the junction as a result of the

[†] Campbell, G.S., Washington State University, U.S.A., 1983, personal communication

TABLE 2.7 $\sqrt{\Sigma D^2/(n-1)}$ for the various data sets indicated and for the various models. Models 5 and 6 will be discussed later (Section 2.4.2)

Source (Table no. in brackets)	No. of calibrations	$\sqrt{\Sigma D^2/(n-1)}$ (%)				
		Model 1	Model 2	Model 3	Model 5	Model 6
Campbell & Gardner(1971)	3	0,83	1,51	3,01	-	-
Chow & de Vries(1973)	3	3,77	6,27	5,96	-	-
Lang & Barrs (1965)	6	0,89	13,61	11,00	-	-
Meyn & White(1972)	4	0,50	3,00	4,74	-	-
Scotter(1972)	5	0,68	0,85	1,30	-	-
Wheeler(1972)	4	1,98	9,71	8,03	-	-
Psychrometer no. 1	9	1,53	4,37	5,14	2,06	1,43
Psychrometer no. 2	8	3,31	7,85	8,39	6,20	4,85
Psychrometer no. 3	9	1,72	5,73	6,33	3,62	3,24
Psychrometer no. 4	8	1,59	6,20	6,89	3,19	2,90

TABLE 2.8 The statistical data for the T vs $1/k_T$ linear relationship and the associated a, b, k_{25} values for the four leaf psychrometers

Psychrometer no.	Slope ($^{\circ}\text{C kPa}/\mu\text{V}$)	Intercept ($^{\circ}\text{C}$)	r	SE(estimate of T on $1/k_T$) ($^{\circ}\text{C}$)	a_{\dagger}	b_{\dagger} ($^{\circ}\text{C}^{-1}$)	k_{25} (kPa/ μV)
1	-8 122,1 \pm 158,9	-5,79 \pm 0,63	0,9985	0,441	0,1975	0,0321	-263,8
2	-8 421,5 \pm 398,8	-5,01 \pm 1,56	0,9933	1,015	0,1675	0,0333	-280,6
3	-7 905,2 \pm 200,8	-5,87 \pm 0,81	0,9978	0,548	0,1900	0,0324	-256,0
4	-7 630,1 \pm 183,5	-3,49 \pm 0,74	0,9983	0,476	0,1225	0,0351	-267,8

[†] Note: Roundoff error affects the third decimal point of a and b. In these calculations, b was calculated and rounded off to four decimals and a determined using $a = 1 - 25 b$ and then rounded off to four decimals

extremely low water potential of a dry contaminant, such as sodium chloride. The heat of condensation would increase the temperature of the sensing junction resulting in a negative voltage output. Chamber contamination disturbs the equilibrium vapour pressure causing erroneous results. A simple test for chamber non-contamination is that $V_T < 1 \mu\text{V}$ for deionized water.

Scotter (1972) maintains that the small V_T value corresponding to 0 kPa and the observation that this output was only weakly dependent on the cooling time, indicates that the previously developed theory of heat energy dissipation at the massive reference junctions (see Fig. 1.1, p7) is inadequate (Fig. 2.5, p 27).

2.4.2 Slope [†]

The calculation of $1/k_T = dV(T_w)/d\psi_T$ using Eq. 1.22 assumes that the radius of the spherical thermojunction is known. The shape of the four sensing thermojunctions were observed to be elliptical. Using a microscope with a measurement error of 0,1 μm , the major and minor axes dimensions, X and Y, respectively, were determined, and a mean effective junction radius \bar{R} calculated from these measured dimensions. These three values were in turn defined to be the thermojunction radius and $1/k_T(\text{theory})$ ($\mu\text{V}/\text{kPa}$) calculated as a function of temperature, T, for each psychrometer. From an *ad hoc* comparison between calculated and measured reciprocal slopes, it was apparent that defining the sensing thermojunctions radius by $r_j = Y$ (Table 2.9) gave consistently good results. Henceforth, $1/k_T(\text{theory})$ is the theoretical slope calculated using the theoretical details of Peck (1968) and Rawlins (1966), with $r_j = Y$ (Table 2.10, p40). Other parameters needed for these calculations are: r_c = thermojunction chamber radius = 2 500 μm ; λ = length of wire from the sensing thermojunction to the chamber wall = 1 000 μm ; r_w = wire radius = 12,5 μm . These values are for leaf psychrometers only.

The model proposed in Section 2.3.2 was applied to the $1/k_T(\text{theory})$ vs T paired data. This model proposes that T as a function of $1/k_T(\text{theory})$ is linear with slope $k_{25}(\text{theory})/b_{th}$ and intercept

[†] Based on the paper by Savage, Cass & de Jager (1982)

TABLE 2.9 Measured (X, Y and r_w) and calculated mean effective (\bar{R}) dimensions for four leaf psychrometers

Psychrometer no.	X (μm)	Y (μm)	Wire radius r_w (μm)	\bar{R} (μm)
1	69,4	60,0	14,1	64,1
2	71,3	50,7	13,1	59,4
3	69,4	48,8	11,3	58,9
4	65,7	52,5	11,3	58,2
Mean			12,5	60,2

$(25 b_{th} - 1)/b_{th}$ where $a_{th} = 1 - 25 b_{th}$ and a_{th} , b_{th} and $k_{25}(\text{theory})$ are the theoretically calculated a , b and k_{25} values. The associated statistical data for these linear regressions are shown in Table 2.11, together with the a_{th} , b_{th} ($^{\circ}\text{C}^{-1}$) and $k_{25}(\text{theory})$ ($\text{kPa}/\mu\text{V}$) theoretical values, for each psychrometer. The regression constants were determined only for the $1/k_T(\text{theory})$ data for which $15^{\circ}\text{C} \leq T \leq 40^{\circ}\text{C}$, at 5°C intervals. We now assume that it is possible to calculate the reciprocal slope at temperature T , $k_T(c)$, via

$$k_T(c) = k_T(\text{theory}) \cdot \frac{k_{T_0}}{k_{T_0}(\text{theory})} \quad 2.19$$

where k_{T_0} and $k_{T_0}(\text{theory})$ are empirical and theoretical reciprocal calibration slopes at a standard temperature T_0 ($\approx 25^{\circ}\text{C}$) respectively. This equation satisfies the condition that if $T = T_0$ then $k_T(c) = k_{T_0}$. Substituting

$$k_T(\text{theory}) = k_{T_{25}}(\text{theory}) / (a_{th} + b_{th}T), \quad 2.20$$

into Eq. 2.19, and rearranging, we get:

$$k_T(c) = \frac{k_{25}(\text{theory})}{k_{T_0}(\text{theory})} \cdot \frac{k_{T_0}}{(a_{th} + b_{th}T)} \quad 2.21$$

TABLE 2.10 The theoretical $1/k_T(\text{theory})$ ($dV/d\psi_V$) values as a function of temperature T (calculated using Eq. 1.22) for the four leaf psychrometers ($r_C = 2\,500\ \mu\text{m}$; $r_W = 12,5\ \mu\text{m}$ and $\lambda = 1\,000\ \mu\text{m}$), with $r_j = Y$ (Table 2.9)

Temperature T ($^{\circ}\text{C}$)	$1/k_T(\text{theory}) \times 10^3$ ($\mu\text{V}/\text{kPa}$)			
	Psychrometer number			
	1	2	3	4
0	-1,290	-1,175	-1,150	-1,200
5	-1,707	-1,565	-1,533	-1,595
10	-2,173	-2,008	-1,970	-2,043
15	-2,704	-2,517	-2,474	-2,557
20	-3,277	-3,074	-3,027	-3,118
25	-3,866	-3,655	-3,605	-3,700
30	-4,460	-4,248	-4,198	-4,294
35	-5,044	-4,836	-4,787	-4,882
40	-5,625	-5,426	-5,378	-5,470
45	-6,169	-5,984	-5,939	-6,025

TABLE 2.11 The statistical data for the T vs $1/k_T(\text{theory})$ linear relationship (where $15\ ^{\circ}\text{C} \leq T \leq 40\ ^{\circ}\text{C}$) and the associated a_{th} , b_{th} and $k_{25}(\text{theory})$ values for the four leaf hygrometers. The $k_T(\text{theory})$ values were calculated using Eq. 1.22 where $r_j = Y$ (Table 2.9)

Psychrometer no.	Slope ($^{\circ}\text{C kPa } \mu\text{V}^{-1}$)	Intercept ($^{\circ}\text{C}$)	r	SE(estimate of T on $1/k_T(\text{theory})$) ($^{\circ}\text{C}$)	a_{th}^{\dagger}	b_{th}^{\dagger} ($^{\circ}\text{C}^{-1}$)	$k_{25}(\text{theory})$ ($\text{kPa}/\mu\text{V}$)
1	$-8\,536,8 \pm 20,2$	$-8,03 \pm 0,09$	1,0000	0,05	0,2425	0,0303	-258,7
2	$-8\,566,4 \pm 43,0$	$-6,42 \pm 0,18$	1,0000	0,11	0,2050	0,0318	-272,4
3	$-8\,579,2 \pm 50,3$	$-6,06 \pm 0,20$	0,9999	0,11	0,1950	0,0322	-276,2
4	$-8\,556,5 \pm 36,6$	$-6,75 \pm 0,15$	1,0000	0,09	0,2125	0,0315	-269,5

† Note: Roundoff error affects the third decimal point of a and b . In these calculations, b was calculated and rounded off to four decimals and a determined using $a = 1 - 25 b$ and then rounded off to four decimals

where if $T = T_o = 25\text{ }^{\circ}\text{C}$, $k_{25}(c) = k_{25}$. Ideally, T_o should be the mean *in situ* block temperature, but generally $T_o \approx 25\text{ }^{\circ}\text{C}$. The calculated a_{th} , b_{th} and $k_{25}(\text{theory})$ values for leaf psychrometers is shown as a function of $r_j = Y$ (Fig.2.7); it is therefore a simple matter to obtain a_{th} , b_{th} and $k_{25}(\text{theory})$ for any value of r_j . For screen-caged soil psychrometers, $r_c = 1\ 000\ \mu\text{m}$ and $\lambda = 1\ 200\ \mu\text{m}$ so that $a_{th} = -0,667 + 0,219 \ln r$, $b_{th} = 0,100 r^{-0,289}$ and $k_{25}(\text{theory}) = -897,412 r^{-0,298}$ where $r = 10^6 \times r_j$.

The essential difference between $k_T(c) = k_{25}/(a + bT)$ (see Eq. 2.14) and Eq. 2.20 is that a and b (Table 2.11) are calculated from the theoretical data (based on the measurement of the junction dimension of the particular psychrometer in question) as opposed to the empirical data of Brown (1970) or Wiebe *et al.* (1970) using

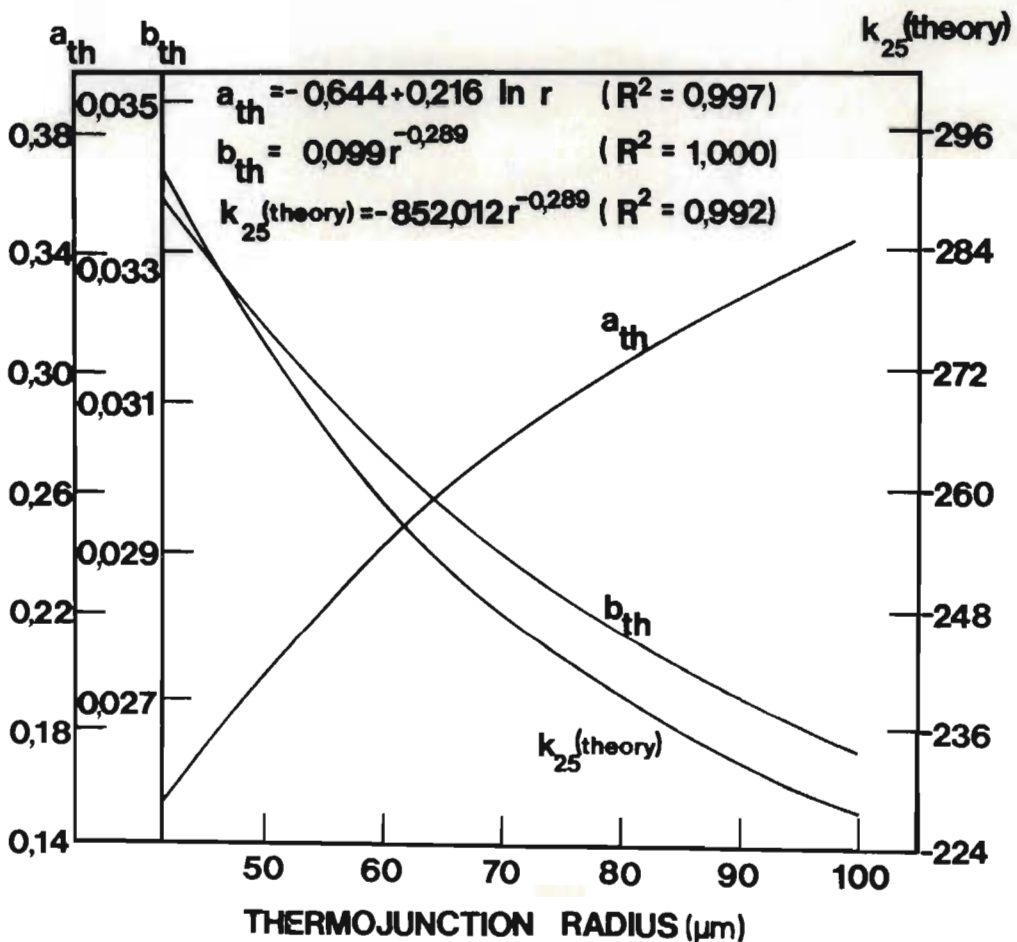


FIG. 2.7 a_{th} , b_{th} ($^{\circ}\text{C}^{-1}$), and $k_{25}(\text{theory})$ ($\text{kPa}/\mu\text{V}$) as a function of the sensing thermocouple radius r_j (μm) over the temperature range 15 to 40 $^{\circ}\text{C}$. In the indicated equations, $r = 10^6 \times r_j$, and R is the sample correlation coefficient

Eq. 2.16 or 2.17.

Equation 2.21 was tested against the model proposed in Section 2.3.2 (model 1), Brown (1970) (model 2) and Wiebe *et al.* (1970) (model 3) for four psychrometers (Tables 2.5 and 2.6), the present model (Eq. 2.21) being model 5. In general, model 1 is far superior than the other models with model 5 second (Table 2.6). Model 5 however only requires calibration at temperature T_o , whereas model 1 requires calibration at a number of temperatures.

Model 5 could be improved by calibrating at two temperatures $T_o(1)$ and $T_o(2)$ (model 6), where $T_o(1) < T_o(2)$, $T_o(1) \approx 20^\circ\text{C}$ and $T_o(2) \approx 30^\circ\text{C}$, for convenience. Equation 2.21, normalized for temperature $T_o(1)$ or $T_o(2)$, becomes:

$$k_T(c) = \frac{k_{25}(\text{theory})}{k_{T_o(1)}(\text{theory})} \cdot \frac{k_{T_o(1)}}{(a_{th} + b_{th}T)}$$

$$\text{or } k_T(c) = \frac{k_{T_o(1)} (a_{th} + b_{th} T_o(1))}{a_{th} + b_{th} T} \quad 2.22$$

for $T \leq (T_o(1) + T_o(2))/2$ (applying Eq. 2.20)

$$\text{and } k_T(c) = \frac{k_{25}(\text{theory})}{k_{T_o(2)}(\text{theory})} \cdot \frac{k_{T_o(2)}}{(a_{th} + b_{th}T)}$$

$$\text{or } k_T(c) = \frac{k_{T_o(2)} (a_{th} + b_{th} T_o(2))}{a_{th} + b_{th} T} \quad 2.23$$

for $T > (T_o(1) + T_o(2))/2$, also applying Eq. 2.20.

The normalization ensures that if $T = T_o(1)$ then $k_{T_o(1)}(c) = k_{T_o(1)}$ in Eq. 2.22 and that if $T = T_o(2)$ then $k_{T_o(2)}(c) = k_{T_o(2)}$ in Eq. 2.23. In practice, the temperatures $T_o(1)$ and $T_o(2)$ will be determined by laboratory facilities. Ideally, if T_{\min} , T_{\max} and \bar{T} are the respective minimum, maximum and mean *in situ* temperatures, then $T_o(1) = (\bar{T} - T_{\min})/2$ and $T_o(2) = (T_{\max} - \bar{T})/2$. In the case of psychrometers 1, 3 and 4, $T_o(1) = 20^\circ\text{C}$, but for 2,

$T_o(1) = 17,4$ °C. For psychrometers 3 and 4, $T_o(2) = 30$ °C, and $T_o(2) = 32,3$ °C for 1 and 2. In each case, the temperature $(T_o(1) + T_o(2))/2$ was taken to be 25 °C, for convenience. The predicted $k_T(c)$ values (Eqs 2.22 or 2.23), using this model (model 6) are compared with the measured k_T values for psychrometer no. 4 (Table 2.5). In general, model 6 is superior to models 2 to 5, but it does require calibration at two temperatures $T_o(1)$ and $T_o(2)$. The various models are also compared using data for all psychrometers (Table 2.6), with the same conclusions reached.

Brown and Bartos (1982) recently proposed a very useful model for calibrating large numbers of Peltier thermocouple psychrometers. Their model predicts water potential from thermocouple psychrometer voltage outputs over ranges in temperature, zero offset and cooling time. It would be very interesting to compare the present model, based on the thermojunction radius, and their model.

2.5 STATISTICAL ASSESSMENT OF ERRORS IN THERMOCOUPLE PSYCHROMETRIC WATER POTENTIAL MEASUREMENT[†]

2.5.1 Introduction

Thermocouple psychrometers are generally considered as the standard for water potential measurements under laboratory conditions (Boyer, 1966). However, this confidence does not extend to field conditions. Provided certain precautions are taken (Chapter 5), thermocouple psychrometers can be used for non-destructive field measurement of leaf water potential. Models for calibrating psychrometers incorporating temperature dependence were discussed in Sections 2.3 and 2.4.

The calculation of error inherent in psychrometric water potential measurement is obviously an important aspect. The aim of this section is to present a method for estimating the standard error of measured water potential, as a function of temperature, for leaf psychrometers employed in laboratory or field situations.

[†] Based on a paper by Savage, Cass & de Jager (1983), submitted for publication to *Crop Science*

2.5.2 Theory

It is possible to estimate the error in a quantity which is calculated from other quantities which themselves contain known measurement errors (Young, 1962, p 99; Barford, 1967, p 34). Suppose f is a function of X^a, Y^b, Z^c, \dots , where X, Y, Z, \dots are quantities determining f and a, b, c, \dots are known exponent values. Then the relative standard error in f , $\sigma(f)/f$, is given by:

$$\frac{\sigma(f)}{f} = \left\{ \frac{1}{f^2} \cdot (\partial f / \partial X)^2 \cdot \sigma^2(X) + \frac{1}{f^2} \cdot (\partial f / \partial Y)^2 \cdot \sigma^2(Y) + \frac{1}{f^2} \cdot (\partial f / \partial Z)^2 \cdot \sigma^2(Z) + \dots \right\}^{\frac{1}{2}} \quad 2.24$$

where $f \neq 0$ and f is a mean value, the variance of which is $\sigma^2(f)$.

Psychrometer block temperature T and the calibration slope $1/k_T$ ($\mu\text{V}/\text{kPa}$) are linearly related with slope S ($\text{kPa}^\circ\text{C}/\mu\text{V}$) and intercept I ($^\circ\text{C}$) (Eqs 2.11 to 2.15). Therefore, for any $T \neq I$,

$$1/k_T = (T - I)/S \quad 2.25$$

and since $\psi_T = k_T V_T$ where ψ_T is the volumetric water potential corresponding to output voltage V_T at block temperature T ,

$$\psi_T = S V_T / (T - I). \quad 2.26$$

From Eq. 2.25, we obtain $\partial \psi_T / \partial S = V_T / (T - I) = \psi_T / S$, $\partial \psi_T / \partial I = S V_T / (T - I)^2 = \psi_T / (T - I)$, $\partial \psi_T / \partial V_T = S / (T - I) = \psi_T / V_T$ and $\partial \psi_T / \partial T = -S V_T / (T - I)^2 = -\psi_T / (T - I)$, so that the relative standard error in water potential, $E_p = \sigma(\psi_T) / \psi_T$ involves a number of subcomponent errors, where

$$\sigma(\psi_T) / \psi_T = \left\{ (\sigma(S)/S)^2 + (\sigma(I)/(T - I))^2 + (\sigma(V_T)/V_T)^2 + (\sigma(T)/(T - I))^2 \right\}^{\frac{1}{2}} \quad 2.27$$

and $E_p = \sigma(\psi_T) / \psi_T$, $E_{p1} = \sigma(S)/S$, $E_{p2} = \sigma(I)/(T - I)$, $E_{p3} = \sigma(V_T)/V_T$ and $E_{p4} = -\sigma(T)/(T - I)$. Hence a 95 % confidence interval for ψ_T is

$$\sigma(\psi_T) \cdot t(n - 1; 95 \%) / \psi_T$$

where n is the number of data points. Alternatively, the error in water potential measurement can be expressed using the percentage standard error of the mean where $E_p = E(\psi_T)$ and:

$$E_p = 100 \cdot \sigma(\psi_T) / \psi_T \quad . \quad 2.29$$

The calibration model (Eq. 2.25) assumes that the voltage intercept of the ψ_T vs V_T curves are zero. There is some evidence for a common voltage intercept for all temperatures (Lang & Barrs, 1965; Chow & de Vries, 1973) but generally, the intercept is non-zero. For this reason, it is necessary to correct V_T to V_T' by subtracting the voltage measured above distilled water, at any temperature, from V_T . Then for zero water potential, the voltage V_T' is zero.

2.5.3 Materials and methods

Calibration of eight Wescor leaf psychrometers were performed under field conditions where temperatures ranged between 15 and 45 °C. In order to encompass lower temperatures, psychrometers were transferred to a refrigerator allowing measurements in the temperature range -2 to 15 °C. Calibration involved using NaCl solutions (0,1; 0,2; 0,3; and 0,5 mol/kg, corresponding to $\psi_T > -2\ 500$ kPa) and deionized water over a range of field temperatures, a 20 s cooling time and 45 min for equilibrium. The psychrometer junction and chamber were steam cleaned whenever resealing took place.

Double filter paper discs (Whatman no. 1) were just saturated (0,05 ml) with calibrating solution, enclosed in an aluminium foil envelope and inserted into the leaf psychrometer slit. The small aperture in the envelope, exposing the filter paper, was positioned to coincide with the thermocouple chamber.

Temperature gradients were controlled by enclosing each psychrometer in a layer of insulating material (Chapter 5) and by using aluminium envelopes small enough to be completely shielded from extraneous radiation when in the slit of the insulated psychrometer block. The psychrometer piston was sealed against the aluminium envelope using a double ring of Parafilm. This ensured

no loss of water from the aluminium envelope over a 24 h period. The top of the psychrometer piston and about 150 mm of lead wire was covered with aluminium foil tape. The slit area was also covered with tape in order to reduce incident radiation and air movement in the vicinity of the block which contributed to the development of temperature gradients. Further precautions associated with the use of the microvoltmeter in the field are discussed in Chapter 5. Output voltages for a range of water potentials, zero offsets and block temperatures were monitored from sunrise to sunset on near cloudless days. Use of a chart recorder, allowed measurement of voltage output to within $0,1 \mu\text{V}$. The definition of the voltage corresponding to the known water potential was that used in Section 2.2.4. Temperature gradients were controlled such that zero offset values ranged between $-0,3$ and $0,2 \mu\text{V}$ and between $-0,2$ and $0,5 \mu\text{V}$ for the field and refrigerator respectively.

Electronic noise associated with laboratory voltage measurements were performed for battery operated Merrill (meter no. 82-22) and Wescor (HR-33T meter) systems. Voltages, to within 5 nV , were measured simultaneously using two chart recorders. To check that the mains driven chart recorders were similar in affecting the voltages, the output from a unit was measured simultaneously using both recorders. This procedure was repeated for the other unit.

2.5.4 Results and discussion

The advantage of the presented theory is that it is possible to evaluate the error associated with a measured water potential when using thermocouple psychrometers. These errors can be converted into measured water potential confidence intervals (Eq. 2.28).

The linear relationship between T and V_T'/ψ_T is shown for a psychrometer with large associated errors (Fig. 2.8, Table 2.12). Each point shown in Fig. 2.8 represents one voltage and block temperature measurement for a given psychrometer. The measured voltages are affected by temperature gradients, and this may account for some of the scatter. However, *in situ* field measurements of leaf water potential are similarly affected. The measured voltage for distilled water, $V_T - V_T'$, was generally less than $0,4 \mu\text{V}$ irrespective of temperature (Table 2.12). Calissendorff & Gardner (1972) showed V_T as a function of T for two different water poten-

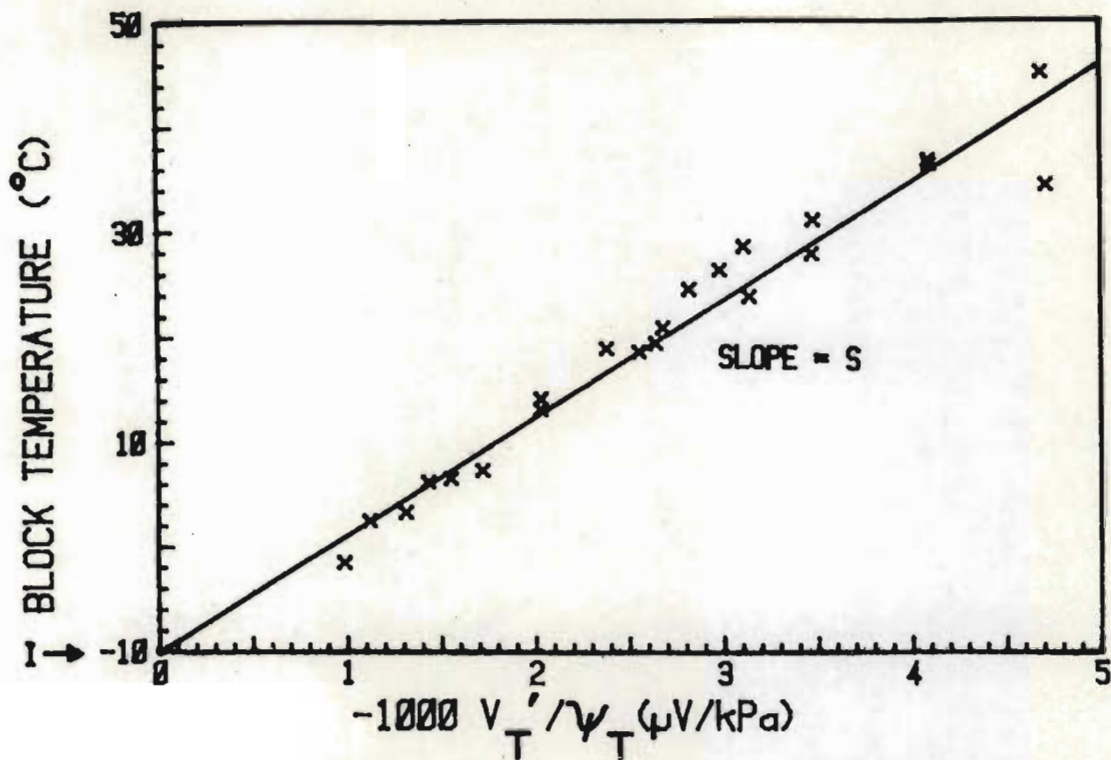


FIG. 2.8 Block temperature T plotted against $-10^3 V_T' / \psi_T$ for psychrometer number 11 (which had the largest associated errors)

TABLE 2.12 Parameters associated with psychrometric error calculation, for a few psychrometers. The total error is calculated from 0 to 45 °C for a zero offset of 0,5 μV and a water potential of -1 250 kPa

	Psychrometer number			
	1A	5A	7A	11A
$S \pm SE(S)$ (kPa °C/ μV)	-10 723±268	-12 937±272	-11 778±199	-11 194±515
$I \pm SE(I)$ (°C)	-8,0±0,7	-15,8±0,8	-12,3±0,6	-10,1±1,5
$r(T \text{ vs } 1/k_T)$	0,9935	0,9969	0,9981	0,9594
$S_{y.x}(T \text{ vs } 1/k_T)$ (°C)	±1,3387	±1,0274	±0,7153	±2,6181
n	23	16	15	22
$V_T - V_T'$ (μV)	0,4±0,05	0,2±0,02	0,2±0,04	0,4±0,05
Total error range (%)	10 to 3	6 to 2	6 to 2	16 to 5

tials, -2 000 and -3 500 kPa. They claimed that their curves were not linear, particularly at lower temperatures (not less than about 4 °C). In our case, temperatures were greater than -2 °C and there appeared to be no marked deviation in T vs V_T'/ψ_T from linearity (Fig. 2.8). This was the case for the eight leaf psychrometers used.

Part of the temperature dependence of the measurement error in psychrometric water potential is contained in the second term of Eq. 2.27 (E_{p2}). This term indicates that the error in psychrometric measurements increases as T approaches the value of I (Eq. 2.26), suggesting limitations in the use of these instruments at low temperatures. The value for I is generally negative and ranged between about -23 and -10 °C for data from the literature (Lang & Barrs, 1965; Campbell & Gardner, 1971; Meyn & White, 1972; Scotter, 1972; Wheeler, 1972; Chow & de Vries, 1973). Extrapolation of the V_T vs T curves of Calissendorff & Gardner (1972) indicated that for $V_T = 0 \mu V$, $T = -20$ °C, or, in our notation, $I = -20$ °C. For the psychrometers used here, I ranged between about -16 and -8 °C (Table 2.12). At low temperatures, T approaches I and the value of E_p increases irrespective of $\sigma(S)/S$ (Eq. 2.27 and Fig. 2.9).

The parameter I appears to be a characteristic of the sensing thermojunction so that in part, the relative standard error as a function of temperature (Fig. 2.9) is dependent on the shape of the thermojunction and the scatter in the field measurements.

Campbell (1979) listed the error subcomponents of $E_{p3} = \sigma(V_T)/V_T$ (Eq. 2.27): (a) zero offset error which has subsequently been quantified as a mathematical function of zero offset voltage, measured voltage and dry junction temperature by Brown & Bartos (1982); (b) zero drift or reference junction temperature changes during cooling; (c) electronic noise.

The zero drift error can be large in the case of field measurements if long cooling times are employed. In this and our other work, we have found 20 s to be suitable for psychrometer measurements greater than -3 000 kPa, although variable cooling times have often been used in the past by other workers. The time taken for the sensing junction to attain the wet bulb value is less than about 30 s for a 20 s cooling time. Further precautions minimizing the

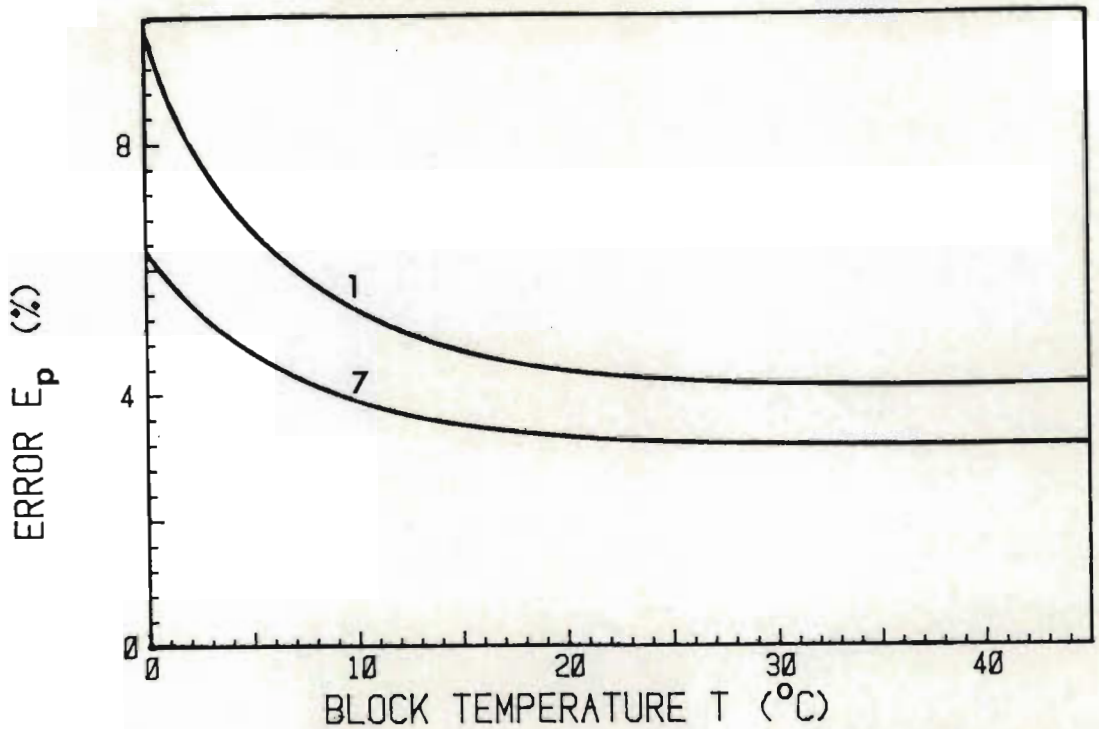


FIG. 2.9 Calculated error, E_p , in measured water potential for the best (no. 7) and the worst (no. 1) psychrometers, as a function of temperature

zero drift error included insulating the leaf psychrometer (Chapter 5) to minimise reference junction changes during the 30 s. With these precautions, this error component is assumed to be relatively small, but is difficult to enumerate.

Campbell (1979) claimed that electronic noise levels are probably about ± 150 nV and that precision in water potential measurements better than ± 50 kPa can be achieved by replicating measurements on the same sample. We measured peak-to-peak noise voltages that were less than ± 25 nV for one commercial microvoltmeter and about ± 50 nV for another. The value of ± 25 nV was measured on two separate occasions months apart. Using Wescor C-52 chamber psychrometers we were able to measure exuded sap water potential of citrus, the average of which was -38 kPa (Chapter 5). At 25°C , 25 nV is roughly equivalent to a potential of 6 kPa.

Assuming that all attempts have been made to minimize the zero drift and electronic noise errors, the major subcomponent of $\sigma(V_T)/V_T$ is the zero offset error, obtained by Brown & Bartos (1982) for empirical data using soil psychrometers. Incorporating this and

the electronic noise error, we define the error in voltage measurement E_{p3} as a combination of two subcomponents E_{p31} and E_{p32} where:

$$\sigma(V_T)/V_T = \{((0,015.dV + 0,00147.T.dV)/10,4)^2 + (0,05/V_T)^2\}^{1/2}, \quad 2.30$$

where dV is the measured zero offset voltage (μV), and V_T the output voltage corresponding to the field measured water potential. The zero offset term is valid for cooling times near 15 s (Brown & Bartos, 1982) and we assume can be used for leaf psychrometers without modification.

The error in water potential due to temperature measurement, $E_{p4} = -\sigma(T)/(T - I)$ using the notation in Eq. 2.27 has previously been investigated by Campbell (1979, Eq. 7). It can be shown that our expression, $-\sigma(T)/(T - I)$, is equivalent to his. Our equivalent of the term c defined by Campbell (1979) is $c' = M/T(T - I)$ where M [= $-S$.thermocouple sensitivity ($\mu V/K$).partial molar volume of water (m^3/mol)/universal gas constant ($J mol^{-1} K^{-1}$)] is a temperature dependent quantity. Applying the product rule for differentiation to c , to obtain dc/dT and hence $(dc/dT)/c$, we get $(dc/dT)/c = -1/T - 1/(T - I)$ and the result $(dc/dT)/c + 1/T = -1/(T - I)$. If we assume that temperature can be measured to within $\pm 0,25$ °C, we have

$$\sigma(T)/(T - I) = \pm 0,25/(T - I). \quad 2.31$$

In order to determine the total error associated with the measurement of water potential using the psychrometric technique, we now apply Eqs 2.27, 2.29 to 2.31. Over the 0 to 45 °C temperature range, the relative mean standard error (total) for data obtained from the literature (Lang & Barrs, 1965; Campbell & Gardner, 1971; Meyn & White, 1972; Scotter, 1972; Wheeler, 1972; Chow & de Vries, 1973) varied between 90 and 30 % (worst case) and between 3 and 1 % (best case) assuming zero offset, temperature and voltage errors were negligible. Our errors were 15 to 5 % (worst psychrometer, Table 2.13) and 6 to 2 % (best psychrometer; Fig. 2.9). The subcomponent errors are also shown in Table 2.13, for a few psychrometers, and as a function of temperature. For a given temperature, there is a slight voltage and hence water potential dependence,

TABLE 2.13 Psychrometric error components (and subcomponents) for a few psychrometers, as a function of temperature (Eq. 2.27). A gap in the table implies a temperature independent error. A zero offset of 0,5 μV is assumed with $\psi_T \approx -1\ 250\ \text{kPa}$

Psychrometer number	T ($^{\circ}\text{C}$)	Total error E_p (%)	Component errors (%) [†]					
			E_{p1}	E_{p2}	E_{p3}	E_{p31}	E_{p32}	E_{p4}
1A	0	9,9	2,5	8,7	2,5	0,1	2,5	3,1
	10	4,9		3,9	1,3	0,1	1,2	1,4
	20	3,7		2,5	0,8	0,2	0,8	0,9
	30	3,2		1,8	0,7	0,3	0,6	0,7
	40	3,0		1,4	0,6	0,4	0,5	0,5
5A	0	6,0	2,1	5,2	1,3	0,1	1,3	1,6
	10	4,1		3,2	1,1	0,1	1,1	1,0
	20	3,3		2,3	0,8	0,2	0,8	0,7
	30	2,9		1,8	0,7	0,3	0,6	0,5
	40	2,7		1,5	0,6	0,4	0,5	0,4
7A	0	5,9	1,7	4,9	2,0	0,1	2,0	2,0
	10	3,5		2,7	1,1	0,1	1,1	1,1
	20	2,8		1,9	0,8	0,2	0,7	0,8
	30	2,4		1,4	0,7	0,3	0,5	0,6
	40	2,2		1,2	0,6	0,4	0,4	0,5
11A	0	15,6	4,6	14,5	2,6	0,1	2,5	2,5
	10	8,8		7,2	1,1	0,1	1,1	1,2
	20	6,8		4,9	0,7	0,2	0,7	0,8
	30	6,0		3,7	0,7	0,3	0,6	0,6
	40	5,5		2,9	0,5	0,4	0,4	0,5

[†] Only error magnitudes are shown

with errors increasing as voltages decrease towards zero, where the major error contribution is from electronic noise. For ease of comparison, we have chosen a water potential near -1 250 kPa (Table 2.13). It is evident that generally, errors in calibration are largest, but for certain conditions such as high temperatures and large zero offsets, all error types contribute significantly. At low temperatures, E_{p2} , E_{p3} and E_{p4} are generally significant.

The application of the proposed error model allows for leaf psychrometers with large inherent error (associated perhaps with large I value) to be identified, and hence allows for the ordering of the units from most accurate to least accurate. It is recommended that all parameters required for the application of the model be known *a priori*, so that when the measured water potential is determined, the error of this value can be calculated.

2.6 SUMMARY

During condensation, steady state of the thermojunction is not attained in a short convenient time (Section 2.2.4). Most workers terminate cooling prior to steady state and this results in a non-equilibrium situation during evaporation (Fig. 2.3). It is therefore necessary to use a fixed cooling time of say 20 s if $\psi_v > -3\ 500$ kPa and 60 s for $\psi_v \leq -3\ 500$ kPa.

The common procedure of correcting calibration slopes (or voltages) at temperature T to that at 25 °C using Eq. 1.24 and the previously published a and b values has the main weakness that these a and b values were determined for a single water potential value over a range of temperatures and cannot be expected to apply to all psychrometers; in general, each psychrometer will possess a unique set of a and b values.

A model (model 1) is devised whereby the thermocouple psychrometer calibration slope $1/k_T$ at a given temperature T may be calculated. The input data for the model is the empirical calibration slope for a number of temperatures. The model is compared with that proposed by Brown (1970) and Wiebe *et al.* (1970) using data found in the literature (Table 2.2) and the empirical data from four leaf psychrometers (Table 2.1). In all cases, the proposed model is superior (Tables 2.5 to 2.7). Irregularly shaped thermojunctions have larger deviations, according to the models

used here (Table 2.7).

If a psychrometer is calibrated at one temperature, then measurement of the junction radius (defined to be the minor axis dimension) enables the theoretical values a_{th} , b_{th} , k_{25} (theory) and hence k_{T_0} (theory), to be determined (Fig. 2.7), T_0 being the calibration temperature (Section 2.4.2). Hence, application of Eq. 2.21 yields the calculated reciprocal calibration slope $k_T(c)$ (kPa/ μ V) as a function of temperature T . For *in situ* measurements, knowledge of the block temperature T enables $k_T(c)$ for the given psychrometer to be determined; for the measured voltage $V(T_w)$ the volumetric water potential ψ_v is $\psi_v = V(T_w) \cdot k_T(c)$. If the psychrometer has been calibrated at two temperatures $T_0(1)$ and $T_0(2)$ then the same procedure is applied for these temperatures using Eq. 2.22 or 2.23. This model is more accurate than the previous one involving a single temperature calibration, and also more accurate than previously used models, for the four leaf psychrometers used in this study.

It was possible to determine the errors involved in water potential measurement using thermocouple psychrometers (Section 2.5.2). These errors arose from the variability in the determination of the slope (S) and intercept (I) of the T vs $1/k_T$ curve (Eqs 2.26 and 2.27), the error in voltage measurement (which included zero offset and electronic noise errors) and error in temperature measurement (Eqs 2.30 and 2.31). Assuming a zero offset of $0,5 \mu$ V and an error in temperature of $0,25 ^\circ$ C, the total error ranged between 15,6 and 5,5 % (at 0 and $45 ^\circ$ C respectively) for the worst psychrometer and between 5,9 and 2,2 % for the best (Table 2.13).

CALIBRATION OF THERMOCOUPLE HYGROMETERS USING THE DEWPOINT TECHNIQUE

3.1 INTRODUCTION

The essential difference between the thermocouple psychrometer and the dewpoint hygrometer is that the former senses the wet bulb temperature in the measuring chamber of the instrument whereas the latter senses the dewpoint temperature. Both of these techniques use identical sensors but different voltmeter circuitry. In this discussion, thermocouple hygrometer will be used as a collective term for both thermocouple psychrometers and dewpoint hygrometers.

Until recently, the psychrometric technique was used almost exclusively compared to the dewpoint technique, for hygrometric water potential measurement. However, the dewpoint technique has recently become increasingly popular, but insufficient knowledge of calibration techniques necessitates investigation of this important aspect. The work reported in this chapter attempts to clarify aspects of the calibration of dewpoint hygrometers and presents a model for the calculation of measurement errors, as a function of temperature.

3.2 DEWPOINT COOLING COEFFICIENT DETERMINATION[†]

3.2.1 Introduction

In order to calibrate the hygrometer in the dewpoint mode, it is necessary to eliminate the effect of all forms of heat energy transfer other than latent heat energy transfer. This is achieved by using a dry atmosphere and setting the cooling coefficient Π to give a constant voltage output, at which $\Pi = \Pi_0$ (Section 1.2.3.1, p 13).

3.2.2 Materials and methods

The dry atmosphere required for correct setting of Π_0 was

[†] Based on the papers by Savage *et al.* (1981a, b, c)

attained by sealing dry finely ground silica gel (on filter paper) in the hygrometer, setting an arbitrary value of Π , cooling the thermojunction and observing the voltage output when the function switch is rotated to "DEWPOINT". If the voltage output increases, then the junction is being cooled (due to a loss of latent heat energy) and if the voltage decreases, then there is condensation (a gain of latent heat energy). The Π value is altered manually until the output voltage is constant, indicating no net transfer of heat energy from the thermojunction. Replacement of the silica gel by a NaCl solution of water potential ψ_v , followed by cooling and switching to "DEWPOINT" will cause the output voltage to converge onto the stationary voltage $V(T_{dp})$ provided Π and T are unaltered, where $V(T_{dp}) \propto \psi_v$ (Eq. 1.25, p 14). This stationary output voltage reflects changes in latent heat energy transfer only if $\Pi = \Pi_0$ is set correctly.

Ungar (1977) used standard NaCl solutions ranging in concentration from 0,1 to 2,0 mol/kg and a cooling time of 10 s for calibration of his hygrometers, while Michel (1979) always used cooling times of between 5 and 6 s when calibrating dewpoint hygrometers. The manufacturers (Anonymous, undated) advocate a cooling time of "a couple of seconds". Cooling times of 20 s were used in this investigation, with calibration performed as a function of temperature. Merrill leaf cutter type hygrometers, Wescor C-52 (chamber), soil and leaf hygrometers were used. All leaf hygrometer calibrations were performed in a constant temperature laboratory and all other hygrometer types in their calibration chambers were placed in a water bath to facilitate temperature control.

3.2.2 Results and discussion

3.2.2.1 *Setting of Π_0*

Dewpoint cooling coefficient values for several hygrometers for various stationary voltage outputs and voltage range settings of "0 TO 100" μV and "0 TO 30" μV , for a "dry" system, are shown (Table 3.1). An analysis of variance indicated significant differences, for a given dewpoint hygrometer, in Π_0 as a function of the stationary voltage and voltage range used. There are also

TABLE 3.1 Comparison between the mean of four Π_0 values[†] (in the body of the table with standard error values in brackets), measured at 25 °C, as a function of the 0 to 100 (R1) and 0 to 30 μ V (R2) ranges and the stationary voltage output, for various dewpoint hygrometers

Hygrometer type and number	Stationary voltage output (μ V)								
	15		20		25		30		
	R1	R2	R1	R2	R1	R2	R1	R2	
Leaf cutter hygro- meter	31	71,6	69,5	70,0	68,4	69,1	67,8	68,6	67,5
		(0,2)	(0,3)	(0,1)	(0,1)	(0,1)	(0,1)	(0,1)	(0,1)
	32	80,1	78,1	78,2	76,8	77,3	76,0	76,6	75,9
		(0,2)	(0,2)	(0,2)	(0,1)	(0,1)	(0,1)	(0,2)	(0,1)
	33	74,6	73,1	73,1	71,8	72,1	71,1	71,5	70,8
		(0,1)	(0,3)	(0,1)	(0,2)	(0,1)	(0,1)	(0,1)	(0,1)
Soil hygro- meter	21	64,1	62,5	63,6	62,2	62,7	61,8	62,0	61,3
		(0,2)	(0,3)	(0,1)	(0,3)	(0,2)	(0,2)	(0,1)	(0,1)
	22	65,3	63,5	64,7	63,6	63,9	63,2	63,2	62,9
		(0,2)	(0,2)	(0,2)	(0,2)	(0,1)	(0,2)	(0,1)	(0,1)
	23	63,4	61,8	62,2	61,0	61,5	60,5	61,0	60,1
		(0,1)	(0,4)	(0,1)	(0,3)	(0,1)	(0,2)	(0,0)	(0,2)
	24	58,8	57,0	58,5	57,3	57,6	57,0	57,0	56,4
		(0,3)	(0,4)	(0,1)	(0,1)	(0,2)	(0,1)	(0,1)	(0,2)
Chamber hygro- meter (C-52)	4	77,3	74,6	75,8	73,8	75,0	73,4	74,4	73,2
(0,1)		(0,2)	(0,2)	(0,2)	(0,1)	(0,1)	(0,2)	(0,1)	

[†] Determined once a day for four consecutive days in the absence of large temperature gradients (less than 0,2 μ V)

significant Π_0 differences between hygrometer types. Besides the fact that there may be electronic differences between the two voltage ranges, the reasons for the voltage range differences are not apparent. The manufacturers (Anonymous, undated) suggest that a stationary voltage between 15 and 30 μV be used. On the basis of data presented in Table 3.1, where it is shown that the dewpoint cooling coefficient is a function of the stationary voltage used, we suggest that only the "0 TO 100" μV range be used and that the cooling coefficient be defined as corresponding to a stationary voltage of 25 μV for 2 minutes.

3.2.2.2 Π_0 as a function of temperature

Slope and intercept differences in the Π_0 vs T relationship is shown for the four leaf hygrometers used in Section 2.3 (Table 3.2). The slope and intercept values shown in Table 3.2 differ, mainly as a result of differences in the electrical resistance between hygrometers. The $d\Pi_0/dT$ values are statistically different as the confidence interval for the slopes for each leaf hygrometer do not overlap except for hygrometer nos 3 and 4 (Table 3.2). For this reason, Π_0 should be determined as a function of temperature, for each hygrometer.

The manufacturers (Anonymous, undated) claim that $d\Pi_0/dT = (0,7 \pm 0,1) \mu\text{V}/^\circ\text{C}$, so that considering means only, we have:

$$\Pi_0(T) = \Pi_0(25^\circ\text{C}) + 0,7(T - 25), \tag{3.1}$$

theoretically and experimentally. The theoretical calculation assumes knowledge of the radius (r_j) and electrical resistance (R) of the sensing junction, as well as the magnitude of the cooling current from the microvoltmeter. Equation 1.26 (p 15) is then applied to determine the voltage (defined as Π_0) corresponding to this given electrical current (defined by Wescor Inc. as the "nominally optimum cooling current"). The three quantities: cooling current magnitude, r_j , and R, required to calculate $d\Pi_0/dT$, vary between hygrometers (r_j and R) and between microvoltmeters (cooling current). Assuming the theory to be correct, each hygrometer will therefore have a unique $d\Pi_0/dT$ value for a given microvoltmeter (Table 3.2). In the case of hygrometer no. 2, $d\Pi_0/dT = 0,55 \mu\text{V}/^\circ\text{C}$,

TABLE 3.2 Statistical data for the Π_0 vs T relationship for four leaf hygrometers

Hygrometer no.	Slope ($\mu\text{V}/^\circ\text{C}$)	Intercept (μV)	r	$S_{y.x}$ (μV)	No. of determinations of Π_0
1	$0,60 \pm 0,01$	$56,74 \pm 0,32$	0,9924	0,58	29
2	$0,55 \pm 0,02$	$55,45 \pm 0,43$	0,9909	0,65	29
3	$0,66 \pm 0,01$	$56,75 \pm 0,27$	0,9975	0,45	29
4	$0,65 \pm 0,02$	$57,07 \pm 0,41$	0,9933	0,63	31

which is less than the minimum value of the range quoted by Anon, undated. It would also seem possible that certain hygrometers could have $d\Pi_0/dT$ values greater than $0,85 \mu\text{V}/^\circ\text{C}$. Hence deviations of actual $d\Pi_0/dT$ values from $0,7 \mu\text{V}/^\circ\text{C}$ could be greater than 20 %.

The application of Eq. 3.1 may be generalized to:

$$\Pi_0(T) = \Pi_0(T_0) + 0,7(T - T_0) \quad 3.2$$

where T_0 is any convenient temperature greater than 20°C at which $\Pi_0(T_0)$ is determined. If the hygrometer is to be used under conditions such that $T \leq 15^\circ\text{C}$, Π_0 should be determined more accurately (Section 3.4).

3.3 CALIBRATION DATA AND SLOPE PREDICTION MODEL[†]

3.3.1 Introduction

Following the approach employed for thermocouple psychrometers (Section 2.4.2, p 38) it would be convenient if the dewpoint calibration slope could be predicted, as a function of temperature.

3.3.2 Results and discussion

The dewpoint curves ($V(T_{dp})$ vs ψ_v) are near linear, devia-

[†] Based on the paper by Savage *et al.* (1982)

ting only at about -3 500 kPa. Generally, with an increase in block temperature T , the output voltage corresponding to $\psi_v = 0$ kPa increases from 0,5 to 1,0 μV . This indicates that the dewpoint technique is not entirely independent of the junction wetting characteristics (Section 1.2.3.2, p 15).

Calibration data (Table 3.3) reveal differences between the leaf hygrometers used. The calibration characteristic that will be used in this discussion is $S_d(T)$ (with unit $\text{kPa}/\mu\text{V}$), the measured reciprocal slope of the dewpoint calibration curve at temperature T (Table 3.3, p 61). The theoretical reciprocal slope $S_d(\text{theory}; T_0)$ may be calculated using:

$$1/S_d(\text{theory}; T_0) = dV(T_{dp})/d\psi_v = -Se_0 \bar{V}_w / RTB. \quad 3.3$$

Using the temperature dependent constants of Table 1.1 (p 11),

$$10^3/S_d(\text{theory}; T_0) = -(6,30211 + 0,04462 T) \quad 3.4$$

where $0^\circ\text{C} \leq T \leq 45^\circ\text{C}$. The regression parameters of $1/S_d(\text{theory}; T_0)$ against T are: $r = 0,9996$, the standard error of the intercept ($-6,30211 \times 10^{-3} \mu\text{V}/\text{kPa}$) is $\pm 0,01207 \times 10^{-3} \mu\text{V}/\text{kPa}$ and that of the slope ($-0,04462 \times 10^{-3} \mu\text{V kPa}^{-1} \text{ }^\circ\text{C}^{-1}$) is $\pm 0,00045 \times 10^{-3} \mu\text{V kPa}^{-1} \text{ }^\circ\text{C}^{-1}$. The standard error of the estimate of $1/S_d(\text{theory}; T_0)$ on T is $\pm 0,02054 \times 10^{-3} \mu\text{V}/\text{kPa}$. Values of $1/S_d(\text{theory}; T_0)$ and $1/S_d(T)$ differ over the temperature range 15 to 35°C for the leaf hygrometers used (Table 3.3). For this reason, there is no substitute for empirical calibration, but this requirement is less exacting than that for thermocouple psychrometers. Baughn (1974) regarded the good agreement between $S_d(\text{theory}; T_0)$ and $S_d(T)$ as fortuitous and calibrated his hygrometers over a wide temperature range. However, calibration at a number of temperatures is tedious and requires good temperature control in the laboratory. A simplified technique would therefore be useful. We assume that a calculated value, $S_d(c)$, may be determined using

$$S_d(c) = S_d(\text{theory}; T) \cdot S_d(T) / S_d(\text{theory}; T_0) \quad 3.5$$

where $S_d(\text{theory}; T)$ and $S_d(\text{theory}; T_0)$ are the reciprocal calibra-

tion slopes at temperatures T and T_0 respectively (cf. Eq. 2.19, p 39). Then

$$S_d(c) = -10^3 \cdot S_d(T_0) / \{S_d(\text{theory}; T_0) \cdot (6,30211 + 0,04462 T)\} \quad 3.6$$

applying Eq. 3.4, where $S_d(\text{theory}; T_0)$ may be calculated also using Eq. 3.4.

For the hygrometers used in this study, a comparison between $S_d(c)$ using Eq. 3.4 (based on $S_d(T_0)$ being the sensitivity at or near 25°C) and the empirically measured values at the same temperature yield a $\sqrt{\Sigma D^2 / (n - 1)}$ value of $\pm 1,5\%$ (Table 3.4). The magnitude of the error relative to the measured value at that temperature, $|D|$, never exceeded 4% (Table 3.4). The use of Eq. 3.6 does not circumvent determining Π_0 as a function of temperature T . For a measured output $V(T_{dp})$ at temperature T ,

$$\psi_V(T) = V(T_{dp}) \cdot S_d(c) \quad 3.7$$

only if $\Pi = \Pi_0(T)$ is the correct dewpoint cooling coefficient.

The dewpoint and psychrometric techniques are compared by evaluating the ratios of the calibration curve reciprocal slopes, $k_T / S_d(T)$ (Table 3.3). Values of k_T were previously determined (Table 2.4, p 34). In general, at 15°C , $1/S_d(T)$ is approximately double $1/k_T$. The dewpoint technique is not as temperature sensitive as the psychrometric, but the relatively favourable temperature characteristics of the former diminish somewhat with an increase in temperature, up to 35°C (Table 3.3).

3.4 STATISTICAL ASSESSMENT OF ERRORS IN DEWPOINT HYGROMETER WATER POTENTIAL MEASUREMENT[†]

3.4.1 Introduction

The calculation of error inherent in hygrometric water potential measurement has apparently received scant attention. The aim of this section is to present a method for estimating the standard

[†] Based on the paper by Savage *et al.* (1983) submitted for publication to *Crop Science*

TABLE 3.3 Statistical data[†] for three leaf hygrometers. The calibration slopes for an ideal hygrometer is also shown together with the $k_T/S_d(T)$ ratio for each hygrometer, as a function of temperature

Hygrometer no.	Temperature T (°C)	$10^3/S_d(T)$ ($\mu\text{V}/\text{kPa}$)	Intercept (kPa)	r	No. of data points	$k_T/S_d(T)$	$S_{y,x}$ (kPa)
2	15,0	$-6,863 \pm 0,023$	$-0,4 \pm 7,7$	0,9999	11	2,89	14,8
	22,0	$-7,176 \pm 0,055$	$13,4 \pm 17,7$	0,9997	11	2,24	34,2
	24,8	$-7,294 \pm 0,043$	$53,9 \pm 14,2$	0,9998	11	2,06	26,9
	35,4	$-7,565 \pm 0,068$	$103,3 \pm 22,7$	0,9996	11	1,58	42,5
3	15,0	$-6,960 \pm 0,068$	$2,6 \pm 22,3$	0,9996	11	2,64	43,1
	22,0	$-7,043 \pm 0,071$	$62,8 \pm 23,7$	0,9995	11	2,00	44,9
	24,8	$-7,109 \pm 0,087$	$119,6 \pm 29,7$	0,9993	11	1,83	55,3
	35,4	$-7,595 \pm 0,076$	$102,6 \pm 25,0$	0,9996	11	1,45	46,9
4	15,0	$-6,875 \pm 0,075$	$-83,2 \pm 23,9$	0,9995	10	2,84	47,6
	22,0	$-7,072 \pm 0,081$	$41,4 \pm 27,0$	0,9994	10	2,12	51,5
	24,8	$-7,276 \pm 0,076$	$38,2 \pm 24,9$	0,9995	10	1,96	47,6
	35,4	$-7,669 \pm 0,076$	$100,3 \pm 24,8$	0,9996	10	1,50	46,6
Ideal hygrometer	15,0	-6,158					
	22,0	-6,439					
	24,8	-6,544					
	35,4	-6,962					

[†] Excluding the point corresponding to 1,0 mol/kg

TABLE 3.4 Comparison of the measured ($1/S_d(T)$) and the calculated ($1/S_d(c)$) calibration slopes at various temperatures for three dewpoint hygrometers. Values of $S_d(c)$ are based on the measured slope at 24,8 °C. The error between the measured and calculated slopes (D) is relative to $S_d(T)$ at the particular temperature

T (°C)	Leaf hygrometer number								
	2			3			4		
	$10^3/S_d(T)$ ($\mu\text{V}/\text{kPa}$)	$10^3/S_d(c)$ ($\mu\text{V}/\text{kPa}$)	D (%)	$10^3/S_d(T)$ ($\mu\text{V}/\text{kPa}$)	$10^3/S_d(c)$ ($\mu\text{V}/\text{kPa}$)	D (%)	$10^3/S_d(T)$ ($\mu\text{V}/\text{kPa}$)	$10^3/S_d(c)$ ($\mu\text{V}/\text{kPa}$)	D (%)
15,0	-6,863	-6,864	0,0	-6,960	-6,689	3,9	-6,875	-6,847	0,4
22,0	-7,176	-7,171	0,8	-7,043	-6,98 ^o	0,8	-7,072	-7,153	-1,1
24,8	-7,294	-7,294	0,0	-7,109	-7,109	0,0	-7,276	-7,276	0,0
35,4	-7,565	-7,760	-2,6	-7,595	-7,562	0,4	-7,669	-7,741	-0,9

error of measured water potential, as a function of temperature, ⁶² for leaf psychrometers. The approach employed is similar, conceptually, to that of the psychrometric technique (Section 2.5, p 43).

3.4.2 Theory

Equation 3.5 may be written in the form (where $V_d = V(T_{dp})$):

$$\psi_v = -10^3 \cdot V_d \cdot S_d(T_0) / \{S_d(\text{theory}; T_0)(6,30211 + 0,04462 T)\} \quad 3.8$$

where it is assumed that the dewpoint cooling coefficient Π is set at its correct value Π_0 (Campbell *et al.*, 1973) and the extrapolation of $S_d(T_0)$ to $S_d(T)$ involves no error. Five sources of error therefore arise: 1. the calibration error (E_{d1}) at temperature T_0 ; 2. the error (E_{d2}) due to extrapolating the calibration curve slope at a reference temperature T_0 to that at temperature T ; 3. the error (E_{d3}) due to incorrectly setting the dewpoint cooling coefficient (Π_0) at a value Π ; 4. error in dewpoint voltage measurement (E_{d4}); 5. error in temperature measurement (E_{d5}).

The value of E_{d1} is defined, for a given hygrometer, by the coefficient of variation for an estimate of ψ_v from a measured V_d , using the appropriate calibration relationship:

$$E_{d1} = S_{y.x}(\psi_v \text{ vs } V_d) / \bar{\psi}_v \quad 3.9$$

where $S_{y.x}(\psi_v \text{ vs } V_d)$ is the standard error of an estimate of ψ_v from V_d and $\bar{\psi}_v$ is the mean water potential of the range of values used for calibration.

The error resulting from extrapolation of the calibration curve slope, E_{d2} , has been calculated (Table 3.4) for a number of temperatures. A value of 1,5 %[†] was therefore used for E_{d2} , independent of temperature.

The third source of error, E_{d3} , is given by

$$E_{d3} = -\{k_T/S_d(T) - 1\} \{1 - \Pi_0/\Pi\} \quad 3.10$$

(Campbell *et al.*, 1973).

The error in dewpoint voltage measurement, E_{d4} , is given by

[†] The mean error magnitude for the hygrometers used (Table 3.4) is 0,9 %, but the variability is large. The value of 1,5 % is between the mean and maximum values and was therefore regarded as representative

$(1/\psi_V)(\partial\psi_V/\partial V_d) \cdot \sigma(V_d)$ (Eq. 2.24, p 44). Hence, from Eq. 3.8,

$$E_{d4} = \sigma(V_d)/V_d. \quad 3.11$$

This error component includes the influence of electronic noise and zero offsets on the measured voltage output V_d , discussed in Section 2.5.4, p 49 and 50.

Similarly, the error in temperature, E_{d5} , is given by

$$E_{d5} = 0,04462 \cdot \sigma(T)/(6,30211 + 0,04462 T), \quad 3.12$$

applying Eq. 3.8.

The total error for the dewpoint technique is therefore

$$E_d = (E_{d1}^2 + E_{d2}^2 + E_{d3}^2 + E_{d4}^2 + E_{d5}^2)^{\frac{1}{2}}. \quad 3.13$$

3.4.3 Results and discussion

The advantage of the presented theory is that it is possible to evaluate the error associated with a measured water potential for any hygrometer used in the dewpoint mode. These errors can be converted into measured water potential confidence intervals (Eq. 2.28, p 45) by substituting V_d for V_p .

The contribution by each of the component errors (E_{d1} , E_{d2} , E_{d3} , E_{d4} , E_{d5}) to the total error differs considerably. The calibration error E_{d1} is usually within $\pm 1\%$ and the extrapolation error E_{d2} within $\pm 4\%$ but averaged $\pm 1,5\%$ (Table 3.4).

The major component of the total error arises from the difficulty in setting Π to its correct value Π_0 (E_{d3}) (Table 3.5). The multiplicative factor $k_T/S_d(T) - 1$ together with $1 - \Pi_0/\Pi$ define the error E_{d3} (Eq. 3.10). The main reason for the large value of E_{d3} is because of the magnitude of the multiplicative factor $k_T/S_d(T) - 1$ (Eq. 3.10). As the temperature T decreases, the ratio $k_T/S_d(T)$ increases because $1/k_T$ approaches zero more rapidly than does $1/S_d(T)$. Consequently, E_{d3} increases to infinity at $T = I$ (Fig. 3.1) where I is defined in Section 2.3.2, p 30. The temperature dependence of $k_T/S_d(T)$ has the form:

TABLE 3.5 Dewpoint hygrometer error components, subcomponents[†] and k_T/S_d as a function of temperature (Eqs 3.9 to 3.16). A gap in the table implies a temperature independent error. A zero offset of 0,5 μ V is assumed

Dew- point hygro- meter no.	T (°C)	Total error E_d (%)	k_T/S_d		Component errors (%) ^{††}							
			E_{d1}	E_{d2}	E_{d3}	E_{d32}	E_{d33}	E_{d4}	E_{d41}	E_{d42}	E_{d5}	
1A	0	5,6	7,1	1,6	1,5	5,0	0,8	0,4	0,7	0,1	0,7	0,2
	10	3,3	3,7			3,2			0,7	0,2	0,6	0,2
	20	2,7	2,7			1,4			0,6	0,2	0,6	0,2
	30	2,5	2,1			0,9			0,6	0,3	0,6	0,2
	40	2,4	1,7			0,6			0,7	0,4	0,6	0,1
5A	0	4,6	4,9	1,6	1,5	4,1	1,0	0,4	0,7	0,1	0,6	0,2
	10	3,1	3,3			1,9			0,6	0,1	0,6	0,2
	20	2,5	2,5			1,6			0,6	0,2	0,6	0,2
	30	2,2	2,0			1,1			0,6	0,3	0,6	0,2
	40	2,1	1,7			1,0			0,6	0,4	0,6	0,1
7A	0	5,1	5,6	1,6	1,5	4,4	0,9	0,4	0,7	0,1	0,7	0,2
	10	3,5	3,4			2,3			0,6	0,1	0,6	0,2
	20	3,0	2,5			1,4			0,6	0,2	0,6	0,2
	30	2,8	2,0			0,9			0,6	0,3	0,6	0,1
	40	2,2	1,6			0,5			0,6	0,4	0,5	0,1
2A	0	8,9	6,5	1,6	1,5	8,4	1,5	0,4	0,7	0,1	0,7	0,2
	10	5,0	3,8			4,2			0,6	0,1	0,6	0,2
	20	3,8	2,7			2,6			0,6	0,2	0,6	0,2
	30	3,3	2,2			1,8			0,6	0,3	0,6	0,1
	40	3,1	1,8			1,2			0,5	0,4	0,5	0,1

[†] The error at low temperatures for hygrometer no. 1A is due to the large $k_T/S_d(T)$ value whereas no. 2A has a slightly smaller $k_T/S_d(T)$ value but a larger E_{d32} value, at low temperatures

^{††} Only error magnitudes are shown

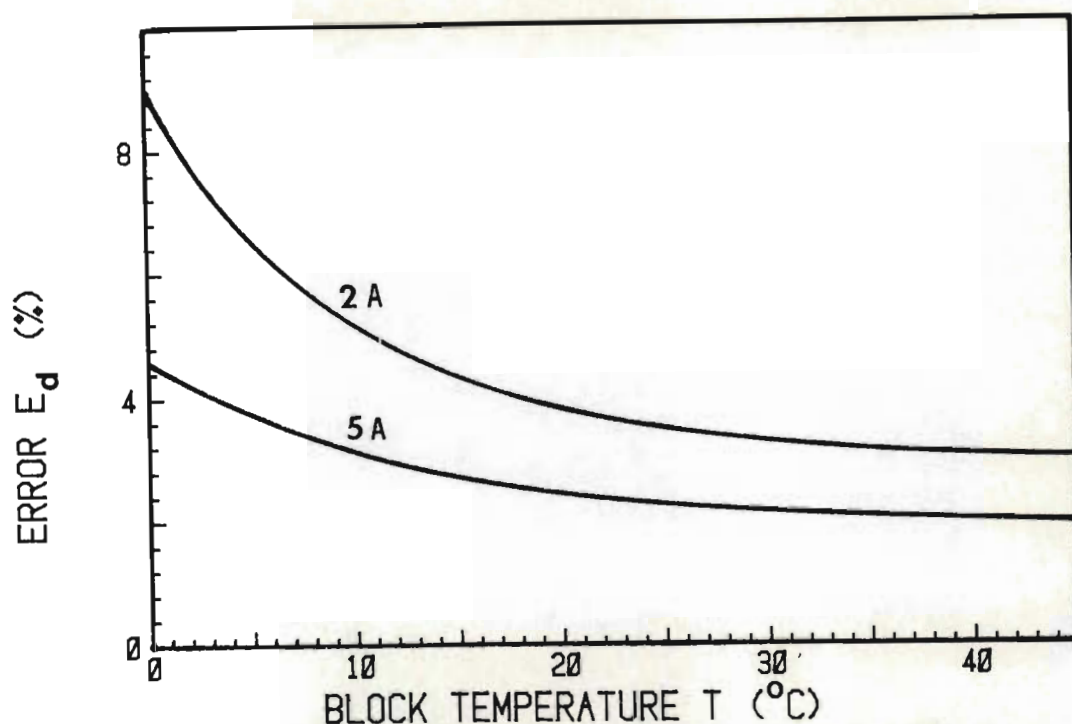


FIG. 3.1 Calculated error, E_d , in measured water potential for the best (no. 5A) and the worst (no. 2A) dewpoint hygrometers, as a function of temperature (cf. Fig. 2.9, p 49)

$$k_T/S_d(T) = A(T - I)^B \quad 3.14$$

for a given hygrometer where I has been defined previously, and A and B are empirical constants. For example, for leaf hygrometer no. 2, $k_T/S_d(T) = 40,76 (T - 9,94)^{-0,797}$ (Fig. 3.2) with a r value of 0,988 (total degrees of freedom of 27). For the leaf hygrometers used in this study, A ranged between 36,0 and 46,6 and B between -0,86 and -0,78 and r between 0,976 and 0,998 (Table 3.6).

In considering the factors which affect the setting of Π at its correct value, it should be noted that: Π_0 is temperature dependent (Campbell *et al.*, 1973); there is random error associated with this temperature dependence determination; there is a physical limitation in setting Π_0 to its predetermined, temperature-corrected value. Each of these error subcomponents has an associated value, E_{d31} , E_{d32} and E_{d33} respectively.

If the temperature dependence of Π_0 is accounted for, then E_{d31} is zero (Campbell *et al.*, 1973). The random error associated with the Π_0 vs T relationship, may be defined by:

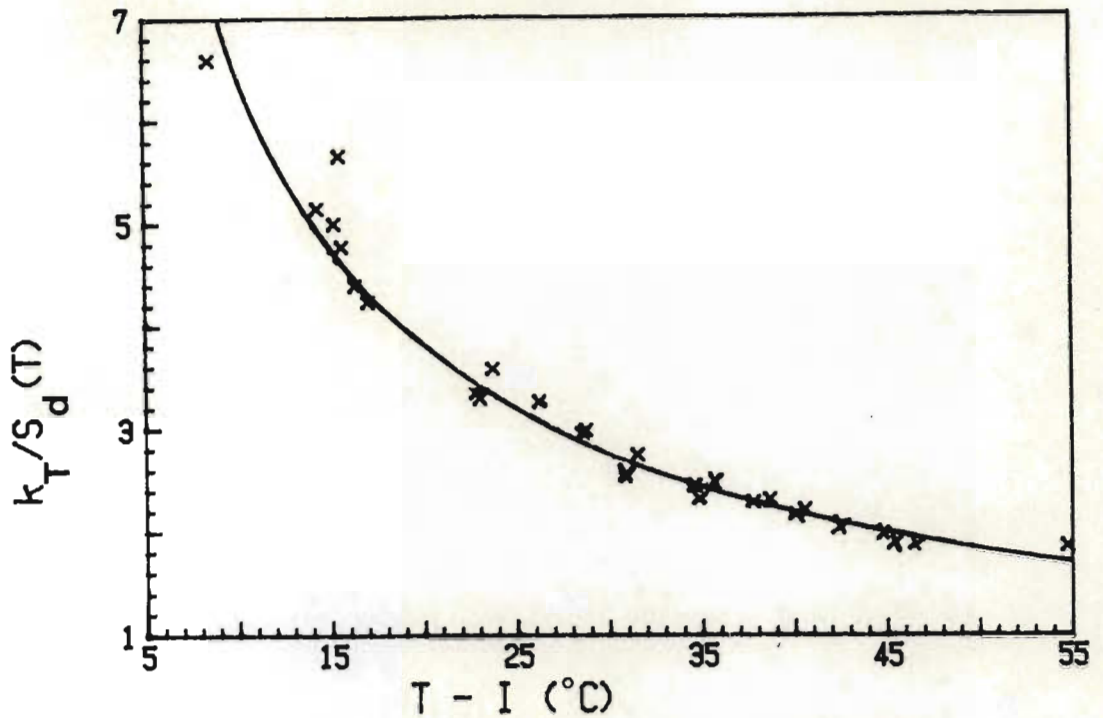


FIG. 3.2 $k_T/S_d(T)$ as a function of $T - I$ for hygrometer no. 2
For this hygrometer, $I = -9,941$ °C (Table 3.6). Each
point represents a voltage measurement for a given
water potential at a measured temperature

TABLE 3.6 Parameters associated with dewpoint error calculation,
for a few hygrometers (Table 3.5)

	Hygrometer number			
	1A	5A	7A	2A
$I \pm SE(I)$ (°C)	$-8,02 \pm 0,695$	$-15,76 \pm 0,820$	$-12,26 \pm 0,602$	$-9,94 \pm 0,685$
A (Eq. 3.14)	35,98	46,64	46,05	40,76
B (Eq. 3.14)	-0,783	-0,818	-0,840	-0,797
r (k_T/S_d vs $T-I$)	0,9904	0,9936	0,9973	0,9877
Total error range from 0 to 40 °C	5,6 to 2,4	4,6 to 2,1	5,1 to 2,2	8,9 to 3,1
(Table 3.5) (%)				

$$E_{d32} = S_{y.x}(\Pi_0 \text{ vs } T) / \bar{\Pi}_0 \quad 3.15$$

where $S_{y.x}(\Pi_0 \text{ vs } T)$ is the standard error of an estimate of Π_0 from T and $\bar{\Pi}_0$ is the mean Π_0 value for the temperature range used. Values of E_{d32} for the hygrometers under consideration did not exceed $\pm 1,5 \%$ over the temperature range 15 to 35 $^{\circ}\text{C}$ (Table 3.5). For the analogue readout microvoltmeter used in this study, there is a physical limitation imposed on the setting of Π_0 to its predetermined value (error E_{d33}), influenced by the electronic resistor that is used to set Π_0 and a temperature limitation arising from changes in the reference junction temperature (zero drift). As in the case of the psychrometric mode, the zero drift error is difficult to enumerate. However, this is expected to be greater for the dewpoint compared to the psychrometric technique. In addition, the zero drift error will result in the originally correct Π_0 value changing to an incorrect value. Since $d\Pi_0/dT \approx 0,7 \mu\text{V}/^{\circ}\text{C}$ (Anonymous, undated), a change in temperature of 1 $^{\circ}\text{C}$ during measurement will result in a Π_0 error of $\pm 0,7 \mu\text{V}$. However, unlike soil psychrometers, it is easier to insulate leaf hygrometers to dampen temperature fluctuations. In order to reduce the magnitude of E_{d33} , the analogue readout unit should be supplemented by a digital display and the Π_0 resistor used should be one that has a lesser effect on Π_0 . Without these changes, generally, it was not possible to set Π_0 to within $0,25 \mu\text{V}$ of its predetermined value, assuming no reference junction temperature changes. We therefore define E_{d33} as $0,25/\bar{\Pi}_0$, where $\bar{\Pi}_0$ was assumed to have the value of $70,5 \mu\text{V}$ (a temperature average value for all leaf dewpoint hygrometers).

Combining these three subcomponent errors, it was possible to calculate $1-\Pi_0/\Pi$ from:

$$1-\Pi_0/\Pi = (E_{d31}^2 + E_{d32}^2 + E_{d33}^2)^{\frac{1}{2}}, \quad 3.16$$

the results of which are summarized in Table 3.5. The total error arising from the difficulty in setting Π_0 (E_{d33}) was usually within $\pm 0,5 \%$, which is much lower than the value of $\pm 2 \%$ suggested by Campbell *et al.* (1973). If it is only possible to set Π to within 2% of Π_0 , the errors shown in Table 3.5 will be greater,

depending on the ratio $k_T/S_d(T)$.

The major error component of voltage (V_d) measurement arises from the presence of large zero offset values. The other subcomponent error (electronic noise) is discussed in Section 2.5.4 (p 49 and 50). Only Michel (1979) appears to have investigated the effect of offsets on the dewpoint voltage measurement. Failing better information, we assume that $E_{d4} = \sigma(V_d)/V_d$ is identical to that for the psychrometric technique (Eq. 2.30), which incorporates the electronic noise error and the zero offset error equation obtained by Brown & Bartos (1982).

As in the psychrometric technique, we assume that $\sigma(T) = \pm 0,25$ °C so that E_{d5} for the dewpoint technique is as presented in Eq. 3.12.

A calculation of the total error associated with the dewpoint technique (incorporating Eqs 3.9 to 3.12 and E_{d2}), shows that in spite of the dewpoint technique calibration curve slopes being less temperature sensitive than psychrometric counterparts, the measurement error in water potential can be greater, particularly at low temperatures (Table 3.5, Fig. 3.1). This is attributable to the difficulty in setting Π_0 accurately. The error curve presented by Campbell *et al.* (1973) appears to account for the error involved in not allowing for the temperature dependence of Π_0 (E_{d31}). The values they show were calculated using a theoretically calculated $k_T/S_d(T)$ value and the $S_d(25$ °C) value, uncorrected for temperature deviations from 25 °C. These authors claim that typical errors are equivalent to Π being within ± 2 % of Π_0 . If this is the case, the total error E_d is typically ± 12 % at 0 °C and ± 6 % at 15 °C, using measured $k_T/S_d(T)$ values and incorporating the other error components (E_{d1} , E_{d2} and E_{d32}). The errors shown in Table 3.5 should be regarded as minimum values for two main reasons. Firstly, the slope extrapolation error was assumed to be 1,5 % on average but can be as high as 4 % (Table 3.4). Secondly, the zero drift error, which also affects the setting of Π_0 , has been neglected. For these reasons, it is not meaningful to compare the psychrometric errors shown in Table 2.13 (p 51) with those in Table 3.5.

3.5 SUMMARY

Because of differences between dewpoint hygrometers, each hygrometer should be individually calibrated. However, it is not necessary to calibrate dewpoint hygrometers at several different temperatures, as is required for thermocouple psychrometers. It is possible to calculate the slope of the calibration curve at any given temperature, using appropriate theory (Eq. 3.5). Errors of magnitude less than 4 % occur using this procedure (Table 3.4), provided the dewpoint cooling coefficient $\Pi_0(T)$ is set accurately for the given temperature.

In spite of the fact that dewpoint hygrometers appear to be much less temperature sensitive than thermocouple psychrometers (Table 3.3), the correct voltage measured depends on an accurate setting of $\Pi_0(T)$. This is particularly true for temperatures $T \leq 15^\circ\text{C}$. It is shown that the setting of $\Pi_0(T)$ may be subjective (Table 3.1). Furthermore, the relationship between Π_0 and T between hygrometers is different (Table 3.2). Hence $\Pi_0(T)$ should be determined for the *in situ* temperature range, for each hygrometer.

A statistical analysis showed that the magnitudes of the error in dewpoint water potential was critically dependent on the dewpoint cooling coefficient Π_0 (Table 3.5). Provided this coefficient is a known function of temperature, can be determined accurately at a given temperature and can then be set within $\pm 0,25 \mu\text{V}$ of this predetermined temperature corrected value when performing field measurements, these errors are generally within $\pm 4 \%$ at 15°C , and $\pm 8 \%$ at 0°C . At low temperatures, the dewpoint technique often has little advantage over the psychrometric technique in terms of the magnitude of the error.

CHAPTER 4

LABORATORY MEASUREMENT OF LEAF WATER POTENTIAL USING
THERMOCOUPLE PSYCHROMETERS, A SCHOLANDER PRESSURE
CHAMBER AND A J-14 HYDRAULIC PRESS[†]

4.1 INTRODUCTION

Two accurate but destructive methods for the measurement of plant leaf water potential involve the use of the Scholander pressure chamber (Scholander, Hammel, Bradstreet & Hemmingsen, 1965; Ritchie & Hinckley, 1975) and the thermocouple psychrometer. Recently however, a new technique using a hydraulic press has been introduced for measurement of leaf water and osmotic potential (Campbell, Papendick, Rabie & Shayo-Ngowi, 1979; Shayo-Ngowi & Campbell, 1980). Very few comparative measurements of total water potential, using the hydraulic press and thermocouple psychrometer or pressure chamber, have been performed. Yegappan & Mainstone (1981) compared field measured cocoa leaf water potentials using the press and the pressure chamber.

The hydraulic press is simple, fast and can be used for soft tissue but requires comparison against either the pressure chamber or the thermocouple psychrometer, for each plant species investigated. The endpoint being somewhat subjective, requires exact definition.

This section involves comparison of leaf water potential measured using the pressure chamber, hydraulic press and chamber type psychrometer. These measurements employ destructive sampling. Commercially available soil psychrometers sealed in stainless steel chambers enable much larger leaf areas to be used compared to using *in situ* leaf psychrometers (Chapter 5). Furthermore, cost limits the number of leaf psychrometers.

4.2 LITERATURE REVIEW

Barrs & Kramer (1969) found that a cut leaf size of 70 mm by 20 mm was large enough to avoid error due to metabolic changes

[†]Adapted from the paper by Grant, Savage & Lea (1981)

which occur in leaf tissue immediately following excision (Macnicol, 1976), in that a piece of size 70 mm by 40 mm yielded the same water potential. However Talbot, Tyree & Dainty (1975) calculated from the data of Barrs & Kramer (1969) that if the ratio of the cut surface area (A) to the volume (V) of leaf material was between 0,07 and 0,12 mm²/mm³, then the water potential of these different sized cut leaf slices were not significantly different. The reason for the lower limit of 0,07 mm²/mm³ is not clear. So for example, a 20 mm by 20 mm leaf section, with cuts on all four sides, has an A/V value of 0,20 mm²/mm³. Consequently, the measured leaf water potential of this segment cannot be expected to represent the true leaf water potential prior to excision (according to Talbot *et al.*, 1975). Ungar (1977) used leaf discs with A/V = 0,60 mm²/mm³ and sealed these in a Wescor C-52 chamber psychrometer. Metabolic changes must be accelerated in a leaf segment having an A/V value of this magnitude and consequently, as noted by Feyen, Belmans & Hillel (1980), water potential values are not representative of the plant.

A minimum time of 1 h for vapour and temperature equilibration has been reported by Phillips (1981) and 2 h by Johnson & Brown (1977) and Brown & Collins (1980) for leaf segments sealed in a psychrometer chamber. Some workers have used times of at least 20 h (Talbot *et al.*, 1975) and others 10 h (Redmann, 1976), but then presumably metabolic changes result in non-representative tissue water potentials (Oertli, Aceves-Navarro & Stolzy, 1975). Walker (1981) found that an equilibration time of 4 h was sufficient for wheat leaves and filter paper material if $\psi_v > -2\ 500$ kPa.

Factors affecting accuracy of leaf water potential measurement using the pressure chamber include:

1. leaf desiccation effects (Boyer, 1967; Puritch & Turner, 1973; Wenkert, Lemon & Sinclair, 1978);
2. rate of increasing pressure (Slavik, 1974, p 71);
3. the increase in leaf water potential following excision (Chapter 5).

The effects of the first factor can be avoided by lining the pressure chamber with wet tissue paper and by covering the leaf prior to excision. Waring & Cleary (1967) suggested a constant pressure

rate increase less than 70 kPa/s. Other factors affecting accuracy are discussed by Turner (1981).

Increasing attention is being paid to leaf osmotic potential measurements in plant water relations research (Acevedo, Fereres, Hsiao & Henderson, 1979; Oosterhuis & Walker, 1982; Walker & Oosterhuis, 1982). The leaf moisture desorption curve was originally derived using the pressure-volume technique (Tyree & Hammel, 1972; Cheung, Tyree & Dainty, 1975; Wilson, Fisher, Schulze, Dolby & Ludlow, 1979) through sequential measurement of cell sap volume obtained by incremental increase in pressure applied to a leaf. The pressure-volume technique has been adapted by others (Talbot *et al.*, 1975; Richter, 1978; Richter, Duhme, Glatzel, Hinckley & Karlic, 1980; Kyriakopoulos & Richter, 1981).

The basic relationship between osmotic potential and volume of solution (Richter *et al.*, 1980), as derived from the Van't Hoff equation is:

$$\psi \text{ (osmotic)}. \quad V = \text{constant}. \quad 4.1$$

More specifically,

$$1/P = (V_0 - V_e)/(RTn_s - f(V)) \quad 4.2$$

where P is the balance pressure, V_0 the original symplasmic volume, V_e the total volume of cell sap expressed, R the universal gas constant, T the absolute temperature, n_s the amount of solute substance and $f(V)$ the volume averaged turgor (Cheung *et al.*, 1975; Ritchie & Hinckley, 1975). At zero turgor potential,

$$1/P = (V_0 - V_e)/RTn_s \quad 4.3$$

and, if there is no change in n_s during the desiccation process, V_e is proportional to the relative saturation deficit[†], RSD:

$$\text{RSD} = \frac{\text{turgid mass} - \text{sample mass}}{\text{turgid mass} - \text{dry mass}} \times 100. \quad 4.4$$

[†]RSD is referred to as water saturation deficit by Richter (1978)

A change in n_s is unlikely in the absence of sunlight (Acevedo *et al.*, 1979).

The point of incipient plasmolysis occurs at the intersection of the line representing the regression of the reciprocal of total potential on RSD and the line representing the regression of the reciprocal of osmotic potential on RSD (Tyree & Hammel, 1972). At lower RSD, the vertical distance between these two curves is related to the magnitude of the turgor component. At higher RSD the two curves are concurrent, and over this range the total leaf water potential is equal to osmotic plus matric potential (zero turgor) (Campbell *et al.*, 1979).

4.3 MATERIALS AND METHODS

The experiment was conducted in a constant temperature (25 °C) laboratory. Newly mature, field-grown soybean trifoliates (*Glycine max* (L) Merr. (cv. Oribi)) were cut and placed in an enclosed glass container with their petioles in distilled water. The following morning the turgid trifoliates were surface dried and their mass determined (turgid mass). The trifoliolate mass was again determined after the leaf material was allowed to dry out on tissue paper for time periods ranging from 0 to 240 min. This mass will be referred to as the sample mass. The trifoliates were then immediately subsampled for total water potential determinations using a thermocouple psychrometer, a pressure chamber[†], and a hydraulic press^{††} (Fig. 4.1). Leaf material was then dried at 100 °C overnight for the dry mass determination.

Metal screen soil psychrometers^{†††} had previously been individually calibrated (20 s cooling time) in metal chambers^{††††} (Brown & Collins, 1980; Fig. 2.2) equipped with rubber O-ring seals. Filter paper (Whatman no. 41) of 20 mm width was rolled around a 5 mm diameter metal rod and inserted into the chamber. The filter

[†]Available from PMS Instrument Co., Corvallis, Oregon, U.S.A.

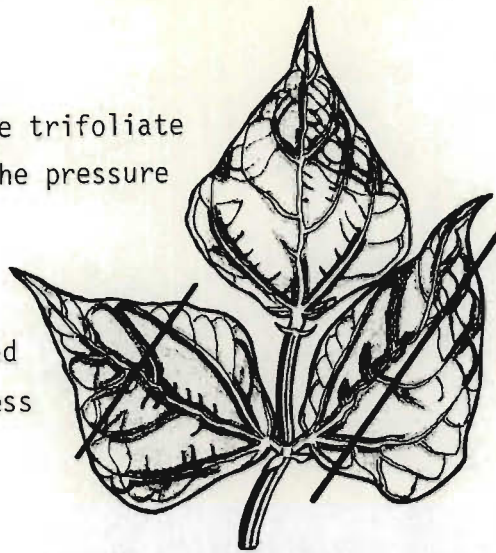
^{††}Campbell Scientific Inc., P.O. Box 551, Logan Utah 84321, U.S.A.

^{†††}Merrill Speciality Equipment, P.O. Box 140A, Logan Utah 84321, U.S.A.; Model no. PSY-200

^{††††}South African Instrumentation, 18 Harvey Road, Durban, South Africa 4001; Swagelok SS1010-C and SS400-R10

Remainder of the trifoliolate
was placed in the pressure
chamber

Subsample placed
in the J-14 press



Subsample sealed in the
psychrometer chamber

FIG. 4.1 Diagrammatic representation of a soybean trifoliolate. The procedure for the leaf subsampling is indicated

paper was saturated with one of a range of NaCl (AR) salt solutions of known water potential. The metal chambers were placed in an insulated chamber to further dampen temperature variations. Subsequent to this study, an insulated water bath was always used. At least 4 h was allowed for temperature and vapour equilibration. The psychrometer output voltage was recorded using a chart recorder.

The 4 h equilibration time used here is a compromise between the previously used times but has recently been confirmed as adequate for wheat (Walker & Oosterhuis, 1982). Equilibration times of less than 2 h caused inaccurate results, especially when using leaf material whose water potential was less than about -1 200 kPa, as measured using the pressure chamber.

Leaf samples for the psychrometers were cut parallel to the midrib (Fig. 4.1) and were approximately 50 mm long and less than 20 mm wide. The ratio of the cut surface area to volume of leaf material varied between 0,05 and 0,10 mm²/mm³ and hence error in ψ_v due to leaf excision was apparently minimal.

When using the pressure chamber, standard procedures were followed (Scholander *et al.*, 1965) with pressure being increased at a rate of 100 kPa per 6 to 8 s.

Leaf samples for the hydraulic press were cut across the distal end of the leaf in order to reduce capacitance and metabolic effects (Macnicol, 1976). Samples were placed on absorptive filter paper to clarify endpoints, this being defined as the pressure at which water along the cut edge of the interveinal tissue first

appears (Heathcote, Etherington & Woodward, 1979). Appearance of moist spots around cut ends of the vascular system was not used as the endpoint (defined as endpoint A by Yegappan & Mainstone, 1981). All endpoints were observed on the abaxial side only.

In this experiment, individual measurements were made on different trifoliates at varying degrees of desiccation to avoid measurement technique effects upon subsequent observations.

4.4 RESULTS AND DISCUSSION

4.4.1 Leaf water potential comparisons

Total leaf water potential, measured with the thermocouple psychrometer, is linearly correlated with that measured using the pressure chamber (Fig. 4.2) and the hydraulic press (Fig. 4.3). Statistical data for the linear regression analyses (Table 4.1, p 77) show that in both cases r is greater than 0,94. The slope of the linear relationship between pressure chamber and psychrometer water potentials (Fig. 4.2) is close to unity but less than unity in the case of hydraulic press and psychrometer water potential (Fig. 4.3). A linear relationship with a slope of unity was established by Shayo-Ngowi & Campbell (1980) for the pressure chamber and the hydraulic press using previously frozen wheat and maize leaves. Bristow, van Zyl & de Jager (1981) found a curvilinear relationship between hydraulic press and pressure chamber measurements compared to the linear relation presented here (Fig. 4.4, p 77). Also, for a given leaf water potential measured using the psychrometer or the pressure chamber, water potentials obtained using the hydraulic press were lower (more negative) than those of Bristow *et al.* (1981). Two reasons for this are postulated:

1. samples used in this study generally had one cut surface and the cut surface area to volume ratio was within the limits suggested by Talbot *et al.* (1975);
2. the endpoint in this study did not include water emergence from severed vascular tissue, but only from mesophyll tissue. Distinction between these two water emergence sources was not made by Bristow *et al.* (1981) (possibly because of the difficulty in doing so with monocotyledonous tissue) nor by Heathcote *et al.* (1979).

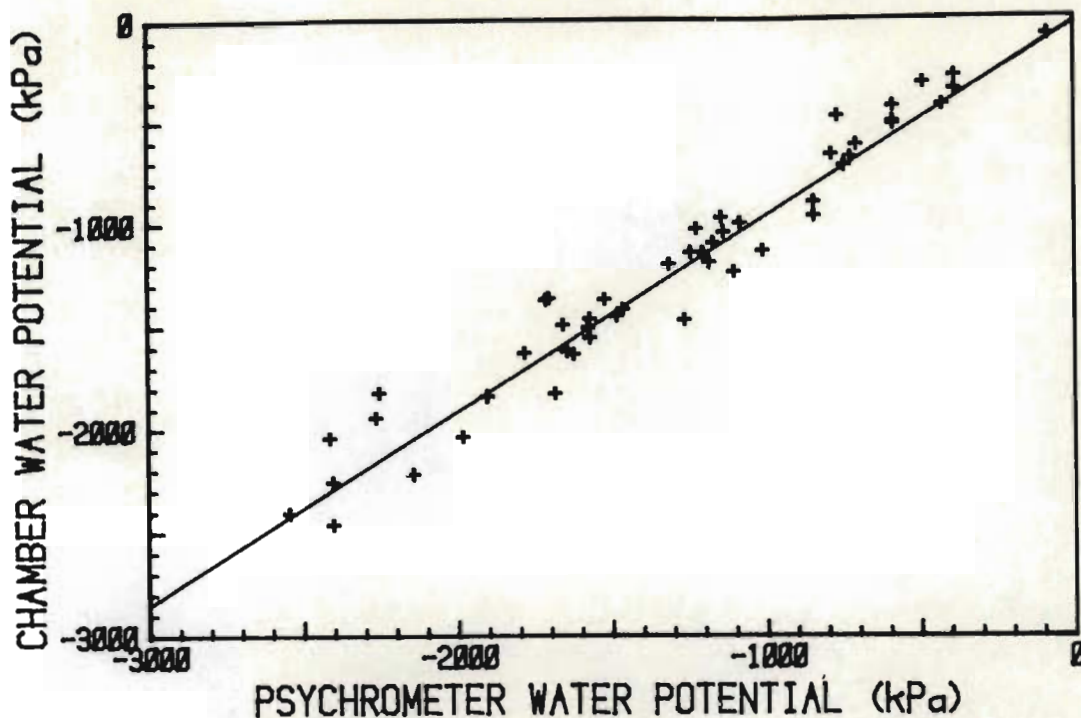


FIG. 4.2 Relationship between total leaf water potential measured using the pressure chamber against that measured using the thermocouple psychrometric technique

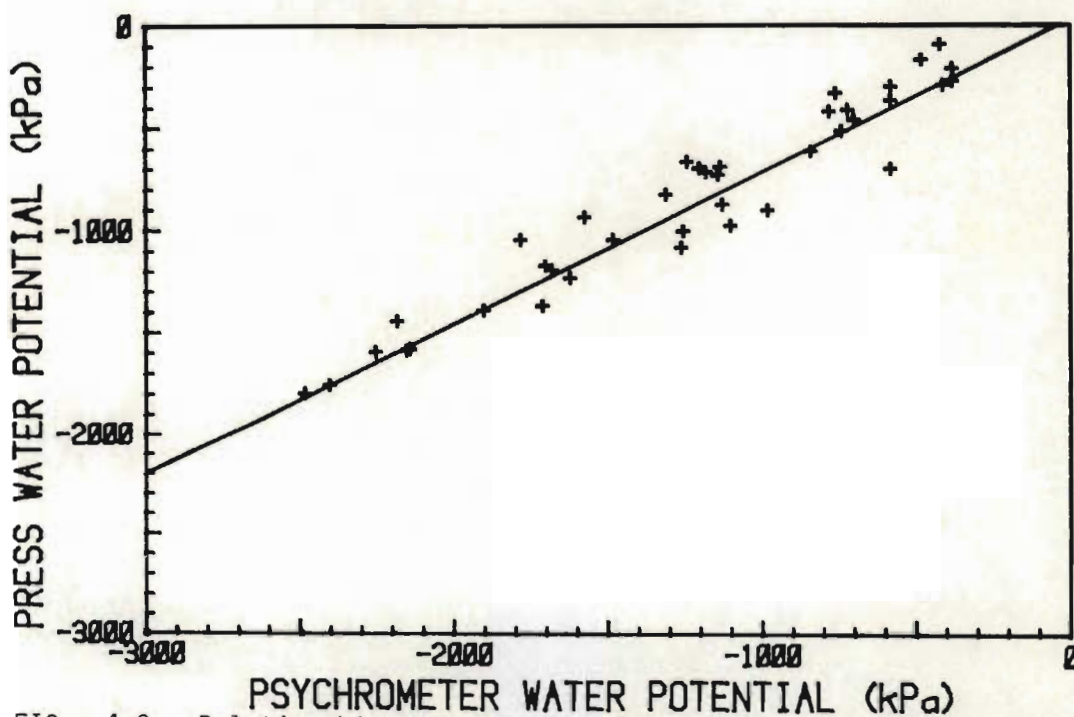


FIG. 4.3 Relationship between total leaf water potential measured using the hydraulic press against that measured using the psychrometric technique

TABLE 4.1 Statistical data for the various psychrometer, pressure chamber and press water potential comparisons (Figs 4.2 to 4.4)

Figure	Slope	Intercept (kPa)	r	SE(estimate of y on x) (kPa)	SE(slope)	SE(intercept) (kPa)
4.2 (Pressure chamber and psychrometer; $n^{\dagger} = 49$)	0,940	-31	0,975	133,8	0,0312	45,7
4.3 (Press and psychrometer; $n = 40$) [¶]	0,742	27	0,964	125,8	0,0330	45,8
4.4 (Press and pressure chamber; $n = 94$) [¶]	0,776	33	0,938	175,9	0,0299	47,6

[†]n is the number of data points

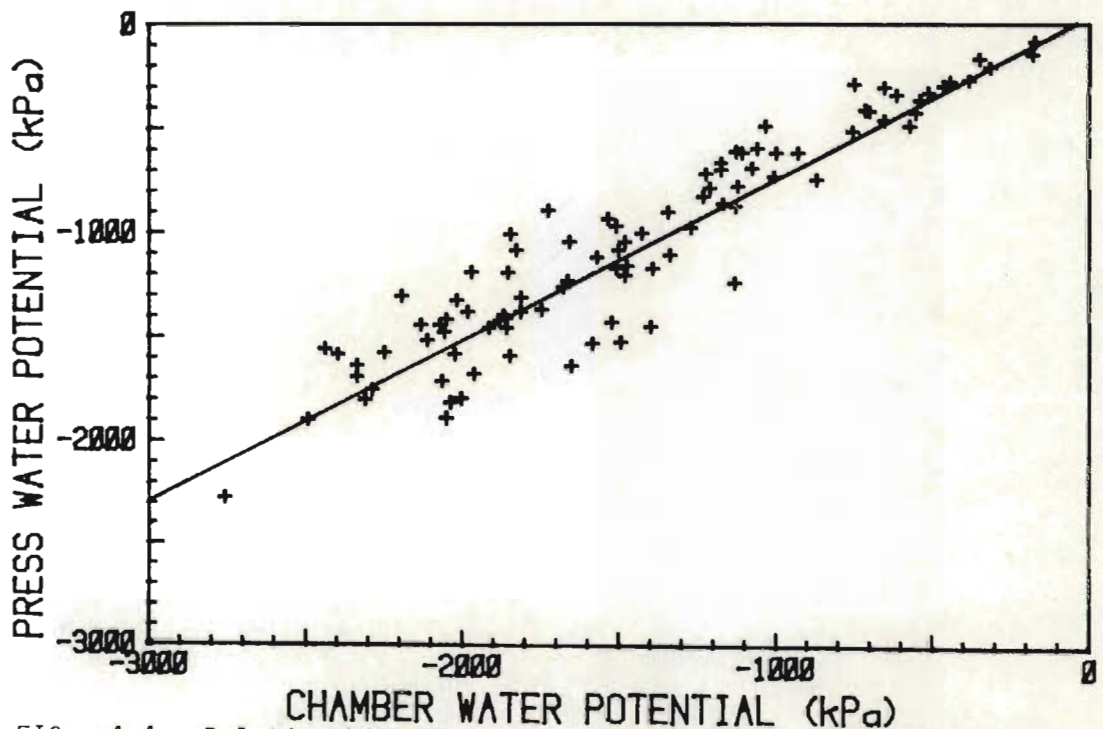


FIG. 4.4 Relationship between total leaf water potential measured using the hydraulic press against that measured using the pressure chamber

[¶] More recent work indicates that the inability of the hydraulic press to estimate low water potentials of cotton is a serious limitation of this instrument (Radulovich, Phene, Davis & Brownell, 1982)

A slope of less than unity for the hydraulic press and psychrometer comparison (Fig. 4.3) also indicates the importance of standardizing the endpoint for the press, for each plant species. Yegappan & Mainstone (1981) point out that the accuracy of the press can be improved by restricting operation to one person. Furthermore, they considered the press to be unsuitable for monocotyledonous leaves which generally have close parallel venation and also dicotyledonous leaves that are intermediately hardened.

In the case of the pressure chamber there is no contact between the leaf and any other surface (except at the rubber stopper surrounding the petiole), and the leaf as a whole is subjected to uniform pressures whereas in the hydraulic press there is contact between the perspex and most of the leaf surface on the upper side and contact with the filter paper on the underside. Water may appear in areas surrounding large veins or the midrib due to pressure exerted by the perspex top on sealing a leaf strip in the press.

The press may be suitable for demarcating broad levels of stress but may not be adequate for physiological investigations which entail examination of pre-dawn and early post-dawn water potentials (Yegappan & Mainstone, 1981).

4.4.2 Pressure-volume curve

In order to compare the accuracy of the psychrometric, pressure chamber and hydraulic press leaf water potential measurements, analyses of variance for the regression of reciprocal leaf water potential on RSD values above the point of incipient plasmolysis, were performed. Only leaf water potentials for which $RSD > 25\%$ is included[†] (corresponding to the region where the total and osmotic potential curves are concurrent). The statistical details for these analyses are shown (Table 4.2). For each curve, the x-intercept, an extrapolated value (corresponding to a very large negative leaf water potential), was very nearly 100% (Figs 4.5 to 4.7). At this point, sample mass \approx dry mass (Eq. 4.3). The x-intercept of slightly less than 100% is attributed to the non-ideal nature of the solutes. The F and r values for the curves of

[†]Richter (1978) seems to indicate that $RSD > 20\%$ would be adequate

TABLE 4.2 Statistical data for linear regressions of reciprocal total leaf water potential measurements (from the three instruments) on relative saturation deficit, RSD (> 25 %)

Instrument	F value	F(0,01)	r	x-intercept (%)	ψ_v (RSD = 25 %) (kPa) [†]
Thermocouple psychrometer (Fig. 4.5; n = 28)	33,3	7,6	0,749	91,8 ± 7,6	-1 466 ± 183
Pressure chamber (Fig. 4.6; n = 54)	56,5	7,2	0,722	104,1 ± 5,0	-1 470 ± 124
Hydraulic press (Fig. 4.7; n = 57)	61,7	7,2	0,727	96,2 ± 7,4	-1 065 ± 96

[†]If a quantity x has a mean \bar{x} and standard error $\sigma(x)$ (so that $x = \bar{x} \pm \sigma(x)$), then a function of x , $f(x)$, has a mean $f(\bar{x})$ and a standard error $\sigma(f(x)) = f'(\bar{x}) \cdot \sigma(x)$, so that $f(x) = f(\bar{x}) \pm f'(\bar{x}) \cdot \sigma(x)$ (adapted from Barford, 1967). In the case here, $1/\psi_v$ is plotted against RSD and the mean and SE of ψ_v (RSD = 25 %) is required from the statistical data. Using previous notation, $f(x) = 1/x$ so that $f(x) = f(\bar{x}) \pm (-1/x^2)\sigma(x)$. This method was used to calculate the values shown in the above table. The assumptions in the method are that the Taylor series expansion of $f(x)$ about $f(\bar{x})$ has insignificant higher order terms and that $f(x)$ and $f'(x)$ are continuous about $x = \bar{x}$.

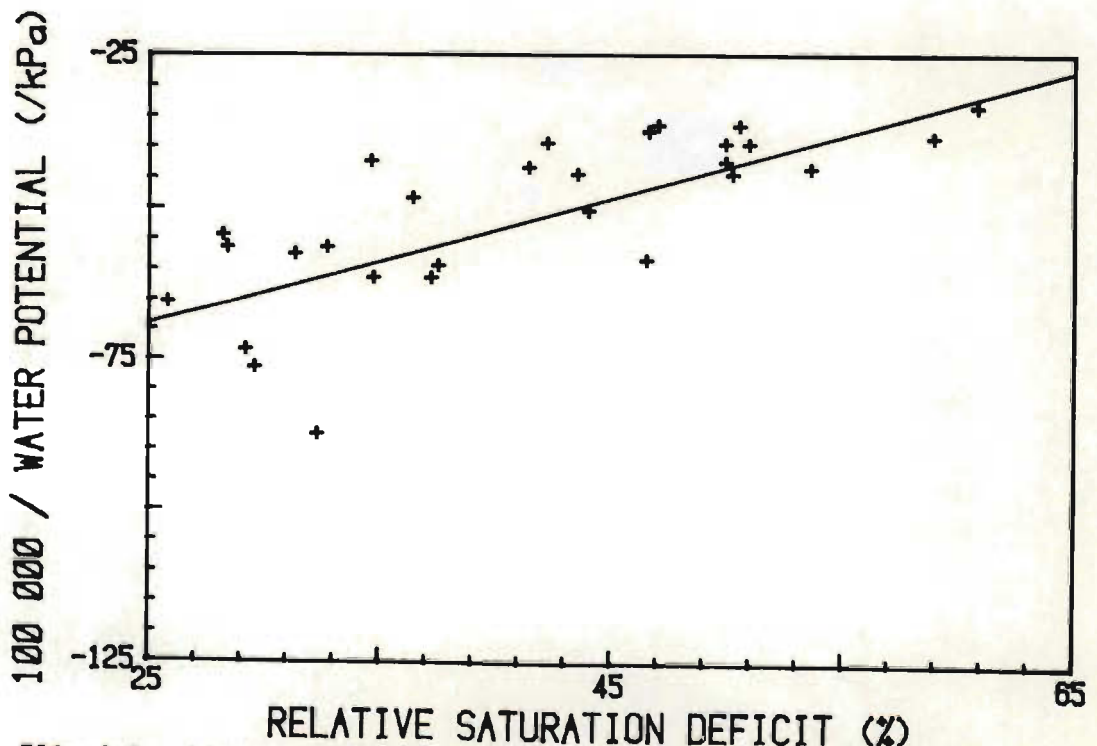


FIG. 4.5 Linear portion of a pressure volume curve as obtained using thermocouple psychrometers

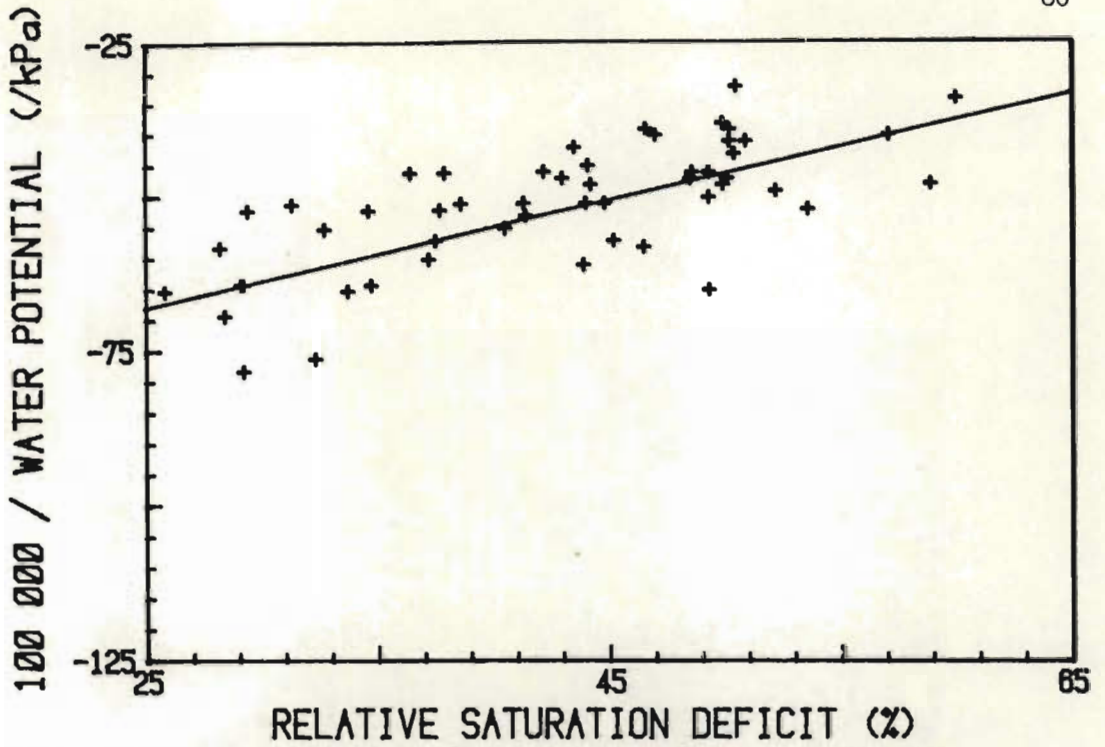


FIG. 4.6 Linear portion of a pressure volume curve as obtained using the pressure chamber

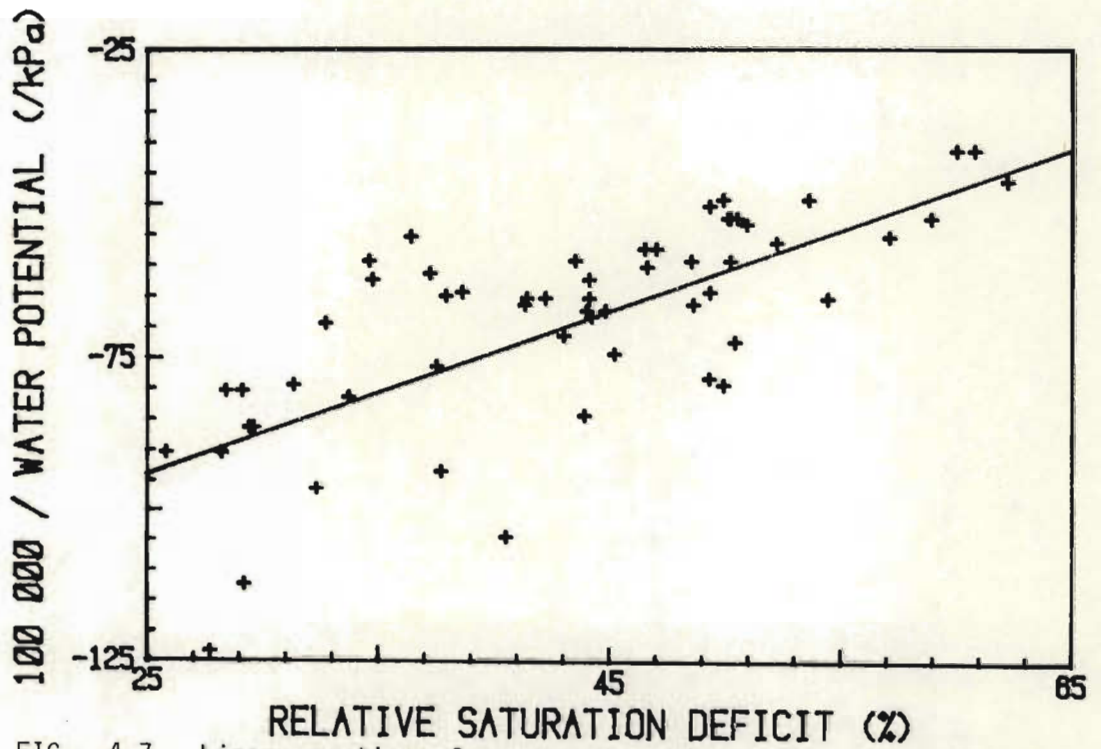


FIG. 4.7 Linear portion of a pressure volume curve obtained using the J-14 hydraulic press

Figs 4.5 to 4.7 indicate the degree of linear correlation in each case (Table 4.2). Some of the scatter in the data is probably due to errors in the determination of RSD, arising mainly from errors in weighing.[†] These errors can be about $\pm 10\%$ of the estimated RSD value for $RSD < 10\%$ and about ± 3 to $\pm 5\%$ if $RSD > 15\%$ (Slavik, 1974, p 149). The lower F value for the psychrometer (Fig. 4.5) is attributable to the fact that there were fewer sample points ($n = 28$ compared to $n > 50$ for the pressure chamber and the hydraulic press). Also, six different psychrometers were used whereas the pressure chamber and hydraulic press measurements were more consistent in that only one instrument was used in each case.

Defining the point of incipient plasmolysis as the total water potential ψ_V (RSD = 25%) value for which RSD = 25%, it is possible to compare these points for the various instruments (Table 4.2). It is apparent that the ψ_V (RSD = 25%) values for the psychrometer and the pressure chamber overlap (-1 446 and -1 470 kPa respectively) but not with that for the hydraulic press (-1 065 kPa). The ratio of the ψ_V (RSD = 25%) value for hydraulic press to that for psychrometer or pressure chamber is approximately 0, 73.

4.5 SUMMARY

Using newly mature trifoliate leaves from field-grown soybean, significant linear correlations between leaf water potential measured using psychrometers, a pressure chamber and hydraulic press, were obtained (Figs 4.2 to 4.4). In each case, the water potential measured using the one instrument plotted as a function of that using another, yielded intercepts statistically indistinguishable from 0 kPa. The slopes obtained were 0,940 for the chamber and psychrometer comparisons, 0,742 for the press and psychrometer, and 0,776 for the press and chamber. The latter two values, being much less than unity, indicate that the press would have to be calibrated for each plant species and the endpoint carefully defined.

[†] Also, individual measurements were performed on different leaves. This may indicate that while Eqs 4.1 to 4.3 may apply to a single leaf left to dry, the equations do not accurately apply when measurements on different leaves are used to define the $1/\psi_V$ vs RSD curve

The leaf pressure-volume curve technique further validated the use of the three instruments for newly mature soybean leaves (Figs 4.5 to 4.7), for two reasons. Firstly, the x-intercept for each method is nearly 100 %. Secondly, the water potential corresponding to the point of incipient plasmolysis was statistically similar for the psychrometer and the pressure chamber but much greater for the hydraulic press (Table 4.2). This again emphasizes the need for calibrating the endpoint defined using the press against one of the more standard techniques. These disadvantages will probably limit the use of the press to applications where standard techniques are impossible, for example, plant water relations studies at remote locations.

IN SITU FIELD MEASUREMENT OF LEAF WATER POTENTIAL
USING THERMOCOUPLE PSYCHROMETERS

5.1 INTRODUCTION[†]

Spanner (1951) developed a thermocouple psychrometer technique for leaf water potential measurement of detached material and this was refined fifteen years later by Brown (1976) and Brown & Johnston (1976). Estimates of *in situ* water potential have been obtained using water potential determinations on detached material and comparisons with pressure chamber measurements performed (Chapter 4) with correlations ranging from poor to good (Duniway, 1971; West & Gaff, 1971; Ritchie & Hinckley, 1975; Walker, 1981). However, very few research workers have attempted non-destructive field measurement of leaf water potential using psychrometric and/or dewpoint methods (Table 5.1). The reason for this is possibly attributable to the presence of large temperature gradients in the field, the diffusion resistance to water vapour offered by the leaf cuticle, the difficulty in affecting a durable seal between leaf and psychrometer cavity and inadequate attention to thermocouple psychrometer calibration procedures and errors involved (Chapter 2).

Large temperature gradients between the leaf and the sensing junctions, which are indicated by large zero offset values between "READ" and "INPUT SHORT" of the microvoltmeter, have generally not been eliminated (Table 5.1). These can cause serious errors in leaf (and soil) water potential determinations when using *in situ* thermocouple hygrometers (Rawlins & Dalton, 1967; Wiebe, Brown & Barker, 1977; Campbell, 1979; Wiebe & Brown, 1979; Brown & Bartos, 1982).

Hoffman & Splinter (1968) postulated that the stomates covered by the psychrometer may have been closed and hence there could be a time lag between measured and actual leaf water potential values (Rawlins, 1964). Zanstra & Hagenzieker (1977) claimed that leaf diffusion resistances may lower *in situ* water potential values obtained using silver-foil psychrometers (designed by Hoffman & Raw-

[†] Based on the paper by Savage, Oosterhuis & Cass (1983)

TABLE 5.1 Relevant details from various literature sources on the use of *in situ* thermocouple leaf hygrometers for non-destructive measurement of water potential (X \equiv no; \checkmark \equiv yes). Some of the early workers enclosed entire leaves
- or ? implies no information or uncertain information

Authors	Dewpoint (D) or psychrometric(P) method	Field use (F) or growth chamber (G)	Comparison with pressure chamber	Magnitude of zero offsets (μ V)	Temperature insulation	Removal of cuticular wax	Air temperature ($^{\circ}$ C)
Lambert & van Schilfgaarde (1965)	P	G	X	Small	\checkmark	X	21 \pm 1
Lang & Barrs (1965)	P	G	X	Small	\checkmark	X	24 to 29
Barrs (1965)	P	G	X	-	X	X	-
Hoffman & Splinter (1968)	P	G	X	-	X	X	-
Hoffman & Rawlins (1972)	P	F	X	-	\checkmark (<25 mm)	X	17 to 32
Neumann & Thurtell (1972)	D	G	X	Small	\checkmark (12 mm)	\checkmark	20 to 24
Beadle, Stevenson, Neumann Thurtell & King (1973)	D	G	X	-	-	?	27 \pm 2 27 \pm 2
Chow & de Vries (1973)	P	G	X	-	X	X	Various but constant
Neumann, Thurtell & Stevenson (1973)	D	G	\checkmark	-	\checkmark	\checkmark	22 \pm 0,5
Baughn (1974); Baughn & Tanner (1974)	D	G	\checkmark	Small	X	\checkmark	20 to 25
Campbell & Campbell (1974)	D	F and G	\checkmark	$< 0,3 $ (?)	X	X	-
Neumann, Thurtell, Stevenson & Beadle (1974)	D	G	X	-	\checkmark	\checkmark	27 \pm 2 22 \pm 2
Brown & McDonough (1977)	P	F	X	-	X	X	-
Herkelrath, Miller & Gardner (1977)	D	G	X	-	?	?	25 \pm 0,5
Wiebe & Prosser (1977)	P and D	G	X	$< 0,3 $	X	X	20(D) 20(N)
Zanstra & Hagenzieker (1977)	P	G	X	-	X	X	22
Ike, Thurtell & Stevenson (1978)	D	G	X	Small	\checkmark	\checkmark	30(D) 25(N)
Liu, Wenkert, Allen & Lemon (1978)	P	G	\checkmark	-	X	X	-
Nulsen & Thurtell (1978)	D	G	X	-	X	X	27 \pm 2(D) 22 \pm 2(N)
Pallas & Michel (1978)	D	G	X	$< 1,0 $	X	X	25(D) 20(N)
Richter (1978)	D	G	X	-	X	\checkmark	20
Pallas, Stansell & Koske (1979)	D	F	X	$> 1,0 $ on occasion	X	X	-
Feyen <i>et al.</i> (1980)	P	G	X	-	X	X	21
Brown & Tanner (1981)	D	F	\checkmark	$< 0,3 $	\checkmark (10 mm)	\checkmark	-
Durand-Campero (1981)	P and D	G	Occasional	-	X	X	25(?)
Ike & Thurtell (1981)	D	G	X	Small	\checkmark	\checkmark	29(D) 26(N)
Balesky, Wilkinson & Pallas (1982)	P	G	X	-	-	X	22(D) 15(N)

lins, 1972). They also claimed, but presented no supporting evidence, that diffusion resistances did not affect water potentials determined using the dewpoint technique and implied that accurate measurements using the psychrometric technique were not possible.

The objectives of this chapter are as follows:

1. investigate the effect of cuticle abrasion on field measured psychrometer water potential;
2. compare these measurements with Scholander pressure chamber (Scholander *et al.*, 1965) measurements on adjacent leaves;
3. investigate the time response of thermocouple psychrometers to leaf water potential changes following excision.

5.2 EFFECT OF CUTICLE ABRASION ON FIELD MEASURED WATER POTENTIAL USING *IN SITU* THERMOCOUPLE PSYCHROMETERS[†]

5.2.1 Introduction

One of the main problems associated with non-destructive measurement of leaf water potential using thermocouple psychrometers is that the substomatal vapour has to diffuse through the leaf cuticle due to presumed stomatal closure under the dark chamber conditions. Thus, leaf diffusion resistances could substantially alter the measured water potential when the psychrometric technique is used (Zanstra & Hagenzieker, 1977).

A common method of reducing cuticular resistance to vapour movement from the substomatal cavity to the psychrometer chamber is to partially perforate the leaf cuticle by abrasion (Neumann & Thurtell, 1972). Apparently only one published work reports on the effect of leaf abrasion (Table 5.1) on the measured water potential (Neumann *et al.*, 1974) after which potential measurements were compared by mounting two dewpoint hygrometers on two sides of a maize leaf, one pretreated with xylene and the other preabraded with a razor blade. They found that potentials measured after these

[†] Based on the paper by Savage, Wiebe & Cass (1983a) submitted for publication to *J. exp Bot.*

cuticle pretreatments differed slightly over their range of measurements (-800 to nearly 0 kPa), particularly in the dry range. However, they made no comparisons with pressure chamber measurements nor did they indicate for how long it was possible to obtain reliable measurements from the same leaf.

Illumination of the leaf material contained within the cavity has been attempted (Neumann & Thurtell, 1972; Brown & McDonough, 1977) but this causes undesirable temperature gradients within the psychrometer chamber.

The use of *in situ* psychrometric technique for the non-destructive measurement of leaf water potential in field situations has apparently been limited (Table 5.1). The psychrometric technique used under controlled temperature conditions resulted in a large scatter in psychrometric measurements compared to pressure chamber measurements (Liu *et al.*, 1978). The variability may have been due to leaf diffusion resistance affecting psychrometric water potential. This study shows that accurate *in situ* measurement of water potential using thermocouple psychrometers is possible provided certain of the abovementioned problems are eliminated.

5.2.2 Materials and methods

Leaf psychrometers (Wescor L-51 and L-51A) were calibrated using 0,1; 0,2; 0,3 and 0,5 mol/kg NaCl solutions at three temperatures (20, 25 and 31 °C). Calibration equations relating water potential to psychrometer voltage output and psychrometer temperature were determined (Section 2.3.2, p 28). Because solar radiation, clouds and winds induced marked thermal gradients in the psychrometer block, it was necessary to insulate the psychrometer block (Campbell & Campbell, 1974) with double coated foam tape[†] covered on the outside with reflective aluminium foil tape^{††} (Section 5.3.2). A mixture of beeswax and lanolin was used to seal the psychrometer piston (or lip) against the leaf surface (Section 5.3.2).

Several abrasion treatments were applied to reduce citrus leaf cuticular resistance to water vapour diffusion and consequent

[†] Scotch mount tape, 4009 by 3M, Industrial Tape Division, St. Paul, MN, U.S.A.

^{††} Aluminium foil tape, Y434 by 3M

lag of the measured water potential behind the true water potential (Table 5.2). The method of abrasion was similar to that used by Brown & Tanner (1981) except that different abrasive materials were used and a single layer of cotton cloth held against the index finger was used to perform the abrasion, in addition to employing their abrasion treatment using cotton buds. The leaf was first cleaned with distilled water. The area to be abraded was marked by a piece of Parafilm[†] wax paper folded around the edge of the leaf and having a punched hole with a diameter slightly larger than that of the psychrometer chamber. The leaf area exposed by the punched hole was marked with the abrasive slurry, and after removal of the wax paper, the marked leaf area was carefully abraded (circular motion) using the index finger covered with thin cotton cloth using the index finger of the other hand as a support. The abrasive slurry was formulated from non-ionic detergent, water and abrasive powder (Table 5.2) as suggested by Brown & Tanner (1981). After abrasion, the leaf was again cleaned with distilled water and gently blotted dry with paper towel. Various abrasion treatments were compared (Table 5.2) by sealing pairs of psychrometers on either side of the midrib of a leaf. Sealing was usually performed in the late afternoon, but not if dew was noted on the leaf surface.

Leaf water potential measurements using the pressure chamber were made on adjacent leaves whenever psychrometer measurements were made. Prior to excision, the leaf was covered with a slightly moistened rectangular piece of cotton cloth folded over the leaf and then covered with adhering plastic wrap (Allen, Nell, Joiner & Albrigo, 1980). Some leaf tissue was trimmed away from the petiole as needed to lengthen it and facilitate insertion into the chamber rubber stopper. Pressure was increased at a rate of about 10 kPa/s, to improve endpoint accuracy.

The plants used in this study were *Citrus jambhiri* seedlings grown in various sized pots holding from 5 to 15 l soil. The heights of the plants varied from about 1 to 3 m. Where more than one psychrometer was sealed on the same leaf, the leaves chosen had a leaf area of about 60 cm². In all other cases, leaf area varied from 30 to 60 cm². Plants were allowed to equilibrate with the

[†]American Can Company, Greenwich, CT, U.S.A.

TABLE 5.2 Abrasion treatments used in this investigation

Treatment	Description
No abrasion	Control treatment
Cotton bud abrasion	As described by Brown & Tanner (1981), but for 30 s
Light abrasion	Gentle leaf abrasion (rotating motion) with a 400 grit carborundum powder (particle size approximately 60 μm) for 30 s
Intensive light abrasion	Identical to light abrasion but performed for 60 s
Coarse abrasion	Gentle leaf abrasion using calcined aluminium oxide, that had been wet-sieved through a 75 μm sieve, for 30 s

natural field environment for 2 weeks prior to measurement.

In order to evaluate the physical effect of leaf abrasion, segments that were cut from abraided leaf areas were fixed, critical point dried, coated with gold and viewed under a scanning electron microscope with an accelerating voltage of 15 kV.

5.2.3 Results and discussion

The time required for water vapour in the psychrometer chamber to reach equilibrium with that in the substomatal cavity is influenced by the abrasion treatments. This time is typically 1 h for an abraided cuticle but in excess of 5 h for an unabraided cuticle (Fig. 5.1) for psychrometers mounted on the same leaf. At the end of the psychrometer measurements, water potential of adjacent leaves was measured using the pressure chamber. Results indicated that the abrasion treatment yielded comparable values to those obtained with the pressure chamber (-589 and -620 kPa respectively) but the unabraided treatment measurements were substantially lower (-825 kPa). The latter treatment apparently had not allowed for equilibrium between leaf substomatal cavity and psychrometer chamber even after the 5 h period of measurement.

The shape of the voltage output vs time curve obtained from

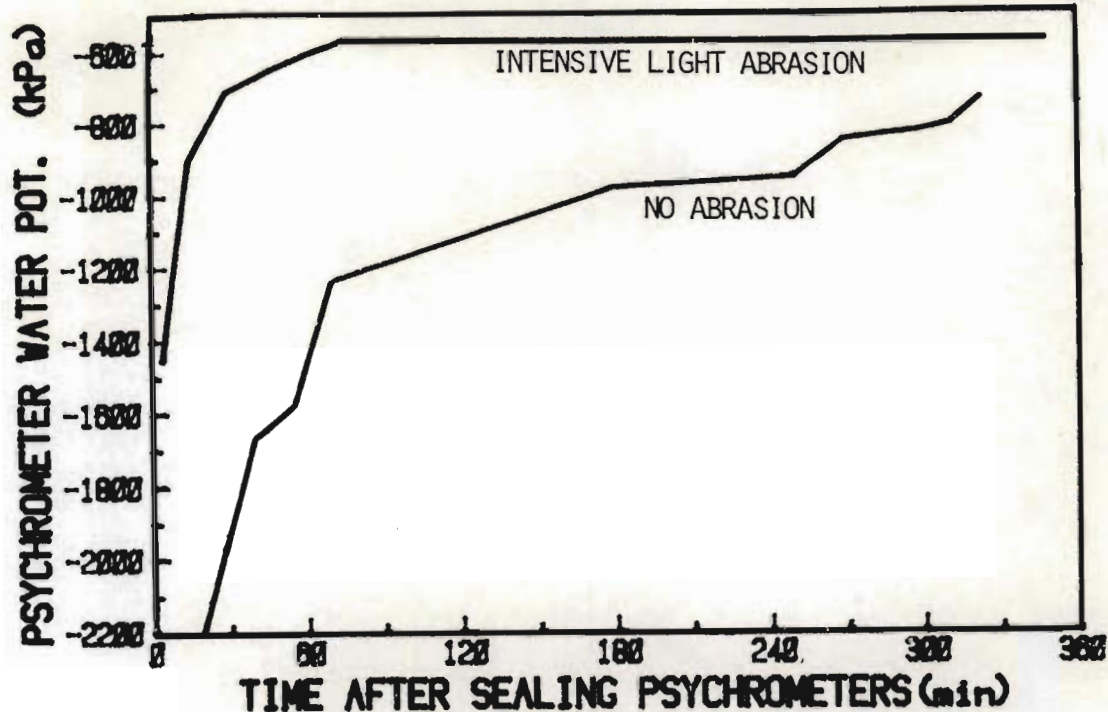
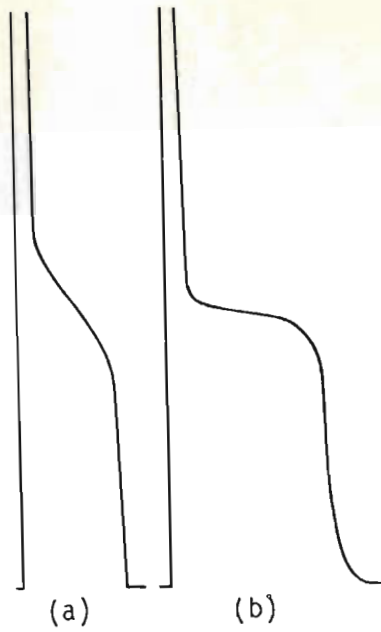


FIG. 5.1 Measured water potentials as a function of time after sealing for the no abrasion and intensive light abrasion treatments. Both psychrometers were mounted on the same leaf for these laboratory measurements

leaf psychrometers were influenced by the magnitude of the diffusion resistance to water vapour across the leaf boundary. Typical examples from the collected data will illustrate this. Voltage output curves shown in Fig. 5.2 indicate that there is a rapid change in the sensing junction temperature during evaporation, in the absence of abrasion (Fig. 5.2a) compared to the light abrasion treatment (Fig. 5.2b). This difference presumably arises from the water flux difference towards the psychrometer sensing junction during cooling. The net effect of this difference is that it is more difficult to determine the maximum point of inflection in the psychrometer output curve as defined by point E of Fig. 2.3 (p 24). These measurements were taken at 14h30 (South African Standard Time, SAST) under almost cloudless conditions. At the time, the abraided treatment water potential had passed the daily minimum and was increasing in time. Presumably the non-abrasion treatment measurements were still converging on the minimum value. Pressure chamber measurements of adjacent leaves were -750, -800 and -850 kPa, which compared favourably with -844 kPa measured over the light abrasion



(a) (b)
FIG. 5.2



(a) (b)
FIG. 5.3

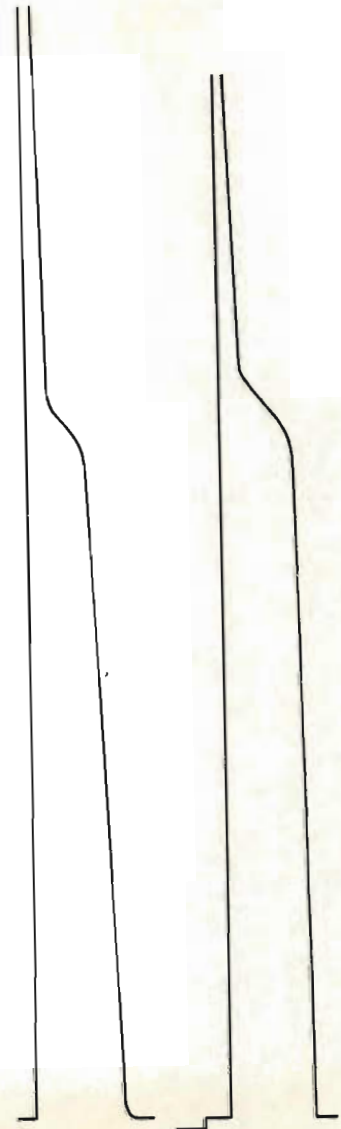


FIG. 5.4

- ¶ FIG. 5.2 Voltage output curves for two psychrometers sealed on the same leaf; The output for (a) is for a no abrasion treatment and that for (b) a light abrasion
- FIG. 5.3 Voltage output curves for two psychrometers sealed on the same leaf. The output for (a) is for a light abrasion treatment and that for (b) a coarse abrasion
- FIG. 5.4 Voltage output curves for two psychrometers sealed on different leaves of the same citrus plant. Treatments used in both cases was an intensive light abrasion

¶ Water potential values for Figs 5.2 to 5.4 are indicated in Table 5.3

treatment (Table 5.3). Control treatment water potential values were always greater in the morning but lower in the afternoon compared to pressure chamber measurements.

As available soil water decreased, it became evident that even light abrasion for 30 s was insufficient to reduce water vapour diffusion resistance to acceptable levels (Fig. 5.3). We therefore found it necessary to intensify the abrasion treatment by applying the light abrasion for 60 s (Table 5.2). In the example shown in Fig. 5.3, the pressure chamber measurements were -1 700, -1 740 and -1 820 kPa for adjacent leaves (Table 5.3).

The coarse abrasion treatment generally resulted in more variable potential values compared to pressure chamber measurements, than did the intensive light abrasion. Furthermore, the intensive light abrasion treatment yielded satisfactory voltage output curves even in the low leaf water potential range (Fig. 5.4). In this case, pressure chamber measurements were -2 860 and -2 910 kPa (average value of -2 885 kPa) compared to an average of -2 765 kPa for the psychrometric measurements (Table 5.3).

Scanning electron microscope photographs (Plate 5.1) were

TABLE 5.3 Comparison of citrus leaf water potential using thermocouple psychrometers (various abrasion treatments for units on the same leaf) and pressure chamber (mean values only from adjacent leaves)

Study	Psychrometer measurements (kPa)				Pressure chamber measurements (kPa)	
	No abrasion	Light abrasion	Intensive light abrasion	Coarse abrasion		
Equilibrium time	-825		-589		-620	
Voltage output curve shape	-1 122	-844			-800	
			-1 396		-1 841	-1 753
				-2 775		-2 885

Scanning electron micrographs for the various abrasion

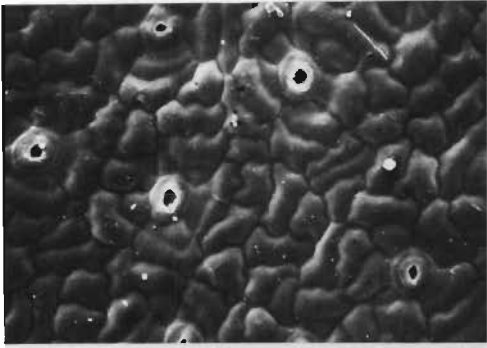
Plate 2.1

treatments (Table 2.2):

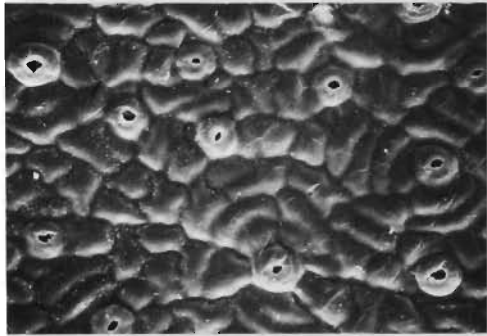
- (a) 500X, control treatment;
- (b) 2 000X, control treatment;
- (c) 500X, bud abrasion (30 s);
- (d) 2 000X, bud abrasion (30 s);
- (e) 500X, light abrasion (30 s);
- (f) 2 000X, light abrasion (30 s);
- (g) 500X, light abrasion (60 s);
- (h) 2 000X, light abrasion (60 s);
- (i) 500X, coarse abrasion (30 s);
- (j) 2 000X, coarse abrasion (30 s).

The treatment of the surface of the material by abrasion from (j) these results show that the surface of the material is much smoother in the case of the coarse abrasion treatment. The results of the light and bud abrasion treatments are also shown in the micrographs.

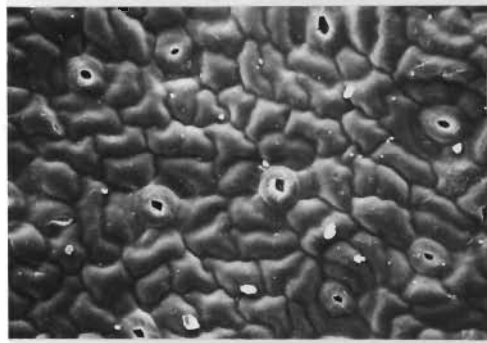
On the basis of the above results it can be seen that the surface of the material is much smoother in the case of the coarse abrasion treatment. The results of the light and bud abrasion treatments are also shown in the micrographs.



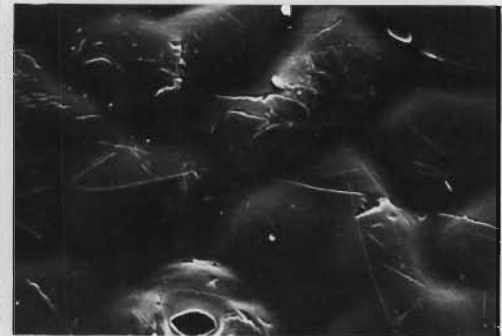
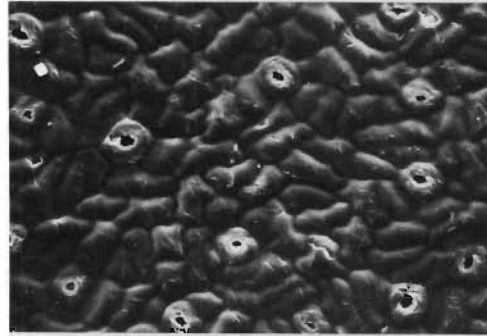
a, b



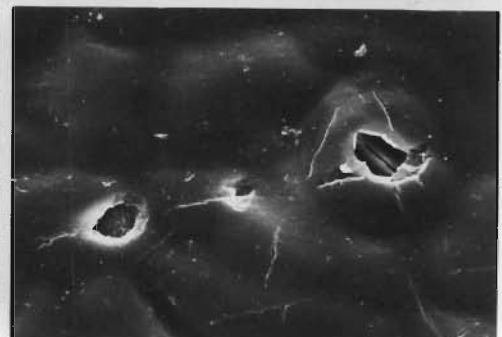
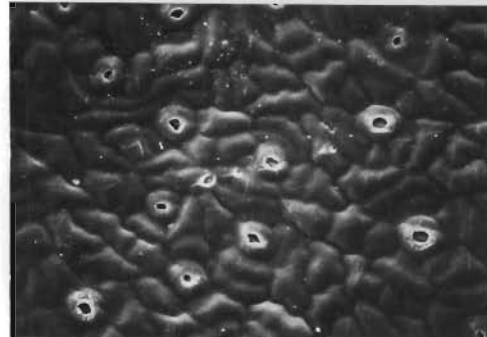
c, d



e, f



g, h



i, j

500X

2 000X

taken of areas abraded using the various abrasion treatments (Table 5.2). Cotton bud abrasion, which yielded unsatisfactory potential values (compared to the pressure chamber apparatus) made little impression on the thick leaf cuticle of citrus (Plate 5.1c and d). Close examination of the plate is necessary. The 30 and 60 s abrasion treatments resulted in greater surface penetration (Plate 5.1e to 5.1h), but the 60 s abrasion resulted in good water potential comparisons with the pressure chamber method over the -3 000 to 0 kPa range. Occasionally, this treatment resulted in small cavities through the epidermal cavity (Plate 5.1g, upper right). In the case of the coarse abrasion treatment, there were very few surface scratches due to the non-angular nature of aluminium oxide compared to the carborundum powder used (Plate 5.1i) but cavities through the epidermal layer were observed (Plate 5.1j). These cavities (Plate 5.1j), or the lack thereof, could explain the apparent variability in psychrometer water potentials as compared to pressure chamber measurements (neighbouring leaves) for this abrasion treatment. Also, it is clear from Plate 5.1h and 5.1j, aside from the cavities observed, that the depth of abrasion scratches were only confined to the surface of the thick citrus leaf cuticle. For this reason, we felt that scanning a cross-section of the leaf was not necessary.

5.3 NON-DESTRUCTIVE FIELD MEASUREMENT OF LEAF WATER POTENTIAL USING THERMOCOUPLE PSYCHROMETERS[†]

5.3.1 Introduction

Lambert & van Schilfgaarde (1965) and Lang & Barrs (1965) were the first to attempt water potential measurement of intact leaves. The latter used a complex temperature control device to eliminate temperature gradients. These early workers and Manchar (1966b, c, d) enclosed an intact whole leaf in the psychrometer chamber but this technique probably changes the water potential of the leaf being measured. Hoffman & Splinter (1968) and Hoffman &

[†] Based on the paper by Savage, Wiebe & Cass (1983b) submitted for publication to *Plant Physiol.*

Herkelrath (1969) were the first to attach miniature psychrometers to plant leaves and monitored water potential changes under strictly controlled temperature environments. By 1972, routine measurement of leaf water potential on intact plants in the field appeared feasible (Hoffman & Rawlins, 1972; Neumann & Thurtell, 1972; Campbell *et al.*, 1973; Campbell & Campbell, 1974) although earlier successes using a beta gauge were published (Rawlins, Gardner & Dalton, 1968). Some workers regard the psychrometric technique as the absolute or primary technique (Boyer, 1966; Ike *et al.*, 1978) but few workers have reported *in situ* field measurements of leaf water potential (Table 5.1). Yet we know from personal communications that many have tried, but with only limited success. A major problem is fluctuating thermal gradients (Calissendorff & Gardner, 1972) within the apparatus under variable radiation and wind conditions. These lead to temperature gradients between the measuring thermojunction and the leaf surface which preclude an acceptable level of precision in the determination (± 200 kPa in one study (Calissendorff & Gardner, 1972) due to temperature gradients). In addition, the diffusion resistance of the cuticle-stomate system may delay equilibrium especially when the resistance is high (Hoffman & Splinter, 1968) as it is likely to be in the dark psychrometer chamber with elevated carbon dioxide concentration levels. The psychrometer should not influence the water potential of the leaf at the point of measurement (Calissendorff & Gardner, 1972); this may be checked using comparative measurements using the pressure chamber. Apparently, only Campbell & Campbell (1974) and Brown & Tanner (1981) have performed *in situ* field comparisons for leaves (Table 5.1), and these comparisons involved the dewpoint technique described by Campbell *et al.* (1973), and Roberts (1977) performed comparisons using pine needles. Campbell & Campbell (1974) applied no temperature corrections to their data.

The basic premise of *in situ* water potential measurements is that the energy of water in equilibrium with the attached leaf gives a measure of that in the conducting elements of the stem xylem (Slatyer, 1966; 1967, p 153). If only a part of the leaf is enclosed by the psychrometer, it may be assumed that the enclosed leaf water potential must be in equilibrium with the more or less unchanged water potential of the rest of the leaf[†] (Slavik, 1974,

[†] Also, every stomate acts independently of every other stomate (Lange, Löscher, Schulze & Kappen, 1971)

p 63). Enclosing a portion of a leaf substantially modifies the local leaf environment by local shading and reduced air movement. This may alter stomatal aperture, transpiration and water potential. It is likely that the local water potential will be that of the leaf veins which traverse the psychrometer area; it may differ from the mesophyll or substomatal cavity water potential, probably being somewhat higher. Hence the enclosed area should be as small as possible (Squire, Black & Gregory, 1981). Boyer (1972b) states that the thermocouple psychrometer probably indicates an average for leaf tissue which approximates a distance average and which requires that cells that are well below the tissue surface contribute to the net vapour flux density at the sensing thermojunction.

The objective of this investigation was to improve non-destructive techniques for measuring leaf water potential in the field using *in situ* thermocouple psychrometers and to compare these measurements with pressure chamber measurements.

5.3.2 Materials and methods[†]

Eleven leaf psychrometers, calibrated according to previous methods (Sections 2.3.2 and 2.4.2), and juvenile plants (*Citrus jambhiri*) grown in 5 to 15 l pots were used in this investigation (Section 5.2.2).

In order to use leaf psychrometers for *in situ* field measurement of leaf water potential, it was necessary to reduce the large temperature gradients associated with exposure of the aluminium block to direct solar radiation and wind. This was done by covering all surfaces of the aluminium housing of a commercial psychrometer with thermal insulation material. Polystyrene covered with aluminium foil tape proved less satisfactory than Scotch mount double coated foam tape (Fig. 5.5a). About 12 mm thick insulation was applied to the top and bottom of the housing and about 6 mm to all sides except the non-slit side (Fig. 5.5a, side A), which was 9 mm thick. This arrangement minimized leaf shading. The insulation material was covered with highly reflective aluminium foil tape ensuring that radiation of all wavelengths is reflected. A

[†] Partly based on the paper by Oosterhuis, Walker & Savage (1983) but mostly on that by Savage *et al.* (1983b)

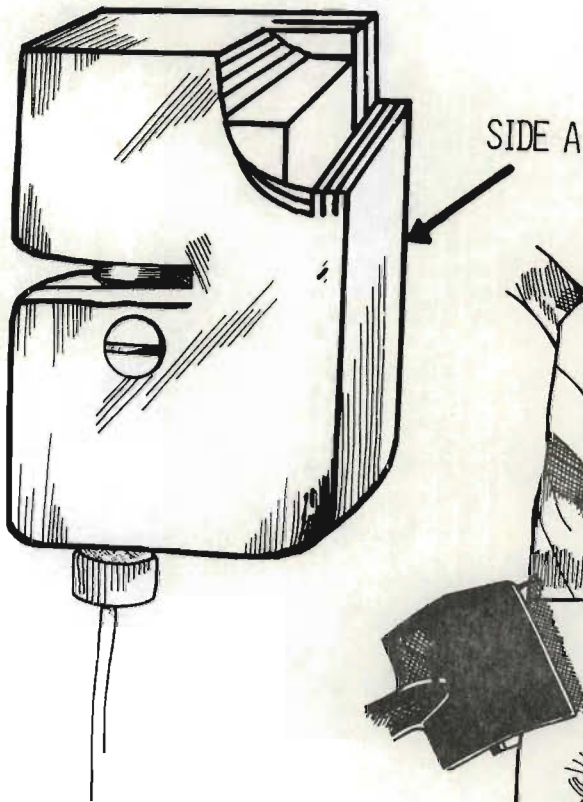


FIG. 5.5 (a)

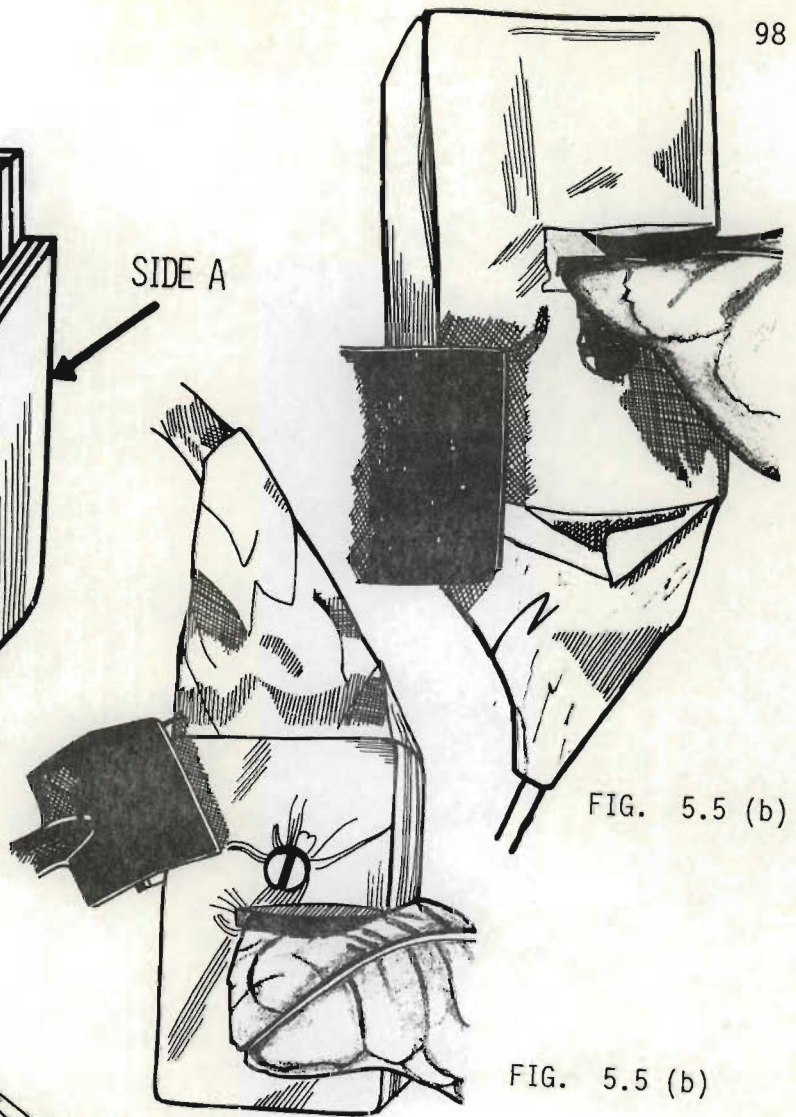


FIG. 5.5 (b)

FIG. 5.5 (b)

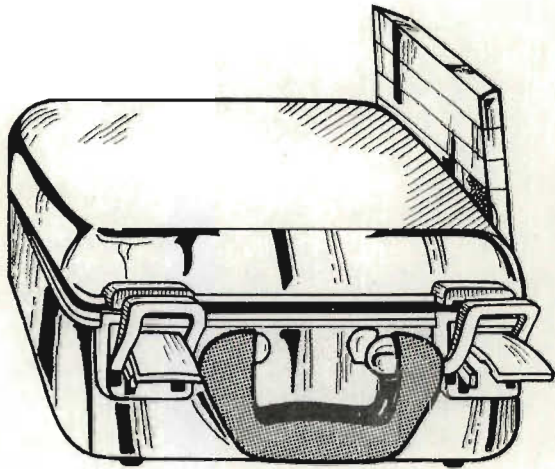


FIG. 5.5 (c)

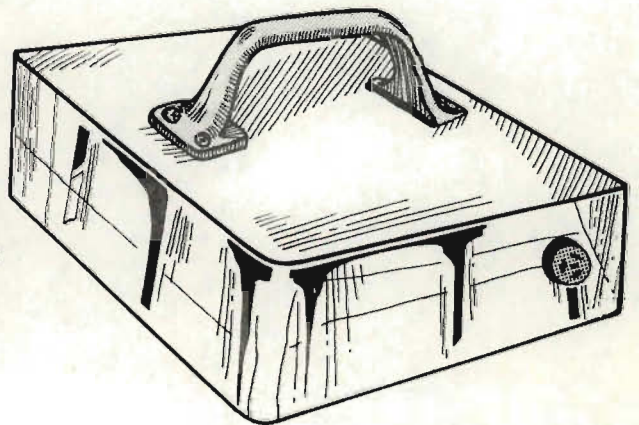


FIG. 5.5 (d)

cylindrical, narrow bore plastic tube was glued to the piston top in order to extend its length, accommodating the increased depth resulting from the insulation material around the psychrometer (Fig. 5.5a).

Cleaning of the leaf psychrometer chamber is important. A toothpick was used to carefully remove any sealant that had entered the psychrometer chamber. The lower piston was then soaked in boiling distilled water, immediately washed in acetone followed by 4 mol/kg ammonium hydroxide, cleaned with a jet of steam and finally rinsed in distilled water. Merrill psychrometers were more difficult to clean if sealant entered the chamber, due to the protective wire screen covering the sensing junction.

The effect of abrasion on the measured leaf water potential was investigated using no abrasion, light particle abrasion and coarse abrasion treatments (Table 5.2). The abrasion technique was similar to that of Brown & Tanner (1981) except that 400 grit (particle diameter of about 60 μm) carborundum powder was used for a light abrasion treatment and calcined aluminium oxide (wet sieved through a 75 μm sieve) for a coarse abrasion treatment. The method of abrasion is discussed in Section 5.2.2.

A beeswax-lanolin mixture was used to seal the psychrometer piston against the leaf. The relative amounts of each wax determines the rheological properties of the mixture. The softening temperature is defined as the temperature at which no beeswax-lanolin mixture flowed off a thermometer dipped into the heated mixture[†]. Generally a mixture was used that had a softening temperature 2 °C greater than the expected 14h00 block temperature. No infiltration of this mixture into the leaf was noted even after a week with temperatures exceeding 35 °C.

The insulated aluminium psychrometer housing supported by metal retort stands and laboratory clamps were positioned so that the abraded areas of the respective leaves fit without stress into the psychrometer slit. Sealant was applied to the edge of the psychro-

[†] If T_s is the softening temperature and R the volume ratio of lanolin to beeswax, then $R = 20,76 - 0,43 T_s$ for the waxes used (with total degrees of freedom of 7, $r = 0,987$ and $S_{y.x} = 0,52$)

meter piston which was then pushed firmly against the leaf surface and secured with a brass set screw (Fig. 5.5a). A screw driver with a long shaft was used to tighten this screw ensuring minimal disturbance to the plant. Psychrometers were usually attached in the late afternoon some 10 min after abrasion, but not if dew was noted on the leaf surface.

For the crops used in this study, psychrometers were always sealed on abaxial leaf surfaces. The leaf angle of citrus changes with water stress and it was necessary to occasionally alter the psychrometer position if measurements continued for extended time periods. When the abaxial leaf surface faced upwards, the plastic rod and lead wire were exposed to incoming solar radiation. In such cases, aluminium foil was taped over the plastic rod (Fig. 5.5b) to reduce heat conduction to the piston. The tape was not used as an umbrella (Pallas *et al.*, 1979), casting minimal shade on the leaf. The psychrometer slit was positioned towards north (or south in the Northern Hemisphere) in order to minimize leaf shading.

It was possible to check whether the psychrometers were successfully sealed against the leaf within 5 min after sealing. A 30 s cool followed by switching to read indicated that the chamber was approaching equilibrium with the substomatal cavity if the output voltage was less than about 15 μ V. If not, the brass screw was released and pressure applied between the psychrometer piston top and the leaf with the piston rotated slightly to improve the vapour seal. The screw was then retightened. Two hours was generally sufficient for vapour equilibration between the substomatal cavity and the psychrometer chamber for the abrasion treatment used; temperature gradients between the leaf and the sensing thermojunction generally diminished within 20 min.

When all psychrometers were sealed, the corresponding stem or branch was tied to the metal support rod and neighbouring stems or branches to reduce the possibility of wind induced stresses breaking the seal. The support rod was also pushed into the soil of potted plants when feasible.

The microvoltmeter lid was covered with aluminium foil tape (Fig. 5.5c) and the inside of the lid filled with polystyrene to reduce sudden temperature changes in the electronic circuit and consequent spurious voltage fluctuations. In particular, the lid of

the microvoltmeter was never fully opened whenever connecting wires or operating the function switch, thus preventing radiation from directly entering the unit. Heating of the psychrometer lead wires was prevented by mounting a polystyrene block covered with aluminium foil tape to the side of the microvoltmeter (Fig. 5.5c). This reduced heat energy flow to the sensor connecting copper posts of the microvoltmeter, and eliminated the apparent temperature gradients and fluctuating zero offsets (Brown & Tanner, 1981).

A rechargeable power supply was substituted for that supplied by the manufacturers. This consisted of six rechargeable batteries (Yuasa, Japan) each 6 V and 6 A h housed in a plastic box covered with aluminium foil tape (Fig. 5.5d) to reduce radiant heating of the batteries in the field. The capacity of the battery pack was sufficient for the microvoltmeter to be kept on continuous power throughout the investigation (after a week, trickle recharging was necessary). The 10 to 15 min drift, on turning the meter on (Brown & Tanner, 1981), was prevented by this procedure.

A mains chart recorder was used to record thermocouple psychrometer output with a Keithley multimeter connected to the Wescor microvoltmeter as a cross-check. For more remote sites, rechargeable battery chart recorders would be necessary.

On a few occasions, the aluminium covering and the thermal insulation resulted in static charge accumulation. This resulted in large apparent zero offset voltages, normally associated with large leaf and sensing junction temperature differences. The accumulation of charge was dissipated by connecting the psychrometer earth lead wire to the chart recorder earth connection.

Generally, psychrometer measurements only commenced at about 09h00 (SAST). Winter dew frequently occurred and pre-dawn measurements were often not possible in windy conditions as droplets of water entered or moved out of the slit area. This water movement often caused large leaf (cavity) and sensing junction temperature differences and also zero drift errors (Section 2.5.4, p 46) during measurement of the wet bulb temperature. Early morning post dawn measurements were also often not possible due to the water movement from the slit area, in particular from the piston. This resulted in large temperature differences (zero offsets) particularly in windy conditions or when the leaf was partially exposed to solar radiation.

5.3.3 Results and discussion

In the field experiment, measured block temperatures ranged between 12 and 29 °C and the zero offsets associated with temperature gradients between the reference[†] and sensing junctions, were never greater than 0,6 μV (Fig. 5.6). This maximum value was measured when direct solar radiation entered the slit area, striking the psychrometer piston. Previous comparisons of measurements obtained from Merrill leaf psychrometers indicated that the Wescor L-51 (wide aperture) and L-51A (narrow aperture) leaf psychrometers exhibited smaller temperature gradients under similar conditions of high energy load than did Merrill psychrometers. Consequently, the latter were not used in the field.

Zero offsets measured during the investigation ranged between -0,1 and 0,6 μV (Fig. 5.6). The zero offsets accepted by Brown & Tanner (1981) were less than 0,3 μV but their psychrometer shaded more of the leaf than ours (9 cm² compared to our 6 cm²). Some workers (Pallas & Michel, 1978) have accepted less than 1 μV. The error analysis of Section 2.5 indicates that zero offset magnitudes less than or equal to 0,5 μV do not result in excessive error in water potential measurement compared to other error components (Table 2.12, p 47).

Agreement between psychrometer and pressure chamber measurements was poor unless the leaves were abraded prior to psychrometer measurements (Figs 5.7 to 5.9). If leaves were not abraded prior to psychrometric measurement, the readings were excessively dry compared to pressure chamber values (Fig. 5.7) and the "plateaus" were poorly developed (Fig. 5.2). The discrepancies became worse with lower (drier) leaf water potentials, ψ_{tot} . In the case of the no abrasion treatment, the wide aperture psychrometer measurements compared more favourably with pressure chamber measurements on neighbouring leaves, compared to the narrow aperture psychrometer measurements (Fig. 5.7). Presumably, diffusion resistances affected narrow aperture leaf water potential measurements than did wide aperture measurements; compare Figs 5.7 and 5.10.

The coarse abrasion treatment resulted in more variable leaf water potential measurements compared to light abrasion (Figs 5.8, 5.9;

[†] We assumed that the reference junction and leaf temperatures were equal. Zero offsets were obtained by comparing dry psychrometer and input short measurements

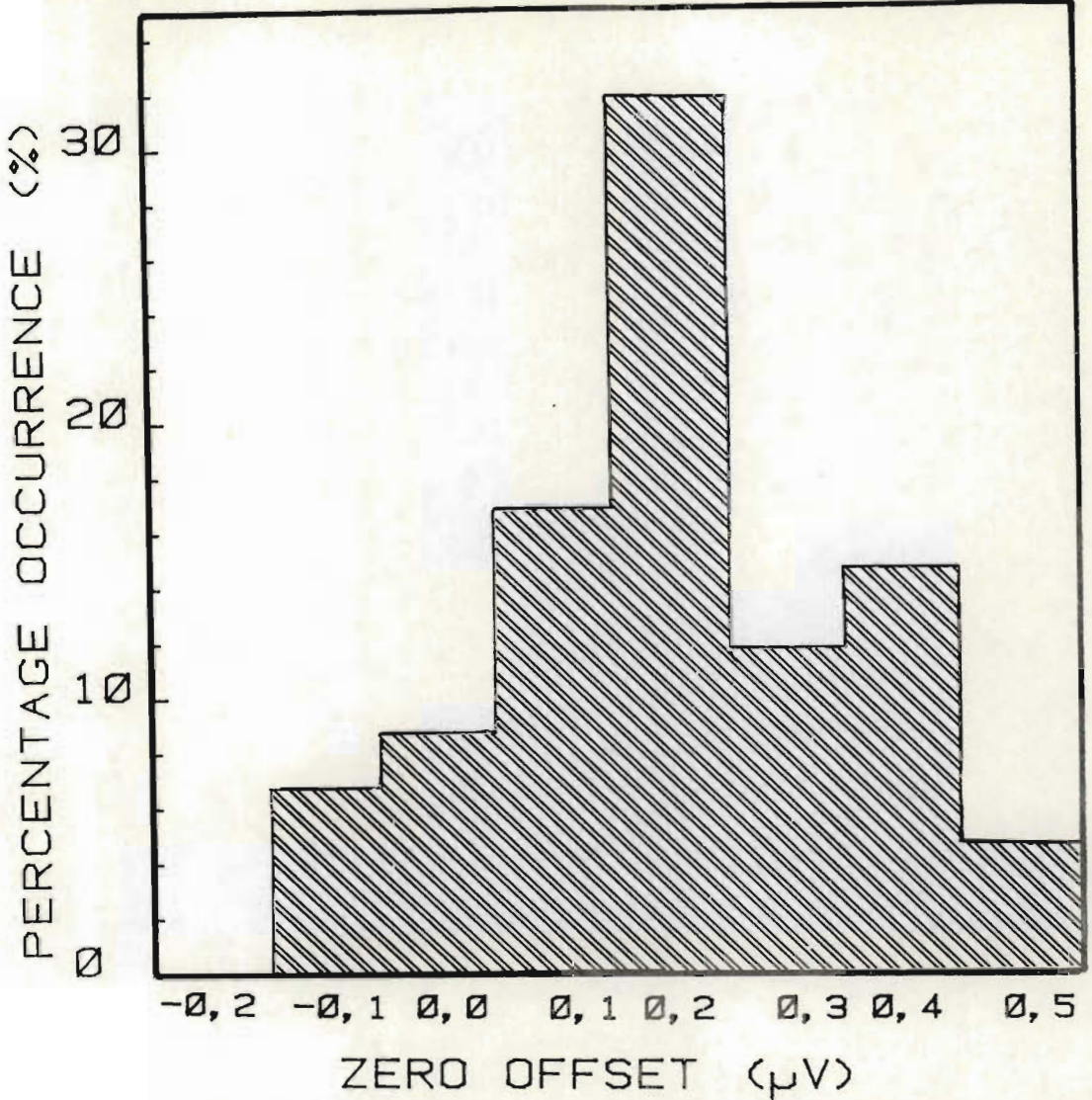


FIG. 5.6 Histogram plot of the percentage occurrence of the various psychrometer temperature gradients occurring in the field situation where block temperature varied between 12 and 29 °C

Zero offset measurements are as important as the measured voltages corresponding to the wet bulb temperature. During this experiment, a total of 243 zero offset measurements were collected. These measurements were obtained using the "0 TO 10" µV range on the HR-33T microvoltmeter and the output recorded on a chart recorder. This enabled voltages to be measured to within $\pm 0,025$ µV (± 25 nV). Generally, negative zero offset values were measured during the night. Most measurements were obtained during hot and dry environmental conditions

shorting out the two poles of the HR-33T gives an instrument zero of about 0,1 to 0,2 µV which is close to the average zero offset shown

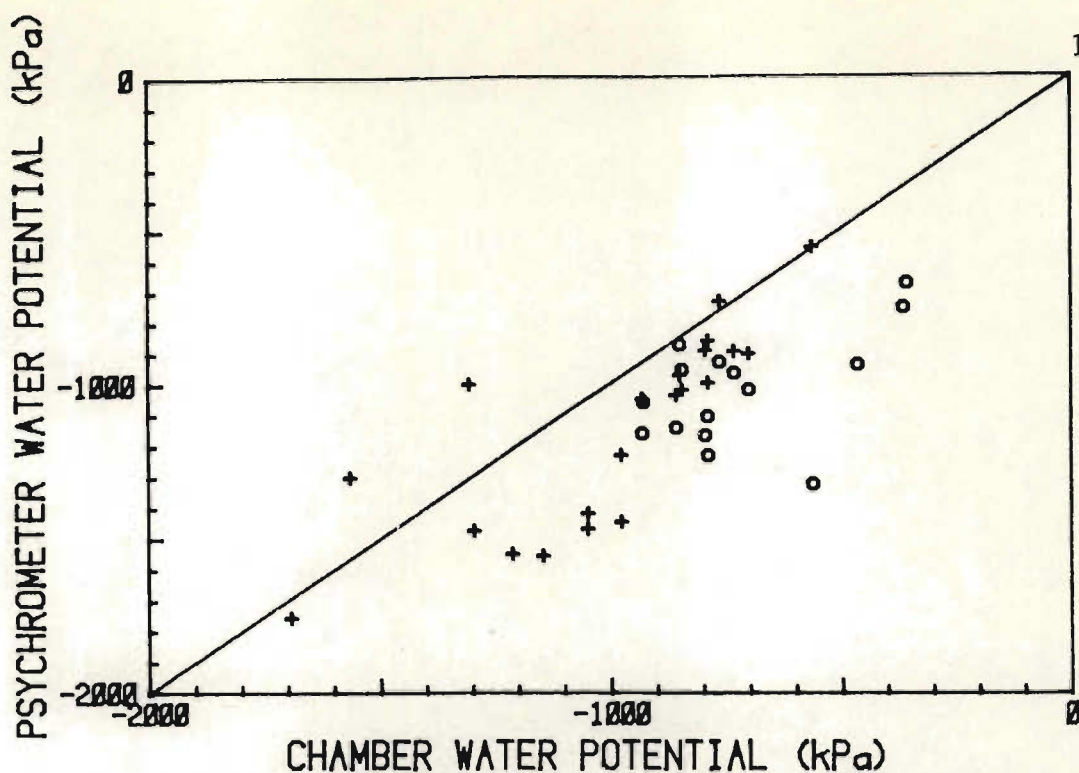


FIG. 5.7 Comparison between psychrometer (no abrasion) and pressure chamber measurements of citrus leaf water potential. Each point represents an average of 2 to 3 pressure chamber measurements using adjacent leaves (+ indicates wide aperture psychrometer measurements and o narrow)

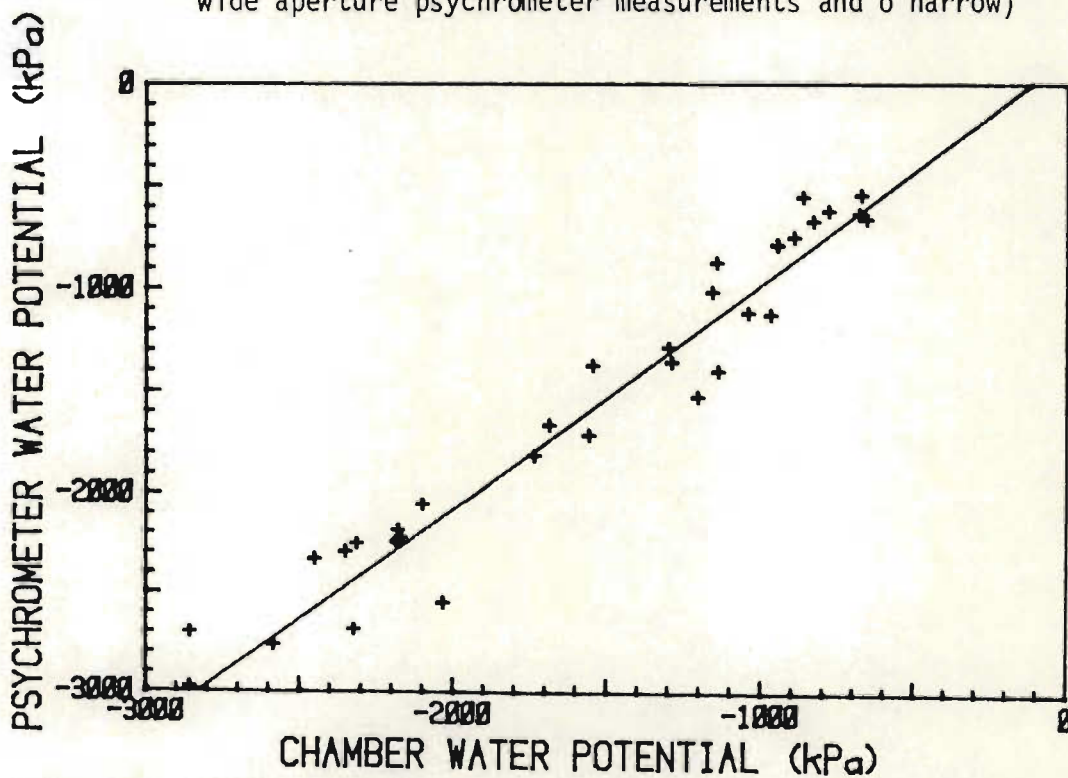


FIG. 5.8 Comparison between psychrometer (coarse abrasion) and pressure chamber measurements of citrus leaf water potential (2 to 3 measurements in each case, from the same plant)

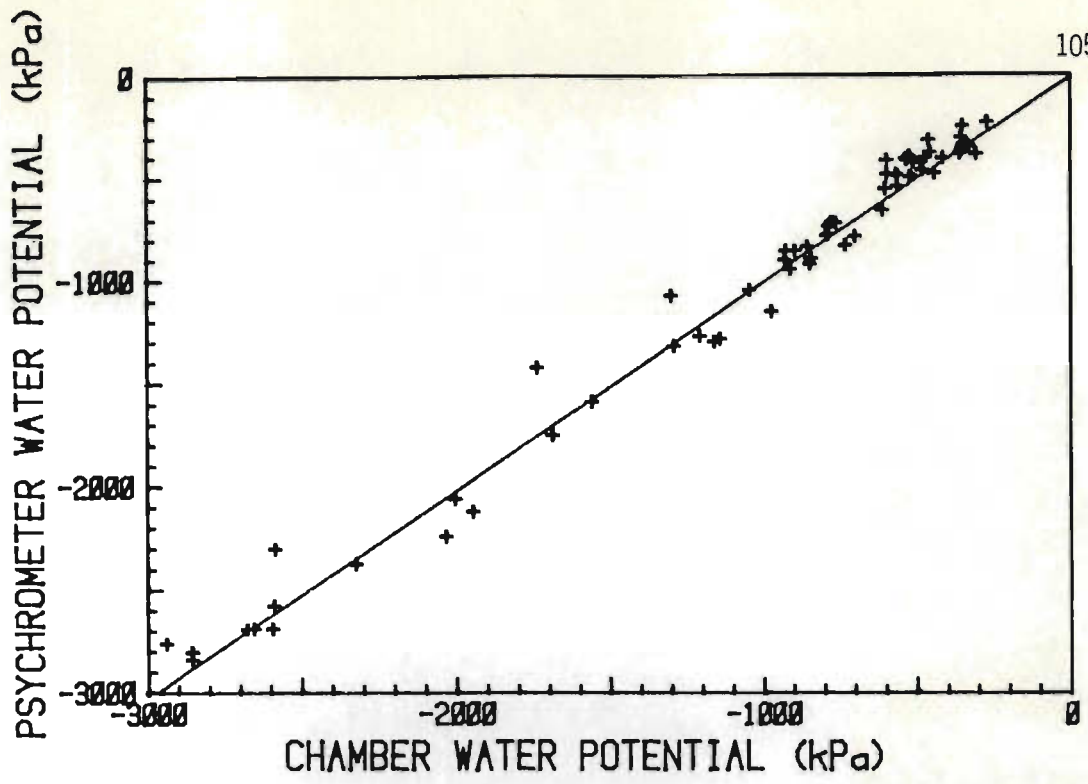


FIG. 5.9 Comparison between psychrometer (light abrasion) and pressure chamber measurements of citrus leaf water potential (2 to 3 measurements in each case, from the same plant)

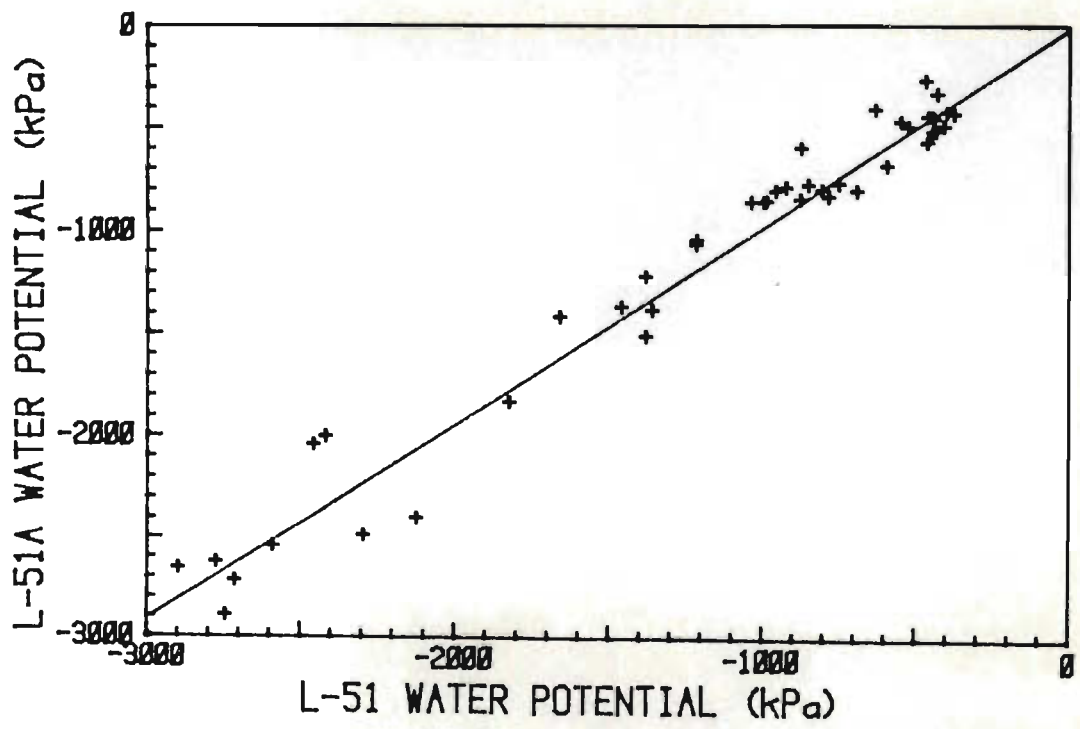


FIG. 5.10 Comparison between psychrometer measurements (intensive light abrasion) using wide aperture unit and those using narrow aperture unit. Individual measurements were performed using the same leaf

TABLE 5.4 Associated statistical parameters for the linear regression curves shown in Figs 5.8 and 5.9 (psychrometric vs pressure chamber measurements) and Fig. 5.10 (narrow aperture psychrometer measurements vs wide aperture) over leaf areas that were pretreated (light abrasion)[¶]

Statistical parameter	Figure number		
	5.8 (Coarse abrasion)	5.9 (Light abrasion)	5.10 (L-51 vs L-51A)
Slope	1,106	1,004	0,996
SE slope	0,0431	0,0159	0,0284
Intercept (kPa)	126	-18	-15
SE intercept (kPa)	76,7	1,6	40,8
r	0,976	0,984	0,982
S _{y.x} (kPa)	179,8	100,0	148,3
Number of points	35	66	44
Slope unity t value [†]	2,451(ns) ^{††}	0,235(hs)	-1,194(s)
Intercept zero t value	-1,659(s)	0,862(hs)	0,374(hs)

[†] Student t value

^{††} ns ≡ non-significant (at 95 % confidence level), s ≡ significant at 95 % and hs ≡ significant at 99 %

TABLE 5.5 Comparison of total leaf water potential ψ_{tot} (kPa) and psychrometric measurements using the slope and intercept parameters of Table 5.4

ψ_{tot} (kPa)	ψ_{PC} (kPa)	LIGHT ABRASION		COARSE ABRASION	
		ψ_{PSY} (kPa)	ψ_{PSY}^W (kPa)	ψ_{PSY} (kPa)	ψ_{PSY}^W (kPa)
- 300	- 262	- 281±21,4	- 231	- 163± 77,9	- 107
- 500	- 462	- 482±22,3	- 432	- 384± 79,8	- 328
- 750	- 712	- 732±24,0	- 682	- 660± 83,3	- 605
-1 000	- 962	- 983±26,2	- 933	- 936± 88,1	- 881
-1 250	-1 212	-1 234±28,8	-1 184	-1 213± 93,8	-1 158
-1 500	-1 462	-1 485±31,7	-1 435	-1 489±100,4	-1 434
-1 750	-1 712	-1 736±34,8	-1 686	-1 766±107,6	-1 710
-2 000	-1 962	-1 987±38,0	-1 937	-2 042±115,4	-1 987
-2 250	-2 212	-2 238±41,4	-2 188	-2 318±123,7	-2 263
-2 500	-2 462	-2 489±44,9	-2 439	-2 595±132,2	-2 539
-2 750	-2 662	-2 740±48,4	-2 690	-2 871±141,2	-2 816

[¶] Intensive light abrasion treatment was used (Table 5.2)

Tables 5.4, 5.5). The coarse abrasion treatment gave psychrometric water potential values, $\psi_{\text{PSY}}(\text{CA})$, greater than the pressure chamber measurements ψ_{PC} , for $\psi_{\text{tot}} > -1\ 250$ kPa, but for drier values the reverse was true (Table 5.5). The slope interval does not overlap with unity at a 95 % confidence level (Table 5.4). The variability of these data may be due to the severity of the abrasion treatment. We found that with this abrasion treatment, damage to the epidermal tissue was more severe, compared to light abrasion (Plate 5.1j) which may account for the lower (drier) psychrometric water potentials for $\psi_{\text{tot}} < -1\ 750$ kPa. The ψ_{tot} values of Table 5.5 are pressure chamber measurements (ψ_{PC}) corrected for the osmotic potential of exuded sap; $\psi_{\text{PSY}}(\text{LA})$ and $\psi_{\text{PSY}}(\text{CA})$ are the respective light and coarse abrasion values calculated from ψ_{PC} ; $\psi_{\text{PSY}}^{\text{W}}(\text{LA})$ and $\psi_{\text{PSY}}^{\text{W}}(\text{CA})$ are the $\psi_{\text{PSY}}(\text{LA})$ and $\psi_{\text{PSY}}(\text{CA})$ values corrected for the apparent effect of "xylem tension relaxation" following petiole excision (Section 5.5.3). We assume that the effect "xylem tension relaxation" increases the actual leaf water potential by 50 kPa.

Light abrasion (60 s) psychrometric water potentials, $\psi_{\text{PSY}}(\text{LA})$, were not statistically different from measured pressure chamber values (Fig. 5.9, Tables 5.4 and 5.5) for $-2\ 700$ kPa $< \psi_{\text{tot}} < -300$ kPa.

Environmental conditions varied widely with measured block temperature ranging between 12 and 29 °C. Brown & Tanner (1981) measured leaf water potential on the same leaf using dewpoint and pressure chamber techniques and found no significant differences between the two. We used adjacent leaves for pressure chamber measurements and hence some of the scatter in our data could arise from spatial separation between psychrometer and pressure chamber leaves (Ritchie & Hinckley, 1975). Also, the pressure chamber water potentials of Table 5.4 and Figs 5.7 to 5.9 were not corrected for the osmotic potential of the exuded sap. The mean osmotic potential of the exuded citrus sap from 28 measurements was -38,0 kPa with a standard error of $\pm 3,6$ kPa (Section 5.4.3). If all pressure chamber potentials are corrected for sap potential, then the psychrometer water potential is closer to the total water potential than to the pressure chamber potential (Table 5.5). The total water potential values shown in this table were calculated from pressure chamber and exuded sap water potential measurements.

Water potential values for the light abrasion treatment were greater than the corrected pressure chamber measurements by approximately 20 kPa, on average. Therefore, the increase of leaf water potential caused by shading the leaf with the psychrometer was small in our case. If however, excision of the leaf releases the "xylem tension" sufficiently to cause a measured increase in pressure chamber water potential (Section 5.5.3), the difference ascribed to shading would be greater than the 20 kPa reported here. If petiole excision increases pressure chamber leaf potential by perhaps 50 kPa, then psychrometric measurements would be greater than the total leaf water potential by about 70 kPa.

Further evidence for the success of the 60 s light abrasion treatment is indicated in Fig. 5.10. Leaf water potential was measured using narrow and wide aperture leaf psychrometers on the same citrus leaf. The good agreement between these measurement values presumably would not be possible if resistance to water vapour diffusion were limiting as the diffusion resistance is double for the narrow aperture psychrometer. There are however, slight differences between these measurements. At low leaf water potentials, say less than -2 500 kPa as measured by the wide aperture psychrometer, the narrow aperture measurements were greater by 70 kPa (calculation based on data from Table 5.4). There was also more variability between these two measurements for water potentials less than about -1 500 kPa (Fig. 5.10). At high leaf water potentials, the narrow aperture psychrometer measurements were lower than their wide aperture counterparts.

5.4 TIME RESPONSE OF THERMOCOUPLE PSYCHROMETERS TO LEAF WATER POTENTIAL CHANGES FOLLOWING EXCISION †

5.4.1 Introduction

The time response of thermocouple psychrometers for dynamic measurement of *in situ* leaf water potential is an aspect of field psychrometry that needs investigation. At present, the response time of these instruments is not known owing to a lack of research in this direction. Lambert & van Schilfgaarde (1965) thought that their psychrometer could respond to leaf water potential changes within 5 min, but chose a time interval of 20 min between measure-

† Based on the paper by Savage & Cass (1983) submitted for publication to *Plant Physiol.*

ments. They maintained that there was a time lag between dynamic changes in water potential of the test leaf and the psychrometer output, but presented no supporting data. Hoffman (1966), cited by Hoffman & Splinter (1968), calculated that this lag would be about 10 s for tobacco if the stomates were open and longer if the stomates were closed. Campbell & Campbell (1974) found that the *in situ* leaf hygrometer appeared to respond to plant water potential changes in less than 30 min and compared dewpoint hygrometer measurements with pressure chamber water potential values. Baughn & Tanner (1976) monitored changes in water potential after leaf excision with a response time of a few minutes. However, their technique introduced thermal gradients that subsided in about 10 min. They measured a 10 to 15 min "wetting transient" of about 10 kPa, but could not separate tissue and thermal effects. Boyer (1972b) altered the water potential of a salt solution sealed in a thermocouple psychrometer cavity by injecting a salt solution of different concentration. He found that the psychrometer reacted to the change in water potential with a response time of 20 s (- he quoted a half life of 30 s). However, it is difficult to separate psychrometer responses from delay in attaining the new water potential because of the finite but unknown diffusion rate of the ionic constituents, with this technique. Neumann & Thurtell (1972) measured the time response of their dewpoint hygrometer measurements by cutting the leaf base in water, and reported a time constant of 110 s. It is possible that the uptake of water by leaves under such conditions is not instantaneous so that this time constant value may reflect internal leaf water and hygrometer responses.

The aim of the work reported here was to investigate the time response of thermocouple psychrometers, particularly short time responses less than about 3 min, as well as the effect of leaf excision on water potential changes under conditions of both high and low atmospheric demand. Whenever possible, psychrometer measurements were compared with pressure chamber measurements.

5.4.2 Materials and methods

Calibration procedures of the eleven leaf psychrometers used in this investigation and other details have previously been described (Section 2.2.3, p 21) modified only by reducing cooling times to 2, 5 and 10 s. All psychrometer measurements obtained were done so using *in situ* leaf psychrometers.

5.4.2.1 *Laboratory investigation*

Potted citrus plants (*Citrus jambhiri*) were equilibrated under laboratory conditions for two days. Leaves were abraded to remove cuticular wax prior to psychrometer sealing (Neumann & Thurtell, 1972; Brown & Tanner, 1981; Section 5.3.2). A commercial psychrometer was modified in order to reduce possible thermal gradients (Section 5.3.2). The psychrometer chamber generally attained water vapour equilibrium with the substomatal cavity within an hour of sealing and measurements were taken after this. A chart recorder was used to record all psychrometer voltage curves. Pressure chamber measurements involved the same techniques outlined previously (Section 5.2.2).

Prior to petiole excision, psychrometric measurements were performed to ensure that measured water potentials were in fact constant.[†] After petiole excision, psychrometer and leaf were carefully moved to positions which minimized leaf shading. In one experiment involving uniform citrus leaves from the same plant, such relocation ensured similar rates of water loss from the leaves without inducing temperature gradients within the psychrometer chamber, nor affecting vapour equilibrium.

In an initial investigation, the potential of exuded leaf sap was measured by over-pressurizing a compound citrus leaf 100 to 200 kPa beyond the pressure chamber endpoint. The sap was collected on a double layer filter paper disc (Whatman no. 541) of diameter 6 mm. The sap potential was then measured using a Wescor C-52 chamber psychrometer.

5.4.2.2 *Field investigation*

Procedures similar to those described for the laboratory investigation were followed. Psychrometer leaves were excised in one of two ways: at the petiole or along the midrib leaving the petiole intact during periods with high and low evaporative demands (Table 5.6) with the psychrometer monitoring water potential changes on the detached leaf portion. In the latter case, movement of the psychrometer containing the cut leaf portion was avoided. The midrib excisions were about 100 to 150 mm long and made with a pair of scissors to avoid pulling the leaf. Leaves were allowed

[†] We therefore assume that the leaf water potential was constant

TABLE 5.6 Leaf excision details for the field measurements and the prevailing climatic conditions

Leaf	Date and local time of excision	Type of excision	Block Temperature ($^{\circ}\text{C}$)	Class A pan (mm) [†]	Wind speed (m/s)
A	10 Sept.'82, 11h58	Petiole	32,8	3,86	0,3
B	10 Sept.'82, 11h12	Petiole	33,1	3,86	0,3
C	31 Aug. '82, 14h27	Petiole	37,6	4,38	2,8
D	1 Sept.'82, 10h44	Petiole	24,0	2,12	0,1
E	1 Sept.'82, 11h14	Midrib	26,8	2,12	0,6
F	1 Sept.'82, 15h03	Midrib	24,5	2,12	2,3
G	1 Sept.'82, 15h21	Midrib	23,6	2,12	2,0

[†] Daily total

to dry out in the position in which they were prior to excision. Two to four pressure chamber measurements on neighbouring leaves were performed to compare with pre-excision psychrometer measurements. Pre-excision psychrometer measurements, as in the laboratory experiment, were performed to determine if the measured leaf water potentials were constant. Post-excision psychrometer measurements were compared with pressure chamber measurements by cutting the leaf petiole, waiting 60 s, cooling the sensing thermojunction for 5 s, monitoring voltage for 55 s (during which time the wet bulb temperature was measured) and then removing the leaf from the psychrometer, and preparing for the pressure chamber measurement. In some cases, the 55 s waiting period was increased. The 5 s cooling time ensured that the sensing junction reached the wet bulb temperature corresponding to the chamber water potential within 55 s.

In other experiments where leaf water potential was high, the leaf was excised and psychrometer water potential monitored at 1 min intervals. In these cases, a cooling time of 2 s was used to ensure that there was no water on the sensing junction at the beginning of the next cooling cycle. As the water potentials decreased during excision, it was sometimes necessary to increase the cooling time from 2 to 5 s. That repetitive cooling of the thermojunction had no effect on the leaf water potential determinations made at 1 min intervals, was confirmed by performing these opera-

tions for a leaf that had not been excised in order to ensure that this procedure did not affect the leaf or measured psychrometric water potential.

5.4.3 Results and discussion

5.4.3.1 Laboratory investigation

The time response of a thermocouple psychrometer[†] was compared with simultaneous pressure chamber measurements using citrus leaves of nearly uniform size, colour, and angle. Psychrometer output was monitored every 10 min up to 50 min after leaf excision. Pressure chamber and psychrometer measurements compared (within 100 kPa) at all times (Fig. 5.11). We conclude that the *in situ* psychrometer response was such that the psychrometer could detect rapid

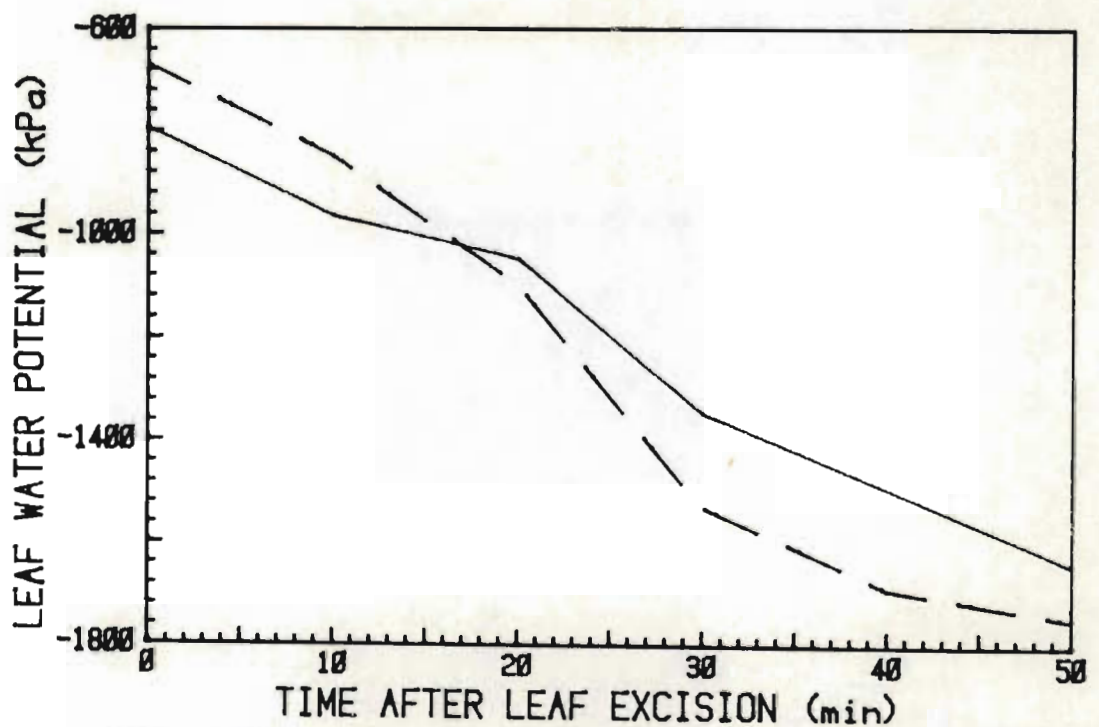


FIG. 5.11 The decrease in citrus leaf water potential following excision in the laboratory as measured by pressure chamber (—) and psychrometric (---) techniques. Only one leaf was used in the case of psychrometric measurements and a different leaf for each pressure chamber measurement. All leaves were of nearly equal area and age and generally of the same colour, for these measurements

[†] In this experiment, leaf water potentials were changing rapidly due to excision

water potential changes resulting from desiccation. Pressure chamber measurements were not corrected for exuded sap potential. The mean value from 28 sap water potential measurements was -38 kPa with a standard deviation of ± 19 kPa (standard error of ± 4 kPa).

A similar investigation involved various plants and eleven leaf psychrometers. Leaves were excised and left to dry for various times ranging from 2 to 200 min. At a set time after excision, psychrometric measurement was made followed by transfer of the leaf from the psychrometer to a pressure chamber and xylem water potential measurement. A total of 24 measurements indicated that the relationship between psychrometer and pressure chamber leaf water potential was linear with a slope of unity and an intercept 0 kPa (Fig. 5.12, Table 5.7). The best fit curve indicates that the psychrometer measurements are generally higher (wetter) than those of the pressure chamber. This could be because of the time delay between psychrometer and pressure chamber measurements (per-

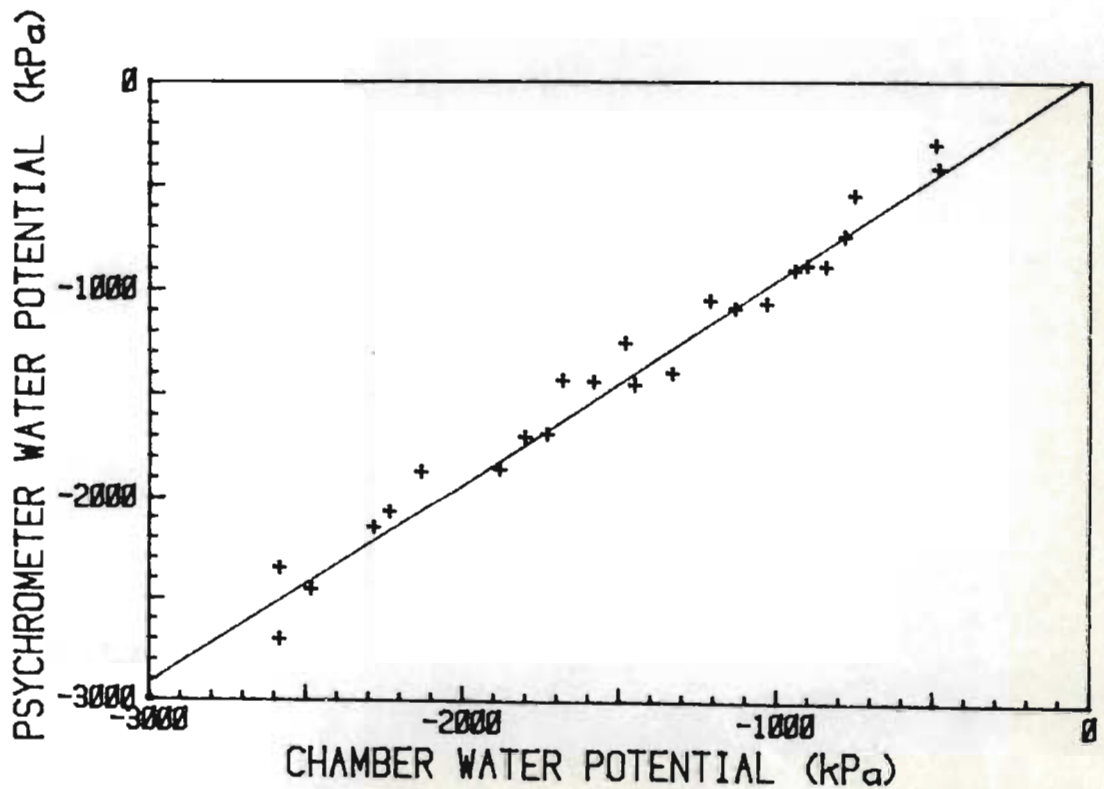


FIG. 5.12 The relationship between pressure chamber and leaf psychrometer measurement for citrus leaves excised in the laboratory. Measurements were performed 2 to 200 min after petiole excision

TABLE 5.7 Associated statistical data for the pressure chamber-
psychrometer curves shown in Figs 5.12 and 5.13

	Laboratory data (Fig. 5.12)	Field data (Fig. 5.13)
Number of points	24	23
Slope and standard error	0,983 ± 0,034	0,912 ± 0,054
Intercept and standard error (kPa)	32,8 ± 56,2	-26,8 ± 65,7
r	0,9869	0,9651
S _{y.x} (kPa)	107,66	87,1
Slope confidence interval (95 %)	(0,911; 1,054)	(0,799; 1,024)
Intercept confidence interval (95 %) (kPa)	(-86,5; 148,6)	(-163,4; 109,9)

formed some 1 to 2 min later) on the same leaf. During pressure chamber measurement therefore, greater pressures are required to force sap to the cut. Presumably the effect of "xylem tension removal" (Section 5.5) affected pressure chamber and psychrometer measurements similarly as both these measurements were performed after leaf excision. The two points of Fig. 5.12 with the highest corresponding leaf water potential were measured about 2 to 3 min after leaf excision indicating that under these laboratory conditions, the time response of the psychrometer is even better than this.

The physical effect of scissors touching the leaf may have induced temperature gradients and hence caused apparent changes in measured leaf water potential. This was investigated by holding a pair of scissors against a leaf without performing a cut while monitoring psychrometric water potential over a 3 min period. There was no detectable change in water potential during this period provided leaf movement was minimized.

5.4.3.2 *Field investigation*

In the field study, water potential in the psychrometer chamber was usually monitored at 1 min intervals after leaf excision. It is possible that this measurement rate could have affected the water potential due to cyclic desiccation and rewetting of the chamber. Control measurements (no excision) were performed to check this. Typically, over a time period of 5 min, water potentials of -708, -734, -708, -721 and -708 kPa at 0, 2, 3, 4 and 5 min respectively after the first cooling cycle (5 s) were measured. The effect of the technique was therefore insignificant in relation to the water potential change induced by leaf excision, in this case.

Comparisons were made between psychrometer and pressure chamber measurements on neighbouring leaves in order to determine the accuracy of the pre-excision psychrometer measurements (Table 5.8). In general, there was a very good correlation over this narrow water potential range. Brown & Tanner (1981) found good correlation using the dewpoint technique (Campbell *et al.*, 1973) for the same alfalfa leaf placed in the pressure chamber apparatus.

Following leaf excision, psychrometric measurements were performed prior to pressure chamber measurements as the same leaf was used for both measurements. An attempt was therefore made to correct for this. Assuming that psychrometer leaf water potential change is a linear function of time after petiole excision it was possible to predict from measurements made before and 1 min after excision, what the psychrometer potentials would have been at the same time as the pressure chamber measurement (Fig. 5.13, Table 5.8). In the case of psychrometer nos 1 and 6, the times were 3 and 5 min after excision respectively, instead of 1 min. The time delay between the psychrometer and corresponding pressure chamber measurement was approximately 1 min. In spite of correcting psychrometer measurements, predicted psychrometer values are slightly greater than the pressure chamber values (Fig. 5.13) under the conditions of a high evaporative demand experienced during the experiment (Table 5.6). Over the measured leaf water potential range (Fig 5.13), the psychrometer measurements are greater (wetter) than the corresponding pressure chamber measurements. This is a similar trend to that found in the laboratory experiments. However, psychrometer measurements do not

TABLE 5.8 Water potential values (kPa) measured using psychrometric and pressure chamber methods and also values corrected for the time lapse (1 min) between psychrometer and pressure chamber measurements. Measurements were performed in the field under high atmospheric demand conditions using citrus plants

Psy- chro- meter no.	Initial psychro- metric measure- ment	Initial pressure chamber measure- ment (adjacent leaves)	Time of and final psy- chrometric measurement	Time of and final pressure chamber measurement (same leaf)	Predicted psychrometer measurement at the time of final pressure chamber measurement
1	-857	-848± 67	3 -1 595	4 -1 960	-1 841
2	-861	-848± 67	1 -986	2 -1 200	-1 111
3	-1 093	-1 081± 81	1 -1 344	2 -1 650	-1 595
4	-951	-1 087± 81	1 -1 126	2 -1 500	-1 301
6	-739	-763±124	5 -1 516	6 -1 900	-1 671
7	-796	-763±124	1 -949	2 -1 200	-1 102

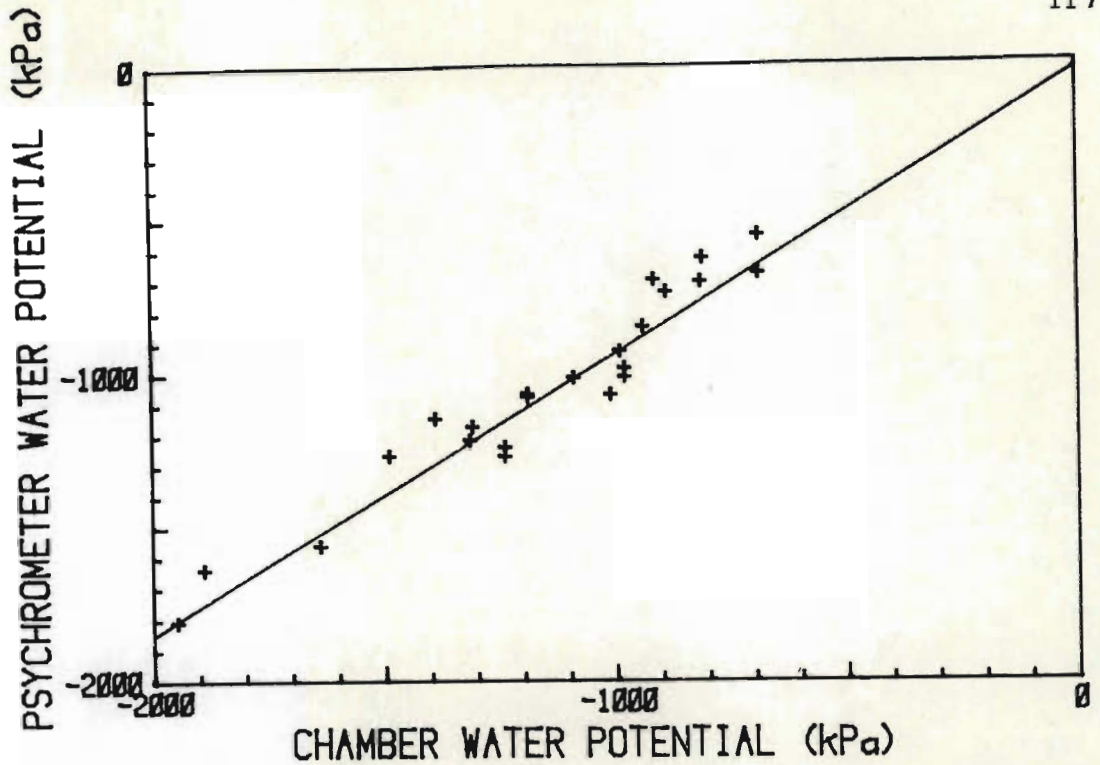


FIG. 5.13 The relationship between pressure chamber and predicted leaf psychrometer measurements (extrapolated to the same time as the former) for various citrus leaves excised in the field. Field measurements were usually within the first two minutes after excision

appear to lag behind the true water potential change, in the first minute after excision, as judged by pressure chamber measurements (Fig. 5.13). Because of the rapid response of the psychrometer, it was possible to monitor changes in leaf water potential at 15 s intervals following excision (Fig. 5.14). For both leaves, there is evidence of a transient increase in leaf water potential, immediately following excision (36 kPa for leaf A and 48 kPa for leaf B). This observation is in conflict with Barrs & Kramer (1969) and Boyer (1968; 1972a) who apparently found that petiole excision itself did not cause an increase in leaf water potential. Barrs & Kramer (1969) postulated that following slicing of leaf tissue, there is passive movement of water from damaged to intact cells. This movement results in an increase in cell volume and corresponding pressure and hence an increase in leaf water potential. Increases in leaf water potential seconds after excision were never

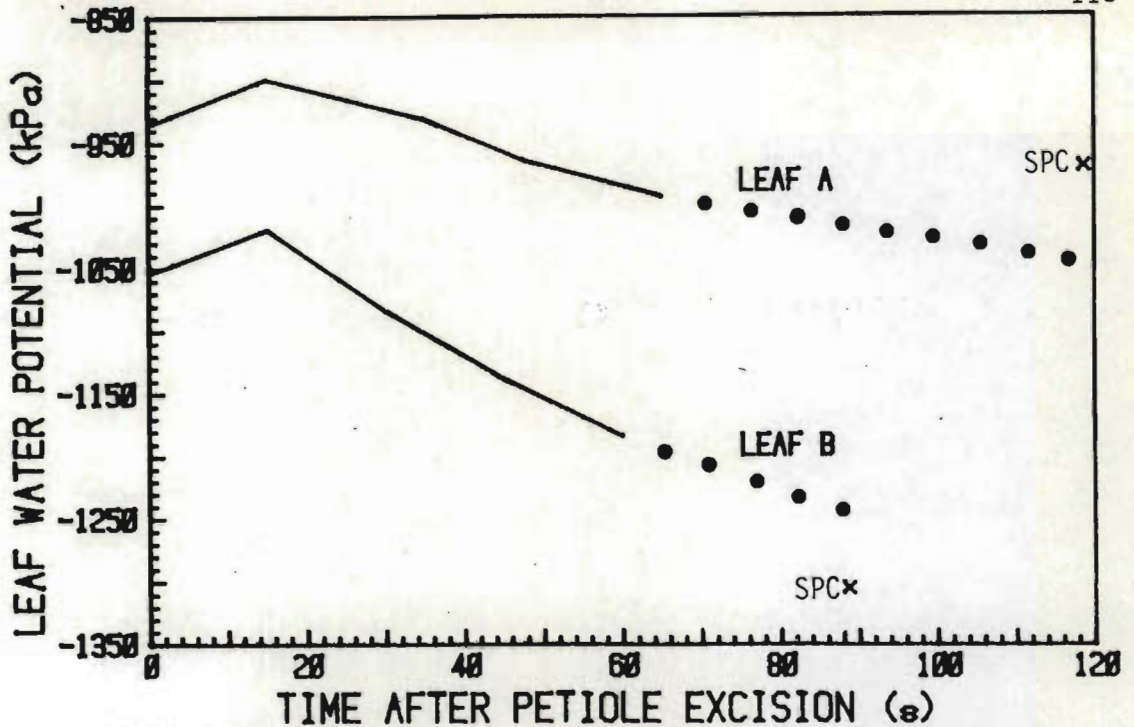


FIG. 5.14 Field measured leaf water potential as a function of time after petiole excision for two leaves from the same citrus plant. The Scholander pressure chamber measurements (SPC) at 90 and 120 s are shown as well as the time predicted psychrometer measurements for these times, respectively

greater than 80 kPa. However, these water potential increases were offset by water potential decreases due to desiccation (Fig. 5.14). Again, there does not appear to be any lag between leaf water potential and that value measured by the psychrometer.

Over a longer period of time, leaf water potential decreases were largely dependent on the climatic conditions. Leaf water potential decreases of 250 to 700 kPa in the first minute after excision were measured (Fig. 5.15; leaves E and C respectively). Under less demanding atmospheric conditions (ambient temperature of 24 °C with scattered cloud, Table 5.6) the decrease in psychrometer water potential was nearly linear in the first 5 min (leaves D, F and G). The effect of transient cloud cover is shown (Fig. 5.15; leaf D). A neighbouring leaf (leaf E) from the same tree was excised along the midrib and the water potential changes of the detached smaller portion monitored about 30 min after leaf D measurements. There does not appear to be any difference in the

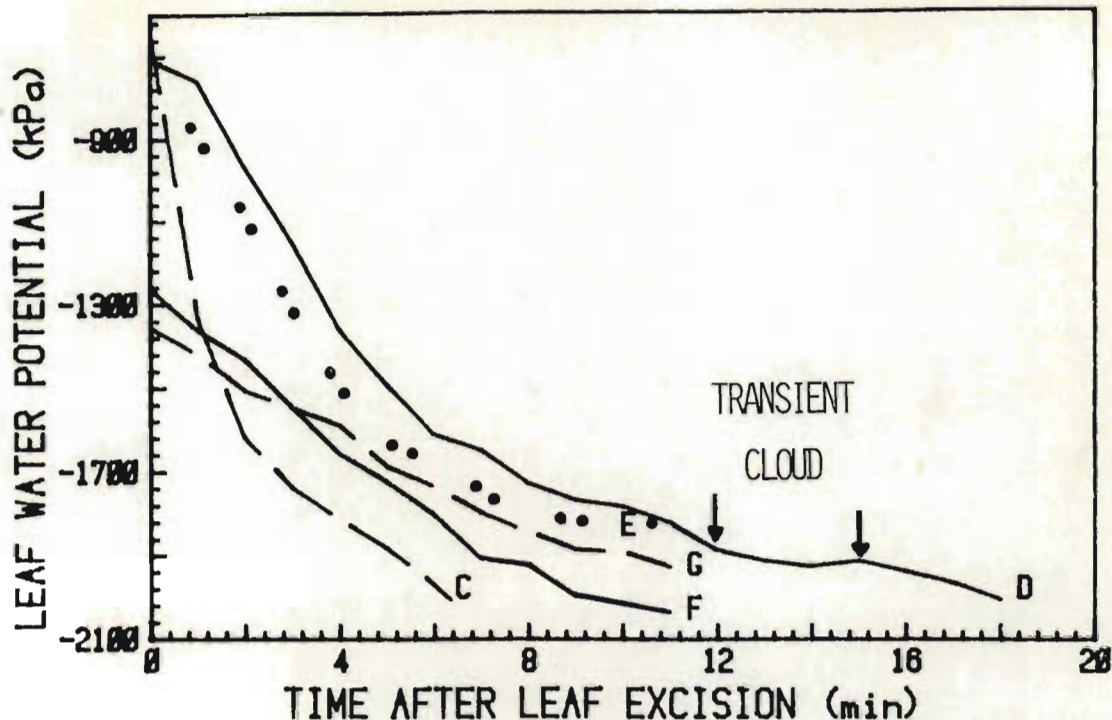


FIG. 5.15 The decrease in citrus leaf water potential following field excision for leaf F and G (low evaporative demand conditions and from the same plant), leaf C (high evaporation) and leaf D and E (low evaporation and from the same plant)

initial water potential decrease (Fig. 5.15; leaf E and D) per unit time, within the first 5 min.

The decrease in psychrometer water potential for two leaves excised along the midrib within 20 min of each other, from the same tree under high evaporative demand conditions is shown (Fig. 5.14 and Table 5.6). Both leaves were on the north side of the tree and a vertical distance of about 150 mm apart. The lower of the two leaves (leaf A) was in a more shaded environment.

5.5 EFFECT OF EXCISION ON LEAF WATER POTENTIAL[†]

5.5.1 Introduction

In view of the excellent time response of *in situ* psychrometers (Section 5.4), this instrument appears ideal for monitoring changes in leaf water potential due to excision to at least within 15 s, provided the resistance to water vapour diffusion is not

[†] Based on the paper by Savage, Cass & Wiebe (1983, submitted to J exp Bot for publication)

significant (Section 5.2). The relevance of this aspect is that all pressure chamber measurements (Section 5.3) were performed after leaf excision, with comparisons being made between these measurements and leaf psychrometer measurements on whole leaves. It is therefore necessary to investigate the effect of excising a leaf petiole on the leaf water potential, assuming that the psychrometer measures the true leaf water potential. The work by Manohar (1966a) and Barrs & Kramer (1969) show that various types of excision cause increases in leaf water potential. Although Manohar (1966a) warns of the danger of using leaf slices placed in chamber type psychrometers for the measurement of leaf water potential, the cuts he used were rather drastic and are not commonly used in performing such measurements except when using small chamber psychrometers used by Ungar (1977) and Cutler, Shahan & Steponkus (1979). For example, Barrs & Kramer (1969) found that 72 mm by 22 mm and 72 mm by 44 mm leaf slices from the same leaf yielded the same measured leaf water potential. Also, Boyer (1968, 1972a) claimed that petiole excision, as measured using an isopiestic psychrometer, did not cause an increase in sunflower leaf water potential.

5.5.2 Materials and methods

Psychrometric and dewpoint hygrometer measurements were performed in a constant temperature laboratory. Dewpoint cooling coefficients (Section 3.2.2, p 54) were determined immediately prior to sealing hygrometers to *Citrus jambhiri* leaves.

All measurements were performed on citrus plants in the laboratory under dark (25 °C) conditions, but unlike the experiment of Baughn & Tanner (1976), leaves were not always covered with aluminium foil to prevent water loss. Petiole cuts were performed using a razor blade and midrib cuts using a pair of scissors. Cooling times ranged between 1 and 3 s and plants were equilibrated for 2 days and watered some 12 h before psychrometer measurements. Abrasion treatment applied to the leaf was the intensive light abrasion treatment (Table 5.2).

5.5.3 Results and discussion

The effect of continuously condensing and evaporating water (every 30 s or so) in the psychrometer chamber was investigated (Fig. 5.16). Generally there was no consistent increase or decrease in measured water potential for up to 3 min after the first measurement, using a 1 s cooling time. The measured water potential was always within 3 % of the time zero leaf water potential. The effect of evaporating and condensing water was therefore ignored. However, it is noted that leaf water potential measurements are only accurate to within 3 %, presumably because of the sensing junction not being allowed to dry completely before the next cooling cycle.

Petiole excision (uncovered leaf) results in immediate (within 15 to 30 s) increase in leaf water potential that can typically amount to more than 60 kPa (Fig. 5.17; leaf C). The reason for this value being a general lower limit is because of the obvious decrease in leaf water potential some 45 s after petiole excision, indicating a loss of water by the uncovered leaf even

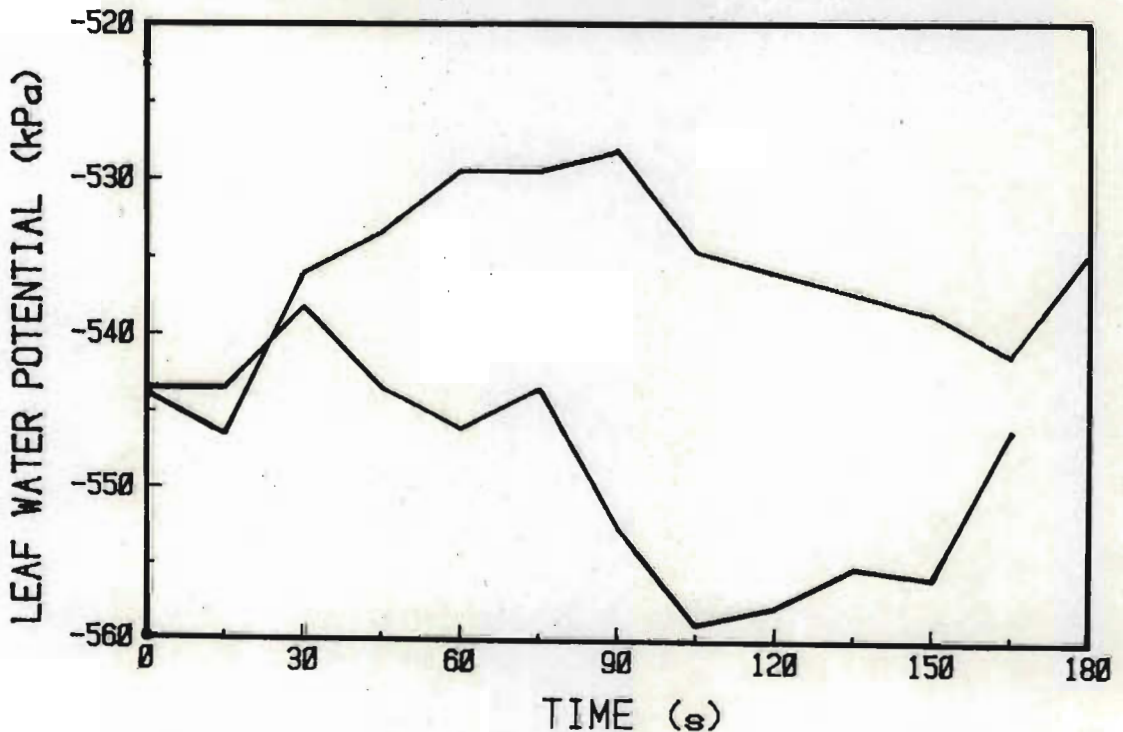


FIG. 5.16 The effect of continuously condensing and evaporating psychrometer chamber water on the measured water potential. Similar measurements were performed on a number of citrus plants; typical results are shown. For the one curve shown, the maximum deviation is 2.9 % relative to the time zero measured leaf water potential.

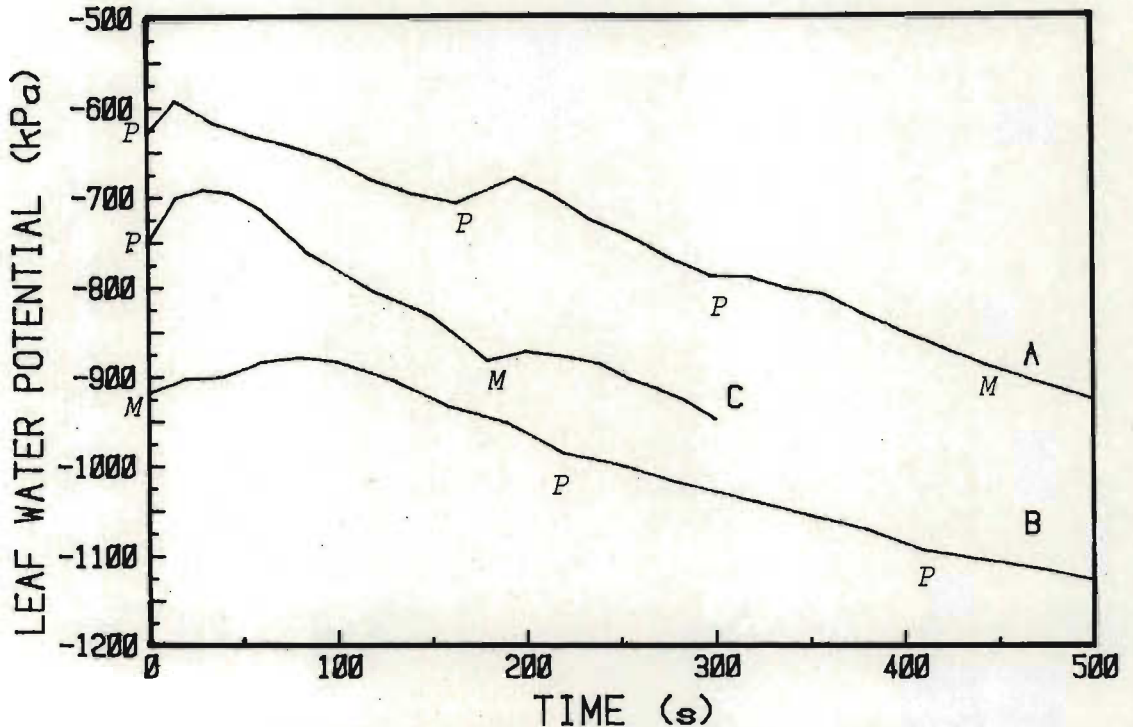


FIG. 5.17 Measured water potential as a function of time for three uncovered leaves excised under dark conditions. P indicates a petiole excision and M a midrib excision

Further "petiole excisions" involved cutting across the midrib, whereas all midrib excisions were parallel to the the midrib axis. Cuts subsequent to the first cut often resulted in smaller increases in measured water potential, compared to the initial cut

under the dark laboratory conditions. A midrib excision on the side opposite the psychrometer, some 3 min after the petiole excision, also resulted in temporary leaf water potential increases that were not as great as the first cut (Fig. 5.17; leaf C). The distance between the petiole cut and the psychrometer sensing area was usually about 100 mm. It is apparent therefore that the rate of change of measured leaf water potential per unit distance is typically of the order $60 \text{ Pa mm}^{-1} \text{ s}^{-1}$, for a petiole cut, assuming that the 60 kPa change in water potential is propagated within 10 s. Presumably, this could be greater if there was some lag

between actual and measured leaf water potentials. Boyer (1968) found that leaf water potentials of intact and petiole excised leaves agreed to within 30 kPa. His (isopiestic) *in situ* chamber type psychrometer had a time response of 30 s and he used different psychrometers for pre- and post-excision measurements. Our results are therefore difficult to reconcile with his.

The experiment was repeated but with a midrib cut on the same side as the psychrometer (Fig. 5.17; leaf B). This typical curve shows that some 100 s is required to attain the peak water potential compared to about 15 to 30 s for a petiole cut (leaf A). The reason for this 100 s period could be that more cells are damaged than a petiole cut, so that a longer time period is required for the water movement through the leaf. There is also a greater quantity of water that is moving passively. The difference between the pre-cut and the 100 s leaf water potential is about 40 kPa, but presumably a significant amount of water had transpired in addition to evaporation from the cut edge during this time period. The type midrib cut performed here is typical of the cut performed when attempting to measure water potential of leaf slices placed in chamber type psychrometers. The size of the leaf slice was about 80 mm by 30 mm. This indicates that even though Barrs & Kramer (1969) found no difference in water potential between leaf slices of 72 mm by 22 mm and 72 mm by 44 mm, there may be differences when water potential of these slices and the potential of the intact leaf prior to excision are compared.

Cuts that were performed after the initial cut generally had peaks that were not as large as the initial one and sometimes did not have peaks but rather a slowing down in the leaf water potential decreases (Fig. 5.17; leaf C). In general though, with every type of cut there was a wetting of the leaf that occurred within about 30 s after cutting (leaves A, B and C).

The experiment was repeated using the dewpoint technique but using covered leaves with plants maintained under dark conditions 24 h prior to and during the experiment. Initially we covered leaves with aluminium foil, but this proved unsatisfactory. If contact with the aluminium foil was made when the petiole was cut, electrical charge conduction resulted in significant shifts in the measured output voltage. Leaves were therefore covered with plastic sheeting.

Using the dewpoint cooling coefficient determined immediately prior to sealing hygrometers to leaves, it was possible to monitor water potential for periods exceeding 30 min, but not in the case of low water potentials ($< -2\ 200$ kPa). In the low water potential case, the output voltage decreased to zero a few minutes after attaining a steady value. This could be due to insufficient available water for the maintenance of the dewpoint temperature, partly because of the low water potential but possibly also because of the diffusion resistance. The dewpoint measurements confirm the results shown in Fig. 5.17; the change in water potential following excision, as expected by J. L. Pallus (in his comments on the paper by Boyer, 1972b) is in fact an increase in measured water potential about 30 s after petiole excision, for *Citrus jambhiri*. The increase varied between about 20 and 80 kPa for plant water potentials ranging between $-2\ 200$ to -300 kPa. From our limited data, increase in measured water potentials appeared to be independent of actual leaf water potentials measured prior to excision.

5.5 SUMMARY

1. Leaf abrasion resulted in decreased diffusion resistance to water vapour movement between the substomatal cavity and reduced the time for the psychrometer water potential to approach the true water potential as defined by the pressure chamber (Fig. 5.1).
2. The extent of abrasion affected the shape of the output voltage curve from thermocouple psychrometers. The shape of the output voltage curve may therefore be used to indicate whether or not leaf diffusion resistance is affecting the water potential measured (Figs 5.2 to 5.4). This is not possible using the dewpoint technique.
3. Pressure chamber measurements on adjacent leaves always compared favourably with psychrometer measurements in the case of citrus if an intensive abrasion treatment was used (Table 5.3). Initial tests should be conducted to determine the extent of abrasion necessary for true water potential measurement using thermocouple psychrometers.
4. *In situ* psychrometer leaf water potential measured on abraded citrus leaves agrees well with that measured on adjacent leaves using the Scholander pressure chamber (Figs 5.8 and 5.9, Tables 5.4 and 5.5).
5. Light abrasion of the leaf resulted in lesser variability in measured water potential values than coarse abrasion. Furthermore, the coarse abrasion psychrometric values measured were greater (wetter) than the pressure chamber counterpart (uncorrected for exuded sap osmotic water potential) for $\psi_w > -1\ 250$ kPa but smaller (drier) for $\psi_w < -1\ 250$ kPa (Fig. 5.9, Tables 5.4 and 5.5).
6. The light abrasion treatment gave psychrometric water potential values that were statistically identical to the pressure chamber values (99 % level of significance), uncorrected for the osmotic potential of exuded sap and the apparent effect of "xylem tension relaxation" following petiole excision (Fig. 5.9, Table 5.4). For this abrasion treatment, water potential measured using a wide aperture psychrometer were typic-

ally 70 kPa greater than those measured using a narrow aperture (at -2 500 kPa), both instruments being sealed on the same leaf (Fig. 5.9, Table 5.4).

7. If pressure chamber measurements are corrected for the osmotic potential of exuded sap for increases in leaf water potential following excision, the psychrometer potentials are greater than the corrected pressure chamber measurements (Table 5.5) by about 70 kPa. This effect may be due to local shading of the leaf by the psychrometer.
8. Post-excision psychrometer field measurements within a minute after cutting the petiole appear to be slightly greater (wetter) than pressure chamber measurements performed on the same leaves 2 min after cutting (Fig. 5.13). In spite of this, the psychrometric technique appears to be more responsive than hitherto thought (Figs 5.14 and 5.15).
9. Petiole excision results in rapid decrease in leaf water potential (as high as 700 kPa in the first minute) for well watered field plants with open stomata (Fig. 5.15). This suggests that large errors will result when using chamber type psychrometers and tissue slices. It is therefore imperative to cover leaves properly prior to excision when performing pressure chamber measurements in order to prevent such rapid decreases.
10. The decrease in water potential under field conditions is generally linear with time after excision, within the first 5 min (Figs 5.14 and 5.15).
11. The favourable response time, elimination of temperature gradients and diffusion resistance to water vapour movement and the non-destructive nature of the psychrometric technique suggest that it is ideally suited for general environmental monitoring of dynamic water potential changes in both controlled and field situations.
12. Petiole excision resulted in increases in measured water potentials (dewpoint and psychrometric) of between 20 and 80 kPa some 15 s after excision, for *Citrus jambhiri*.

GENERAL DISCUSSION

This work has concentrated on the measurement of leaf water potential using *in situ* thermocouple psychrometers. In general, psychrometric measurements of leaf water potential on excised samples should be avoided if other, more reliable, methods are possible (Baughn & Tanner, 1976). Attention to the calibration of thermocouple hygrometers is a first step towards accurate measurement of water potential. If such units are only used in the laboratory, then calibration at a single constant temperature using a range of salt solution concentrations is adequate. If hygrometers are used in the field, it is best to calibrate units under cloudless and calm field conditions. This would ensure that the calibration conditions are as nearly similar to measurement conditions as possible. The method for obtaining the calibration curves for thermocouple psychrometers used in the field is described in Section 2.5.4 (p 46) and the calculated error in water potential on p 49 to 52. Alternative temperature calibration models were described and tested (Section 2.3.3, p 31; Section 2.4.2, p 38). The error calculation for the dewpoint hygrometer is similar to that for psychrometers and is described in Section 3.4.3 (p 63).

Leaf abrasion techniques (Section 5.2.2, p 86) are necessary for accurate citrus leaf water potential measurements using *in situ* thermocouple psychrometers (Fig. 5.9, Table 5.4). Through experience, the abrasion technique used resulted in different psychrometers sealed on the same leaf yielding comparable measured water potential (Fig. 5.4, p 90). The extent of tissue damage following abrasion was found to be surface localized (Plate 5.1h, p 93). Provided psychrometric water potentials were corrected for the osmotic potential of exuded sap (Section 5.3.3, p 107) and the increase in water potential due to excision (Section 5.5.3, p 121), psychrometer measurements compared favourably with pressure chamber measurements (Table 5.5, p 106). For these comparisons, it was necessary to insulate the psychrometer and the microvoltmeter from sudden temperature changes (Fig. 5.5, p 98). A compromise was reached between the thickness of the insulation material (Fig. 5.5, p 98) and the field measured zero offset values (Fig. 5.6, p 103) for a variety of environmental conditions. To determine the time response of thermocouple hygrometers, we induced sudden leaf water potential changes by excising leaves. We showed that hygrometers respond rapidly and certainly within 15 s.

In spite of the artificial situation whereby it is necessary to abrad leaf surfaces and clamp thermocouple psychrometers to leaves, these instruments can be used to measure dynamic changes in leaf water potential non-destructively, with an accuracy that compares favourably with that of the pressure chamber.

REFERENCES

- Acevedo E, Fereres E, Hsiao TC, Henderson D (1979) Diurnal growth trends, water potential and osmotic adjustment of maize and sorghum leaves in the field. *Plant Physiol* 64: 476-480
- Allen JJ, Nell TA, Joiner JN, Albrigo LG (1980) Effects of leaf position and storage conditions on pressure bomb measurement of leaf water potential in *Chrysanthemums*. *HortScience* 15: 808-809
- Anonymous (undated) Interim HR-33T manual. Wescor Inc, Utah
- Babcock KL (1963) Theory of the chemical properties of soil equilibrium. *Hilgardia* 34: 417-542
- Barford NC (1967) Experimental measurements: precision, error and truth. Addison Wesley Pub Co Inc, London
- Barrs HD (1965) Psychrometric measurement of leaf water potential: lack of error attributable to leaf permeability. *Science* 149: 63-65
- Barrs HD, Kramer PJ (1969) Water potential increase in sliced leaf tissue as a cause of error in vapour phase determinations of water potential. *Plant Physiol* 44: 959-964
- Baughn JW (1974) Water potential in plants: comparative measurements using the pressure chamber, psychrometer, and in situ dewpoint hygrometer. PhD thesis, University of Wisconsin, 121 pp
- Baughn JW, Tanner CB (1976) Leaf water potential: comparison of pressure chamber and in situ hygrometer on five herbaceous species. *Crop Sci* 16: 181-184
- Beadle CL, Stevenson KR, Neumann HH, Thurtell GW, King KM (1973) Diffusive resistance, transpiration, and photosynthesis in single leaves of corn and sorghum in relation to leaf water potential. *Can J Plant Sci* 53: 537-544
- Begg JE and Turner NC (1976) Crop water deficits. *Adv Agron* 28: 161-217
- Belesky DP, Wilkinson SR, Pallas JE (1982) Response of tall fescue cultivars grown at two nitrogen levels to low soil water availability. *Crop Sci* 22: 93-97
- Bolt GH, Frissel MJ (1960) Thermodynamics of soil water. *Neth J Agric Sci* 8: 57-78
- Bolt GH et al. (1975) Soil physics terminology. *Bull Int Soc Soil Sci* 48: 26-36
- Boyer JS (1966) Isopiestic technique: measurement of accurate leaf water potentials. *Science* 154: 1459-1460
- Boyer JS (1967) Leaf water potentials measured with a pressure chamber. *Plant Physiol* 42: 133-137
- Boyer JS (1968) Relationship of water potential to growth of leaves. *Plant Physiol* 43: 1056-1062
- Boyer JS (1972a) Use of isopiestic technique in thermocouple psychrometry II. Construction. In Brown RW, van Haveren BP (eds) *Psychrometry in water relations research*. Utah Agric Res Stat and Utah State Univ, pp 98-102
- Boyer JS (1972b) Use of isopiestic technique in thermocouple psychrometry III. Application to plants. In Brown RW, van Haveren BP (eds) *Psychrometry in water relations research*. Utah Agric Res Stat and Utah State Univ, pp 220-223

- Briscoe RE, Tippetts EL (1982) Development of a microprocessor-controlled water potential data system. *Agron Abst*, p 158
- Bristow KL, de Jager JM (1980) Leaf water potential measurements using a strip chart recorder with the leaf psychrometer. *Agric Meteorol* 22: 149-152
- Bristow KL, van Zyl WH, de Jager JM (1981) Measurement of leaf water potential using the J14 press. *J exp Bot* 32: 851-854
- Brown PW, Tanner CB (1981) Alfalfa water potential measurement: a comparison of the pressure chamber and leaf dewpoint hygrometers. *Crop Sci* 21: 240-244
- Brown RW (1970) Measurement of water potential with thermocouple psychrometers: construction and application. *USDA For Ser Res Pap INT-80*, 27 pp
- Brown RW (1972) Determination of leaf osmotic potential using thermocouple psychrometers. In Brown RW, van Haveren BP (eds) *Psychrometry in water relations research*. Utah Agric Res Stat and Utah State Univ, pp 198-209
- Brown RW (1976) New technique for measuring the water potential of detached leaf samples. *Agron J* 68: 432-434
- Brown RW (1977) Water relations of range plants. In Sosebee RE (ed) *Rangeland plant physiology*. Society for Range Management, pp 97-140
- Brown RW, Bartos DL (1982) A calibration model for screen-caged Peltier thermocouple psychrometers. *USDA For Ser Res Pap INT-293*, 155 pp
- ✓ Brown RW, Collins JM (1980) A screen-caged thermocouple psychrometer and calibration chamber for measurements of plant and soil water potential. *Agron J* 72: 851-854
- Brown RW, Johnston RS (1976) Extended field use of screen-covered thermocouple psychrometers. *Agron J* 68: 995-996
- Brown RW, Mc Donough WT (1977) Thermocouple psychrometer for in situ leaf water potential determinations. *Plant and Soil* 48: 5-10
- Calissendorff C, Gardner WH (1972) A temperature compensated leaf psychrometer for in situ measurements of water potential. In Brown RW, van Haveren BP (eds) *Psychrometry in water relations research*. Utah Agric Exp Stat and Utah State Univ, pp 224-228
- Campbell EC (1972) Vapour sink and thermal gradient effects on psychrometer calibration. In Brown RW, van Haveren BP (eds) *Psychrometry in water relations research*. Utah Agric Exp Stat and Utah State Univ, pp 94-97
- Campbell EC, Campbell GS, Barlow WK (1973) A dewpoint hygrometer for water potential measurement. *Agric Meteorol* 12: 113-121
- Campbell GS (1979) Improved thermocouple psychrometers for measurement of soil water potential in a temperature gradient. *J Phys E* 12: 739-743
- Campbell GS, Campbell MD (1974) Evaluation of thermocouple hygrometer for measuring leaf water potential in situ. *Agron J* 66: 24-27
- Campbell GS, Gardner WH (1971) Psychrometric measurements of soil water potential: temperature and bulk density effects. *Soil Sci Soc Am Proc* 35: 8-12
- Campbell GS, Papendick RI, Rabie E, Shayo-Ngowi AJ (1979) A comparison of osmotic potential, elastic modulus, and apoplastic water in leaves of dryland winter wheat. *Agron J* 71: 31-36
- Cheung YNS, Tyree MT, Dainty J (1975) Water relations parameters on single leaves obtained in a pressure bomb and some ecological interpretations. *Can J Bot* 53: 1342-1346

- Chow TL, de Vries J (1973) Dynamic measurement of soil and leaf water potential with a double loop Peltier type thermocouple psychrometer. *Soil Sci Soc Am Proc* 37: 181-188
- Cook RJ, Papendick RI (1978) Role of water potential in microbial growth and development of plant disease, with special reference to postharvest pathology. *HortScience* 13: 559-564
- Cutler JM, Shahan KW, Steponkus PL (1979) Characterization of internal water relations of rice by a pressure-volume method. *Crop Sci* 19: 681-685
- Duniway JM (1971) Comparison of pressure chamber and thermocouple psychrometer determinations of leaf water status in tomato. *Plant Physiol* 48: 106-107
- Durand-Campero G (1981) A comparison of dewpoint and psychrometric mode in leaf water potential measurement. MS thesis, Utah State Univ, 57 pp
- ✓Easter SJ, Sosebee RE (1974) Use of thermocouple psychrometry in field studies of soil-plant-water relationships. *Plant and Soil* 40:707-712
- Feyen J, Belmans C, Hillel D (1980) Comparisons between measured and simulated plant water potential during soil water extractions by potted ryegrass. *Soil Sci* 129: 180-185
- Grant RF, Savage MJ, Lea JD (1981) Comparison of hydraulic press, thermocouple psychrometer, and pressure chamber for the measurement of total and osmotic leaf water potential in soybeans. *S Afr J Sci* 77: 398-400
- Heathcote DG, Etherington JR, Woodward FI (1979) An instrument for non-destructive measurement of the pressure potential (turgor) of leaf cells. *J exp Bot* 30: 811-816
- Hill AV (1930) A thermal method of measuring the vapour pressure of an aqueous solution. *Proc Roy Soc Lon A*127: 9-19
- Hoffman GJ (1966) Thermocouple psychrometer measurements of water potential in an intact plant-soil system. PhD thesis, North Carolina University
- Hoffman GJ, Herkelrath WN (1968) Design features of intact leaf thermocouple psychrometers for measuring water potential. *Am Soc Agric Eng Tran* 11: 631-634
- Hoffman GJ, Rawlins SL (1972) Silver-foil psychrometer for measuring leaf water potential in situ. *Science* 177: 802-804
- ✓Hoffman GJ, Splinter WE (1968) Water potential measurements of an intact plant-soil system. *Agron J* 60: 408-413
- Hsiao TC (1973) Plant responses to water stress. *Ann Rev Plant Physiol* 24: 519-570
- Ike IF, Thurtell GW (1981) Response of indoor-grown cassava to water deficits and recovery of leaf water potential and stomatal activity after water stress. *J exp Bot* 32: 1029-1034
- Ike IF, Thurtell GW, Stevenson KR (1978) Evaluation of the pressure chamber technique for measurement of leaf water potential in cassava (*Manihot* species). *Can J Bot* 56: 1638-1641
- Johnson DA, Brown RW (1977) Psychrometric analysis of turgor pressure response: a possible technique for evaluating plant water stress resistance. *Crop Sci* 17: 507-510
- Kramer PJ (1969) *Plant and soil water relationships: a modern synthesis*. Mc Graw-Hill, New York
- Kramer PJ (1972) Contributions of thermocouple psychrometers to plant science. In Brown RW, van Haveren BP (eds) *Psychrometry in water relations research*. Utah Agric Res Stat and Utah State Univ, pp 187-193
- Kriakopoulos E, Richter H (1981) Pressure-volume curves and drought injury. *Physiol Plant* 52: 124-128

- Lambert JR, van Schilfgaarde J (1965) A method of determining the water potential of intact plants. *Soil Sci* 100: 1-9
- Lang ARG (1967) Osmotic coefficients and water potentials of sodium chloride solutions from 0 to 40 C. *Aust J Chem* 20: 2017-2023
- Lang ARG, Barrs HD (1965) An apparatus for measuring water potentials in the xylem of intact plants. *Aust J Biol Sci* 18: 487-497
- Lange OL, Löscher R, Schulze ED, Kappen L (1971) Responses of stomata to changes in humidity. *Planta* 100: 76-86
- List RJ (1951) *Smithsonian meteorological tables*. Smithsonian Institution, Washington DC
- Liu WT, Wenkert W, Allen LH, Lemon ER (1978) Soil-plant water relations in a New York vineyard: resistances to water movement. *J Am Soc Hort Sci* 103:226-230
- Macnicol PK (1976) Rapid metabolic changes in the wounding response of leaf discs following excision. *Plant Physiol* 57: 80-84
- Manohar MS (1966a) Effect of the excision of leaf tissue on the measurement of their water potential with thermocouple psychrometer. *Experientia* 27: 386-387
- Manohar MS (1966b) Measurement of the water potential of intact plant tissues I. Design of a microthermocouple psychrometer. *J exp Bot* 17: 44-50
- Manohar MS (1966c) Measurement of the water potential of intact plant tissues II. Factors affecting the precision of the thermocouple technique. *J exp Bot* 17: 51-56
- Manohar MS (1966d) Measurement of the water potential of intact plant tissues III. The water potentials of germinating peas (*Pisum sativum* L). *J exp Bot* 17: 231-235
- Meidner H, Sheriff DW (1976) *Water and plants*. Blackie, London
- ✓Meyn RL, White RS (1972) Calibration of thermocouple psychrometers: a suggested procedure for development of a reliable predictive model. In Brown RW, van Haveren BP (eds) *Psychrometry in water relations research*. Utah Agric Res Stat and Utah State Univ, pp 56-64
- Michel BE (1977) A miniature stem thermocouple hygrometer. *Plant Physiol* 60: 645-647
- Michel BE (1979) Correction of thermal gradient errors in stem thermocouple hygrometers. *Plant Physiol* 63: 221-224
- ✓Milburn JA (1979) *Water flow in plants*. Edward Arnold, London
- ✓Millar BD (1971a) Improved thermocouple psychrometer for the measurement of plant and soil water potential I: thermocouple psychrometry and an improved instrument design. *J exp Bot* 22: 875-890
- ✓Millar BD (1971b) Improved thermocouple psychrometer for the measurement of plant and soil water potential II: operation and calibration. *J exp Bot* 22: 891-905
- ✓Millar BD (1974) Improved thermocouple psychrometer for the measurement of plant and soil water potential III: equilibration. *J exp Bot* 25: 1070-1084
- Monteith JL (1973) *Principles of environmental physics*. Edward Arnold, London
- Moore RT, Caldwell MM (1972) The field use of thermocouple psychrometers in desert soils. In Brown RW, van Haveren BP (eds) *Psychrometry in water relations research*. Utah Agric Exp Stat and Utah State Univ, pp 165-169
- Myrold DD, Elliott LF, Papendick RI, Campbell GS (1981) Water potential-water content characteristics of wheat straw. *Soil Sci Soc Am J* 45: 329-333

- Neumann HH, Thurtell GW (1972) A Peltier cooled thermocouple dewpoint hygrometer for in situ measurement of water potential. In Brown RW, van Haveren BP (eds) Psychrometry in water relations research. Utah Agric Exp Stat and Utah State Univ, pp 103-112
- Neumann HH, Thurtell GW, Stevenson KR (1973) Resistance to water flow in corn, soybean, and sunflower at several transpiration rates. *Can J Plant Sci* 54: 175-184
- Neumann HH, Thurtell GW, Stevenson KR, Beadle CL (1974) Leaf water content and potential in corn, sorghum, soybean, and sunflower. *Can J Plant Sci* 54: 185-195
- Nnyamah JU, Black TA (1977) Field performance of the dewpoint hygrometer in studies of soil-root water relations. *Can J Soil Sci* 57: 437-444
- Nnyamah JU, Black TA, Tan CS (1978) Resistance to water uptake in a Douglas-fir forest. *Soil Sci* 126: 63-76
- Nulsen RA, Thurtell GW (1978) Recovery of corn leaf water potential after severe water stress. *Agron J* 70: 903-906
- Oertli JJ, Aceves-Navarro E, Stolzy LH (1975) Interpretation of foliar water potential measurements. *Soil Sci* 119: 162-166
- Oosterhuis DM (1981) Hydraulic conductivity and drought acclimation of cotton root systems. PhD thesis, Utah State University 128 pp
- Oosterhuis DM, Walker S (1982) Field measurement of leaf water potential components using thermocouple psychrometers. II Application in plant water relation studies in wheat. *Crop Prod* 11: 5-8
- Oosterhuis DM, Walker S, Savage MJ (1982) Field comparison of leaf in situ and screen-caged psychrometers, and pressure chamber measurements of soybean water potential. *Agron Abstr*, p 106
- Pallas JE, Michel BE (1978) Comparison of leaf and stem hygrometers for measuring changes in peanut plant water potential. *Peanut Science* 5: 65-67
- Pallas JE, Stansell JR, Koske TJ (1979) Effects of drought on Florunner peanuts. *Agron J* 71: 853-858
- Papendick RI, Campbell GS (1980) Theory and measurement of water potential. In Parr JF, Gardner WR, & Elliott LF (eds) Water potential relations in soil microbiology. *Soil Sci Soc Am*, pp 1-22
- Peck AJ (1968) Theory of the Spanner psychrometer, 1. The thermocouple. *Agric Meteorol* 5: 433-447
- Peck AJ (1969) Theory of the Spanner psychrometer, 2. Sample effects and equilibration. *Agric Meteorol* 6: 111-124
- Phillips DL (1981) End-point recognition in pressure chamber measurements of water potential of *Vigniera porteri* (Asteraceae). *Ann Bot* 48: 905-907
- Puritch GS, Turner (1973) Effects of pressure increase and release on temperature within a pressure chamber used to estimate plant water potential. *J exp Bot* 24: 342-348
- Radulovich CJ, Phene CJ, Davis KR, Brownell JR (1982) Comparison of water stress of cotton from measurements with the hydraulic press and the pressure chamber. *Agron J* 74: 383-385
- Rauscher HM, Smith DW (1978) A comparison of the water potential predictors for use in plant and soil thermocouple psychrometry. *Plant and Soil* 49: 679-683
- Rawlins SL (1964) Systematic error in leaf water potential measurements with a thermocouple psychrometer. *Science* 146: 644-646

- Rawlins SL (1966) Theory for thermocouple psychrometers used to measure water potential in soil and plant samples. *Agric Meteorol* 3: 293-310
- Rawlins SL (1972) Theory of thermocouple psychrometers for measuring soil and plant water potential. In Brown RW, van Haveren BP (eds) *Psychrometry in water relations research*. Utah Agric Stat and Utah State Univ, pp 43-50
- Rawlins SL, Dalton FN (1967) Psychrometric measurement of soil water potential without precise temperature control. *Soil Sci Soc Am Proc* 31: 297-300
- Rawlins SL, Gardner WR, Dalton FN (1968) In situ measurement of soil and plant water potential. *Soil Sci Am Proc* 32: 468-470
- Redmann RE (1976) Plant-water relationships in a mixed grassland. *Oecologica (Berl)* 23: 283-295
- Richter H (1978) Water relations single drying leaves: evaluation with a dewpoint hygrometer. *J exp Bot* 29: 277-280
- Richter H, Duhme F, Glatzel G, Hinckley TM, Karlic H (1980) Some limitations and applications of the pressure-volume curve in ecophysical research. In Grace J, Ford ED, Jarvis PG (eds) *Plants and their atmospheric environment*. Blackwell Scientific Publications, Oxford, pp 263-272
- Ritchie GA, Hinckley TM (1975) The pressure chamber as an instrument for ecological research. *Adv Ecol Res* 9: 165-254
- Roberts J (1977) The use of tree-cutting techniques in the study of water relations of mature *Pinus sylvestris* L. *J exp Bot* 28: 751-767
- Rose DA (1979) Soil water: quantities, units and symbols. *J Soil Sci* 30: 1-15
- Savage MJ (1978) Water potential terms and units. *Agrochemophysica* 10: 5-6
- Savage MJ (1979) Use of the international system of units in the plant sciences. *HortScience* 14: 492-495
- Savage MJ (1980) The effect of fire on the grassland microclimate. *Herb Abstr* 50: 589-603
- Savage MJ, Cass A (1983) Time response of thermocouple psychrometers to leaf water potential changes following leaf excision. Submitted for publication to *Plant Physiol*
- Savage MJ, Cass A, de Jager JM (1981a) Calibration of thermocouple hygrometers. *Irrig Sci* 2: 113-125
- Savage MJ, Cass A, de Jager JM (1981b) Calibration of thermocouple hygrometers using the dewpoint technique. *S Afr J Sci* 77: 323-324
- Savage MJ, Cass A, de Jager JM (1981c) Measurement of water potential using thermocouple hygrometers. *S Afr J Sci* 77: 24-27
- Savage MJ, Cass A, de Jager JM (1982) An accurate temperature correction model for thermocouple hygrometers. *Plant Physiol* 69: 526-530
- Savage MJ, Cass A, de Jager JM (1983) Statistical assessment of error in thermocouple hygrometric water potential measurement. Submitted for publication to *Crop Sci*
- Savage MJ, Cass A, Wiebe HH (1983) Effect of excision on leaf water potential. Submitted for publication to *J exp Bot*
- Savage MJ, de Jager JM, Cass A (1979) Calibration of thermocouple hygrometers using the psychrometric technique. *Agrochemophysica* 11: 51-56
- Savage MJ, Oosterhuis DM, Cass A (1983) Some aspects on the non-destructive measurement of in situ leaf water potential. *Crop Prod* 12 (in press)
- Savage MJ, Vermeulen K (1983) Microclimate modification of tall moist grasslands of Natal by spring burning. *J Range Mgt* 36: 172-174

- Savage MJ, Wiebe HH, Cass A (1983a) Effect of cuticular abrasion thermocouple psychrometric in situ field measurement of leaf water potential. Submitted for publication to *J exp Bot*
- Savage MJ, Wiebe HH, Cass A (1983b) In situ field measurement of water potential using thermocouple psychrometers. Submitted for publication to *Plant Physiol*
- Scholander PF, Hammel HT, Bradstreet ED, Hemmingsen EA (1965) Sap pressure in vascular plants. *Science* 148: 339-346
- Schimmelpfennig H (1972) Semi-automatic thermocouple psychrometer readout. In Brown RW, van Haveren BP (eds) *Psychrometry in water relations research*. Utah Agric Exp Stat and Utah State Univ, pp 120-122
- Scotter DR (1972) The theoretical and experimental behaviour of a Spanner psychrometer. *Agric Meteorol* 10: 125-136
- Shayo-Ngowi AJ, Campbell GS (1980) Measurement of matric potential in plant tissue with a hydraulic press. *Agron J* 72: 567-568
- Slack DC, Riggall ER (1980) Effects of joule heating of thermocouple psychrometer water potential determinations. *Trans Am Soc Agric Eng* 23: 877-883
- Slatyer RO (1966) Some physical aspects of internal control of leaf transpiration. *Agric Meteorol* 3: 281-292
- Slatyer RO (1967) *Plant-water relationships*. Academic Press, London
- Slavik B (1974) *Methods of studying plant water relations*. Springer-Verlag, Berlin
- Sojka RE, Stolzy LH, Fischer RA (1979) Comparison of diurnal drought response of selected wheat cultivars. *Agron J* 71: 329-335
- Spanner DC (1951) The Peltier effect and its use in the measurement of suction pressure. *J exp Bot* 2: 145-168
- Squire GR, Black CR, Gregory PJ (1981) Physical measurements in crop physiology II. Water relations. *Expl Agric* 17: 225-242
- Talbot AJB, Tyree MT, Dainty J (1975) Some notes concerning the measurement of water potentials of leaf tissue with specific reference to *Tsuga canadensis* and *Picea abies*. *Can J Bot* 53: 784-788
- Taylor SA, Ashcroft GL (1972) *Physical edaphology*. WH Freeman and Co, San Francisco
- Turner NC (1981) Techniques and experimental approaches for the measurement of plant water status. *Plant and Soil* 58: 339-366
- Turner NC, Begg JE (1978) Responses of pasture plants to water deficits. In Wilson JR (ed) *Plant relations in pastures*. CSIRO, pp 50-66
- Turner NC, Begg JE (1981) Plant-water relations and adaptation to stress. *Plant and Soil* 58: 97-131
- Turner NC, Jones MM (1980) Turgor maintenance by osmotic adjustment: a review and evaluation. In Turner NC, Kramer PJ (eds) *Adaptation of plants to water and high temperature stress*. John Wiley and Sons, New York, pp 87-103
- Tyree MT, Hammel HT (1972) The measurement of the turgor pressure and the water relations of plants by the pressure bomb technique. *J exp Bot* 23: 267-282
- Ungar IA (1977) The relationship between soil water potential and plant water potential in two inland halophytes under field conditions. *Bot Gaz* 138: 498-501
- van Haveren BP (1972) Measurements of relative vapor pressure in snow with thermocouple psychrometers. In Brown RW, van Haveren BP (eds) *Psychrometry in water relations research*. Utah Agric Exp Stat and Utah State Univ, pp 178-185

- van Haveren BP, Brown RW (1972) The properties and behaviour of water in the soil-plant-atmosphere continuum. In Brown RW, van Haveren BP (eds) Psychrometry in water relations research. Utah Agric Exp Stat and Utah State Univ, pp 1-27
- Walker S (1981) Field measurement of leaf water potential components using thermocouple psychrometers. MSc (Agric) thesis, University of Natal, 65 pp
- Walker S, Oosterhuis DM (1982) Field measurement of leaf water potential components using thermocouple psychrometers. I Techniques. *Crop Prod* 11: 1-4
- Walker S, Oosterhuis DM, Savage MJ (1983) Field use of screen-caged thermocouple psychrometers in sample chambers. Accepted for publication by *Crop Sci*
- Waring RH, Cleary BD (1967) Plant moisture stress: evaluation by pressure bomb. *Science* 155: 1248-1254
- Weast RB (1978) CRC handbook of chemistry and physics (5th edition), The Chemical Rubber Co, Cleveland
- Wenkert W, Lemon ER, Sinclair TR (1978) Changes in water potential during pressure bomb measurement. *Agron J* 70: 353-355
- West DW, Gaff DF (1971) An error in the calibration of xylem-water potential against leaf-water potential. *J exp Bot* 22: 342-346
- Wheeler ML (1972) Application of thermocouple psychrometers to field measurements of soil moisture potential. PhD thesis, University of Arizona, 132 pp
- Wheeler ML, Qashu HK, Evans DD (1972) Psychrometric measurement of water potential under desert conditions. In Brown RW, van Haveren BP (eds) Psychrometry in water relations research. Utah Agric Exp Stat and Utah State Univ, pp 171-174
- Wiebe HH (1981) Measuring water potential (activity) from free water to oven dryness. *Plant Physiol* 68: 1218-1221
- Wiebe HH, Brown RW (1979) Temperature gradient effects on in situ hygrometer measurements of soil water potential II Water movement. *Agron J* 71: 397-401
- Wiebe HH, Brown RW, Barker J (1977) Temperature gradient effects on in situ hygrometer measurements of water potential. *Agron J* 69: 933-939
- Wiebe HH, Brown RW, Daniel TW, Campbell EC (1970) Water potential measurements in trees. *BioScience* 20: 225-226
- Wiebe HH, Campbell GS, Gardner WH, Rawlins SL, Cary JW, Brown RW (1971) Measurement of plant and soil water status. *Utah State Univ Bull* 484, 71 pp
- Wiebe HH, Kidambi RN, Richardson GH, Ernstrom CA (1981) A rapid psychrometric procedure for water activity measurement of foods in the intermediate moisture range. *J Food Prot* 44: 892-895
- Wiebe HH, Prosser RJ (1977) Influence of temperature gradients on leaf water potential. *Plant Physiol* 59: 256-258
- Wilson JR, Fisher MJ, Schulze ED, Dolby GR, Ludlow MM (1979) Comparison between pressure-volume and dewpoint hygrometry techniques for determining the water relations characteristics of grass and legume leaves. *Oecologia (Berl)* 41: 77-88
- Yegappan TM, Mainstone BJ (1981) Comparisons between press and pressure chamber techniques for measuring leaf water potential. *Expl Agric* 17: 75-84
- Young HD (1962) Statistical treatment of experimental data. McGraw-Hill Book Co Inc, New York

- Zanstra PE, Hagenzieker F (1977) Comments on the psychrometric determination of leaf water potentials in situ. *Plant and Soil* 48: 347-367
- Zemansky MW (1957) *Heat and thermodynamics*, 4th ed. McGraw-Hill Book Co Inc, New York